# FINITE ELEMENT ANALYSIS OF HOLLOW STRUCTURAL SECTIONS SUBJECT TO TORSION AND COMBINED LOADING

© By: Steven Bartlett

A thesis submitted to The School of Graduate Studies

in partial fulfillment of the requirements for the degree of

**Master of Engineering**

**Faculty of Engineering and Applied Science**

Memorial University

**October 2021**

St. John's Newfoundland and Labrador Canada

# Abstract

The reliability of steel structures is governed by design codes which may vary between countries. These codes may stipulate factors of safety, quality, and loading conditions. The approved steel design codes ensure each structure is designed with the same quality, recommended loading conditions, and safety standards for the design life of the structure. In Canada, steel structures are governed by the Canadian Standards Association (CSA) and designed to CAN/CSA S16-19 – Design of Steel Structures [1]. In the United States, steel structures are governed by the American Institute of Steel Construction (AISC) and designed to ANSI/AISC 360-16 – Specification for Structural Steel Buildings [2]. Both Canada and the United States have similar design principles included in their structural design codes. Therefore, the Canadian steel code and the load-resistant factored design sections of the American steel code are almost interchangeable.

From the literature review comparing the most current Canadian and American principle clauses, it was identified ANSI/AISC 360-16 [2] provides mathematical equations for checking HSS in torsion and combined loading while CAN/CSA S16-19 [1] advises the user to complete an elastic analysis for verification. While the approach of completing a finite element analysis to the torsion stress is a very precise method, having the option to use theoretical formulas in accordance with limit state design to analyze this condition could be beneficial to practicing engineers. This thesis concentrates on strength verification of the American torsional clause using non-linear FEA techniques with calculated section capacities to determine if the clause can be a potential recommended method of torsion loading assessment. The objective of this work is to develop a practical method of evaluating hollow structural sections subject to torsion and combined loading in Canada.

From the research performed, conclusions are made based on the results of the analysis. Recommendations are provided according to the application of the ANSI/AISC 360-16 [2] torsion clause along with the additional research required for validation as an approved design approach in Canada.

# Acknowledgments

I would like to thank Dr. Stephen Bruneau and Dr. Amgad Hussein for their input, guidance, and recommendations on this thesis. Without their invaluable contribution completion of this thesis would not have been possible.

Also, I want to thank my family for the continued support and encouragement to finish this thesis.

# Table of Contents

# List of Figures

# List of Tables

# Chapter 1 Introduction

## 1.1 Background

Structural steel systems are designed daily by practicing structural engineers for many different applications. These engineered systems have a very broad range of purposes and specific load requirements. Structural engineering systems vary from complex structures such as buildings, bridges, offshore platforms to simpler structures such as a single spreader beam used for lifting equipment. One aspect all engineered systems have in common is they are designed to a specified design code that has predetermined reliability parameters. Reliability is a very important aspect in the design of any system, as it allows for the quantification of the probability that a system will behave as intended over a definite time period and under specific loading conditions [3].

In general, when engineers design a system they are trying to achieve an appropriate utilization of a structure within governing code requirements but also an economical design. Commonly structural design codes are formatted to be optimal for a wide assortment of structures and their intended purpose. Most structural design codes are founded upon probability and structural reliability principles. The two primary aspects of designing a structure are optimization of the total anticipated efficiency by the engineer and optimization of the design code which would be previously written [4]. The required levels of safety that must be achieved are decided by the code writing committee. Fundamentally design codes are structured on risk tolerance in specific loading conditions. Depending on the probability and possible types of failure of a structural element, the risk tolerance can vary.

In Canada, steel structures are governed by the Canadian Standards Association (CSA) and designed to CAN/CSA S16-19 – Design of Steel Structures [1]. In the United States, steel structures are governed by the American Institute of Steel Construction (AISC) and design to ANSI/AISC 360-16 – Specification for Structural Steel Buildings [2]. Both Canada and the United States have similar design principles included in their structural building codes. Based on this, the Canadian steel code and the load-resistant factored design sections of the American steel code are essentially compatible.

Limit states design is a design methodology that checks the adequacy of a structural system against several limiting loading conditions at relevant load magnitudes. The loading conditions that are checked for structural systems are ultimate limit states and serviceability limit states. Ultimate limit states are states which are associated with safety such as loading capacities and failure due to cyclic fatigue of a structure. Serviceability limit states are states that are related to the structure's performance under normal operating circumstances, an example of this would be deflection in a building under the live load of people occupying the building. Limit states provide the margin of safety between loads imposed on the structure and the resistance of the structure [3]. As stated by Kulak and Grondin, "In essence, the designer attempts to ensure that the maximum strength of a structure (or elements of a structure) is greater than the loads imposed upon it, with a reasonable margin against failure". [5]

The ultimate limit states condition is shown in Figure 1, which presents the distribution curves for the effect of loads and the resistance on a structure. Load and strength are independent variables used for the design of a structure, when the loading effect is greater than the resistance the structure will ultimately fail. Structures are designed so the overlap of the strength and resistance curve is small therefore providing an acceptable probability of failure while keeping the design as economical as possible. It is known that in the design of any structure the probability of failure is never 0. [5]

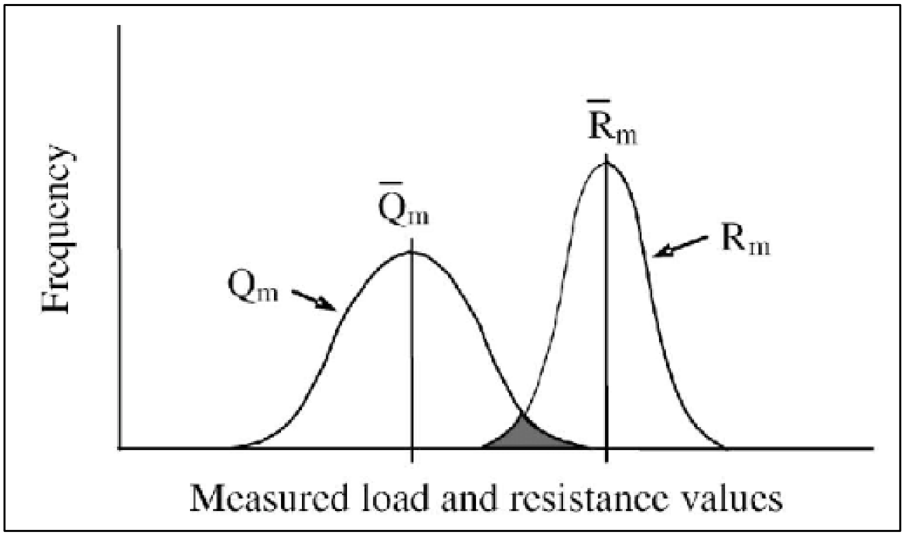


Figure 1: Frequency of Distribution Curves [6]

Ultimate limit states are checked by satisfying the equation that a resistance factor multiplied by the resistance of a structural element is greater than a load factor multiplied by the loading magnitude. The resistance factor is applied to the strength of a member to consider any strength uncertainness such as dimensions, material properties, and workmanship. The load factor is applied to the imposed loads on the structure, which accounts for the inconsistency of load magnitudes and how combined loadings are acting on the structure. [5]

## 1.2 Objective and Approach

The overall objective of this thesis is to determine a concise design approach through the application of theoretical equations to assess hollow structural sections (HSS) subject to torsion and combined loading for designs in Canada. The primary motivation for this research originated from the literature review, specifically from the gap analysis between CAN/CSA S16-19 – Design of Steel Structures [1] and ANSI/AISC 360-16 – Specification for Structural Steel Buildings [2]. Through the comparison of the codes and examining the principal design clauses, it was identified

ANSI/AISC 360-16 [2] provides mathematical equations for checking HSS in torsion and combined loading while CAN/CSA S16-19 [1] advises the user to complete an elastic analysis for verification. Although the method of completing a finite element analysis to determine the torsion or combined loading stress is a very effective and accurate design approach, having theoretical formulas following limit states design to analyze this condition as well could be a beneficial option to practicing engineers. Torsion is a fundamental stress state experienced in structural steel design [7], it is developed when a section is twisted about its geometric center. Torsion and combined loading are unique scenarios that are not typically present in building design but more common in structural systems such as pipe support designs where eccentric loads are present in multiple directions. HSS subject to torsion and combined loading are important loading scenarios that should be considered during the design phase of a structure if the loading behavior exists. An example of a pipe support column loaded in combined torsion, bending, and shear is shown in Figure 2.

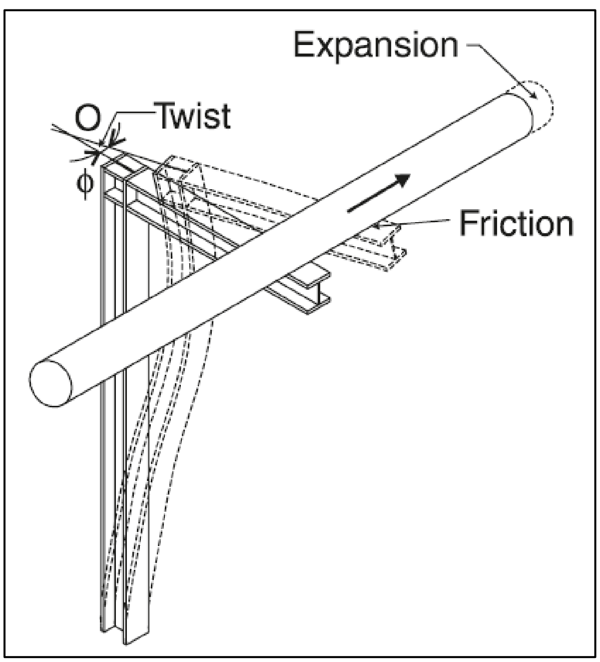


Figure 2: Column Subject to Combined Loading [7]

The clause identified in ANSI/AISC 360-16 [2] was Chapter H, Section H3 – Members Subject to Torsion and Combined Torsion, Shear, Flexure, and/or Axial Force. Specifically, the equations provided in parts 1 & 2 in clause H3 for HSS. To consider the use of this clause for HSS torsion design in Canada it was understood the reliability indexes between both codes needed to be examined to assess if the American code provides the same level of safety as the Canadian code. For further information on calibration between the Canadian and American code through reliability techniques refer to the companion study to this paper, "Reliability-Based Development of Torsional Strength Equations for the CSA S16 Standard" [8]. It was also identified for this clause to be a potential recommended method of torsion loading assessment, it would need to be verified through a detailed strength analysis. This thesis focuses on verification of the American torsional clause using FEA techniques with calculated section capacities from both the American and Canadian codes. The approach used in this thesis to verify the application of this clause is illustrated in Figure 3.

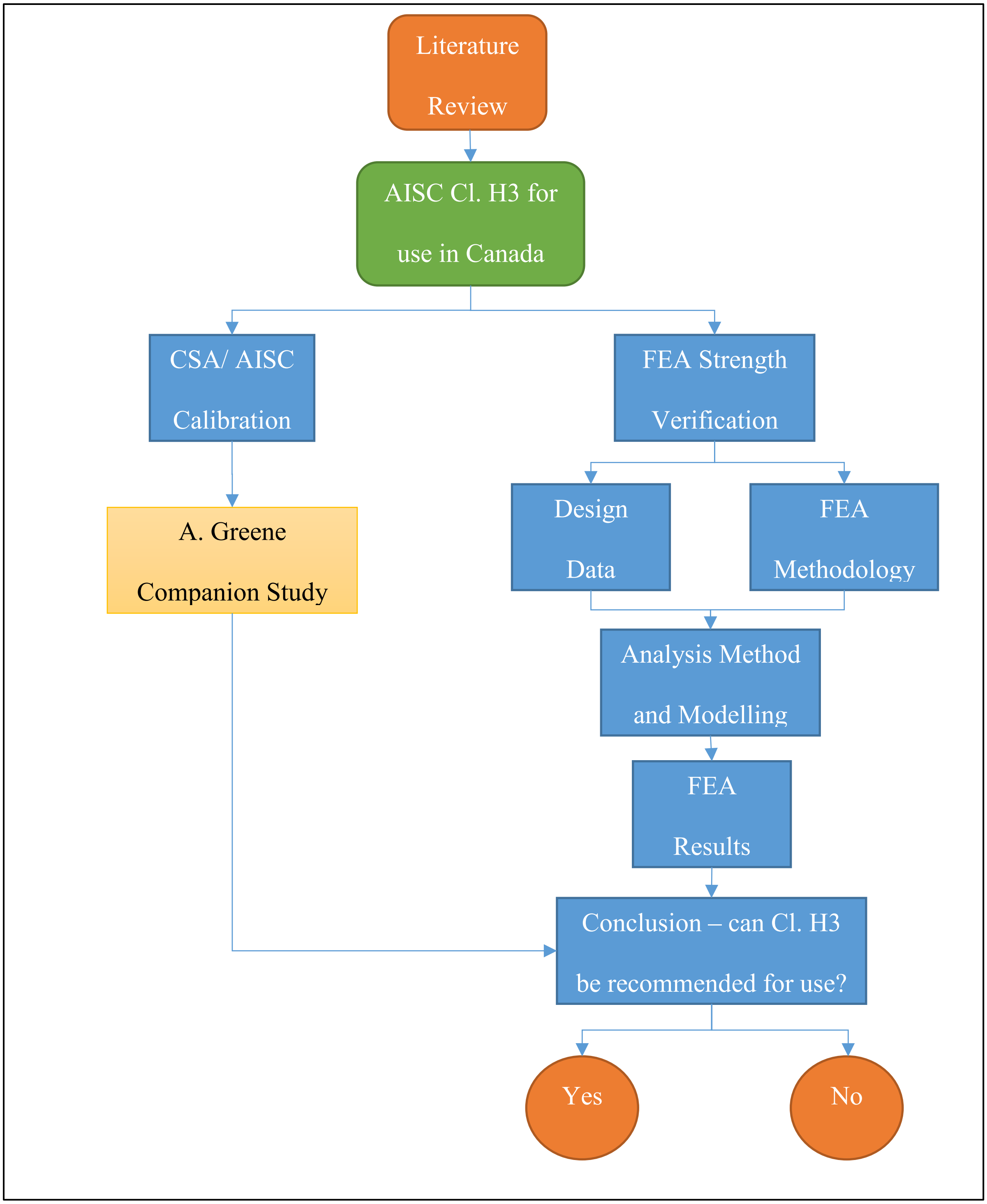


Figure 3: Objective of Thesis Flowchart

## 1.3 Outline of Thesis

This thesis begins with a literature review in Section 2.0 which discusses some research that has been previously completed comparing CAN/CSA S16-19 [1] and ANSI/AISC 360-16 [2] clauses, relevant past research using finite element analysis on steel members, finite element model validation and applicable research of steel beams loaded in torsion. Section 3.0 provides the detailed design data and principles that were used in the analysis. Section 4.0 documents the design loads and conditions which were used for all the FEA models. The results of the research are discussed in Section 5.0 and Section 6.0 documents conclusions that were determined from this study. Recommendations for future work are presented in section 7.0, outlining areas where additional research could be completed to advance this field of torsion verification work in HSS and other section types.

# Chapter 2 Literature Review

## 2.1 Comparison of Canadian and American Codes

This chapter highlights some of the relevant research of comparisons between the Canadian and American codes. It is well understood that developed countries such as Canada and the United States have internationally recognized established steel design standards for practicing engineers. Galambos [9] completed a comparison of the Canadian, Mexican, and United States steel design standards concentrating on stability design of plates, columns, beams, and beam-columns. It is stated in the paper, while the academic and experimental foundation for the three codes is similar, the details of assessment principles are not equivalent. Clauses for columns, beams, and beam-column design have different formulas. Even though the formulas for design resistances are different, Galambos [9] determines the outcome of the section sizes that are adequate for certain loads are not very different. It was concluded that the primary concepts and experimental background for the three steel codes are essentially identical [9]. Most of the criteria for strength checks in the codes are either the same or very similar but it is noted there are some functional differences in the codes. Galambos concludes there is no main issue to fundamentally exchange the design standards between Canada, Mexico, and the United States [9]. For example, a plot of the design column strength is shown in Figure 4 which presents the slenderness ratio on the x-axis vs the critical load multiplied by the material resistance factor for each code. The variables used in Figure 4 are defined as $\phi$ = resistance factor, $P_{cr}/P_y$ = critical buckling load, and $\lambda_c$ = slenderness ratio. It is noted by Galambos the applicable curves for the majority of column sizes from each code are nearly corresponding. Although differences between the three North American design codes for steel buildings do exist, the result of these differences is not significant enough to affect the safety of the public or the economy [9]. Galambos did not specifically compare the torsion of steel sections in his study between the three codes.

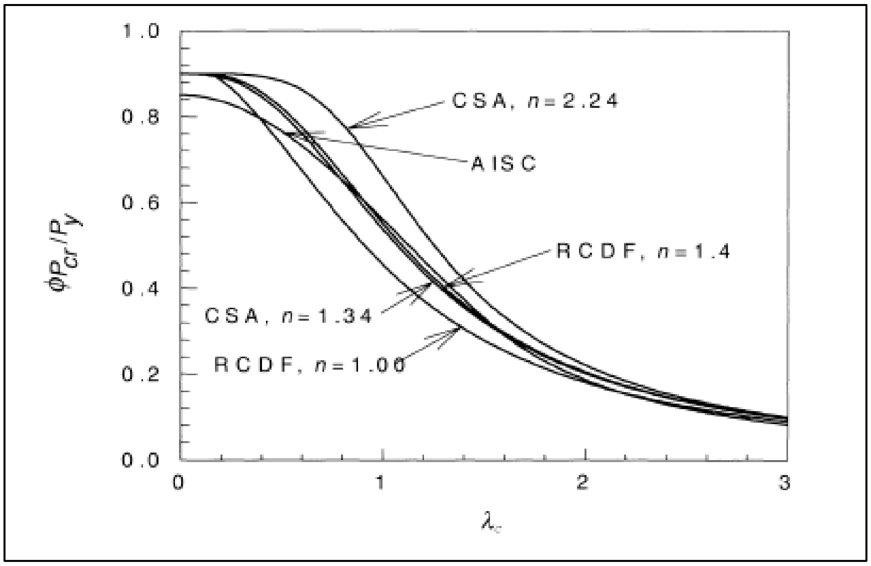


Figure 4: Design Column Strength [9]

A study was performed by Liu et al. [10] that investigates slenderness ratios of built-up compression members used in AISC-ASD [11], AISC-LRFD [12], AS-4100 [13], and CSA S16-01 [14]. Liu et al. [10] did not compare beams loaded in torsion but focused on compression elements between the different codes. Slenderness ratios and compressive strength for various sections were calculated in accordance with each code. For the Canadian code parameters, an effective length factor of 1.0 was used for snug tight bolted built-up members and 0.65 was used for members connected with welds or pre-tensioned bolts. It was concluded from this study for back-to-back snug tight bolted members, such as angles or channels, the calculated compressive resistance using the slenderness ratios from AISC-LRFD [15] and CSA S16-01 [14] were essentially the same [10]. The results from this research also showed the codes are very similar providing equal capacities for the same section in compression.

A paper was written by Rhodes et al. [16] comparing the differences in steel bridge member resistances in AASHTO LRFD 8th edition [17], Eurocode EN1993-2 [18], and CSA S16-14 [19] under identical loadings. AASHTO provides steel bridge design specifications in the United States which are in line with AISC specifications. AASHTO also adopts some clauses from the AISC steel code for the design of certain elements. Rhodes et al. [16] completed assessments of members in tension, compression, bending, shear, and, utilization ratios in an FEA model of a steel truss footbridge. Certain differences in the codes and design approach were noted, but when the results were compared it was determined all three codes provided equivalent outcomes. Easterling et al. [20] performed a similar study comparing AISC [21], CSA [22], and Eurocode [23] focused on the strength of shear studs in steel deck on composite beams and joints. They noted the bolt resistance factors and calculated shear strengths differ between the three codes. The authors partially attributed these differences to the uncertainty that existed at the time the codes were developed in the shear strength of bolts. The calculated shear strength of bolts in a composite deck without resistance factors are shown in Figure 5 and with resistance factors in Figure 6. The variables used in Figure 5 and Figure 6 are defined as $f_c$' = specified compressive strength of concrete, $Q_n$ = nominal shear strength of a stud, and $\phi$ = resistance factor.

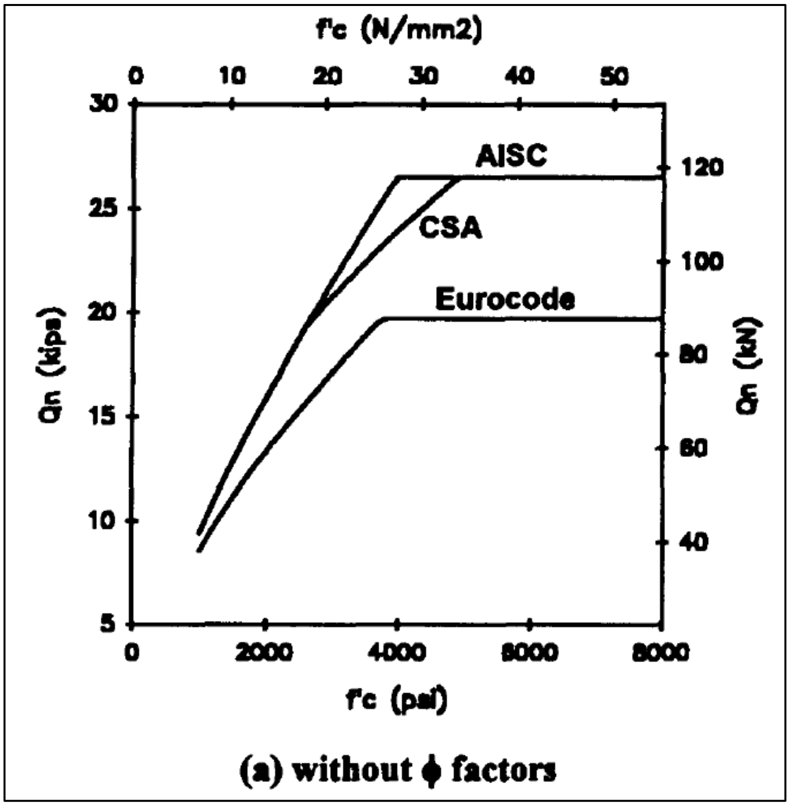

Figure 5: Shear Strength of Bolts without Resistance Factors [20]

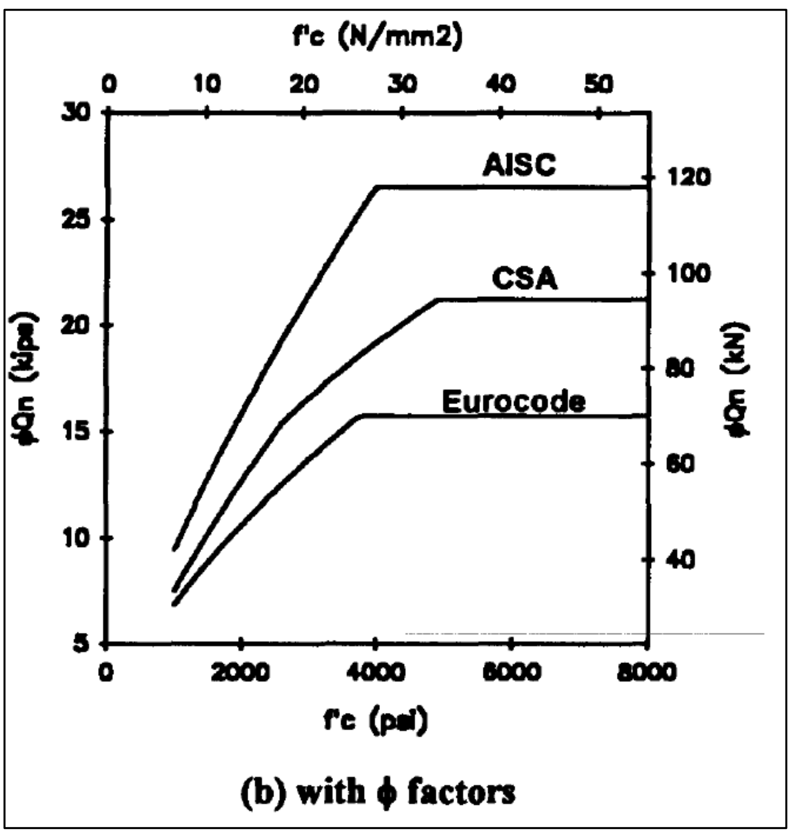

Figure 6: Shear Strength of Bolts with Resistance Factors [20]

Kabir [24] completed research on lateral-torsional buckling of welded wide flange beams, where he evaluated the consequence of welding residual stress on the beam capacity before failure. Kabir stated that the different steel design codes such as CSA S16-14 [25], AISC 360-10 [26], AS 4100 [13], and Eurocode 3 [27] all have different formulas to determine lateral-torsional buckling resistance but generally the methodology is similar. He also explains that in both North American codes CSA S16-14 [25] and AISC 360-10 [26] the calculated capacity of rolled and welded beams is the same therefore using the same strength curves, whereas Eurocode 3 [27] provides two separate curves. Similar research was conducted by Eamon et al. [28] focused on the effect of moment gradient and load height on wide flange steel beams subject to lateral-torsional buckling. The authors explain in this paper some of the international codes such as Eurocode 3 [27], Australian Standard AS-4100 [13], CSA S16-14 [25], and AISC 360-10 [26] include the effects of moment gradient in calculating beam lateral-torsional buckling loading. They further indicate while the European, Australian, and Canadian standards include corrections for load application height, the American standard does not have adjustments built in the equations and refers the user to the commentary for guidance. In this paper Eamon et al. [28] concentrate on the AISC code and how it deals with lateral-torsional buckling resistance under specific loading.

Kabir and Bhowmick [29] completed related research on the effect geometric imperfections have on the lateral-torsion buckling capacity of I-beams. Using ABAQUS they performed nonlinear FEA of 30 different laterally unsupported I-beams with various geometric imperfections. The authors compared how CSA S16-14 [25], AISC 360-10 [26], AS 4100 [13], and Eurocode 3 [27] standards follow different strength curves to determine the lateral-torsional buckling capacity of unbraced I-beams. The authors explain CSA S16-14 [25] doesn’t offer different strength curves for welded and rolled sections like Eurocode 3 [27] and it also does not specify an out-of-tolerance limit for initial straightness for determining lateral-torsional buckling capacity. Kabir and Bhowmick [29] determined from the FE analysis results that the extent of geometric deficiencies has a significant impact on the moment capacity of the sections. They concluded a direct relationship can be made between the initial beam out of straightness and the moment-resisting capacity. In a recent study, Manarin [30] performed similar research on lateral-torsional buckling but on T-shape beams while comparing methodologies for determining capacities in CSA S16-14 [25], AISC 360-16 [2], and Eurocode 3 [27]. The author provided a detailed assessment of clauses used to determined lateral-torsional buckling capacities in each code. He highlights that while the CSA and AISC standards provide equivalent moment gradient factors for W shapes that are singly or doubly symmetrical, they do not include a moment gradient factor for calculating lateral-torsional buckling resistance of T-shapes. He notes currently there isn't considerable literature available on lateral-torsional buckling of tees for both elastic and plastic regions. The scope of the research included using ABAQUS for FEA of eighteen T sections cut from common rolled wide-flange sections with varying flange and web dimensions. The FE model was utilized to study the lateral-torsional behavior of the T-shapes under three loading scenarios. The separate load cases were applying a uniform distributed load, a point load, and a moment with all models having simply supported boundary conditions, therefore allowing the T section beams to resist all induced moments. From the model results, Manarin [30] recommended the existing CSA S16-14 [25] moment gradient factor for singly and doubly symmetric W sections be used for tee shapes loaded with the flange in compression for the above-mentioned load cases. He also proposed revisions to be made to CSA to contain the moment gradient factor recommended by Wong and Driver [31]. Another interesting comparison between the codes he provided was "CSA S16 underestimates the inelastic LTB moment and AISC 360 underestimates both the cross-sectional capacity—when the limit of $1.6 \cdot M_y$ is included since this factor is meant to address the serviceability of the beam and not the ultimate limit state—and the inelastic LTB moment. The underestimation of the inelastic LTB moment in both standards is due to a combination of the moment gradient factor being neglected and the assumption that the inelastic LTB curve is linear." [30]. For this study, the variable $M_y$ is defined as the yield section moment.

The above four studies focused on lateral-torsional buckling of beams, where complex research was completed and experimentally justified conclusions are drawn. The studies contained very beneficial and thorough information but did not explore HSS torsion or combined loading.

In a recent study, Leblouba and Tabsh [32] indicated the current North American design standards do not take into account the shear design of corrugated web steel beams, as the codes were developed for the design of welded plate girders. They explained in the paper the existing resistance factors in AISC 360-16 [2] and CSA S16-14 [25] were established for welded girders. Therefore, applying these resistance factors to corrugated web steel beams could potentially lead to member resistances with a lower factor of safety that is outside of the LRFD methodology. Leblouba and Tabsh [32] noted for the full incorporation of the shear design of corrugated web steel beams into the codes, specific resistance factors need to be determined through reliability-based methods and calibrated to be in line with the codes LRFD philosophy. The authors performed various reliability analyses on previous experimental beam shear data and verified the experimental results using non-linear finite element analyses. These reliability analyses were used to determine the target reliability for both AISC and CSA codes. They then looked at the dead, live, wind, and snow loads for AISC 360-16 [2] and CSA S16-14 [25] utilizing probability methods to calibrate the resistance factors for corrugated web steel beam shear design. Leblouba and Tabsh [32] concluded that when the existing AISC resistance factor is used for corrugated web beam shear design it produces a safety factor outside of code target reliability, therefore a factor of 0.85 is recommended. Further to this for CSA, the authors determined the current resistance factor of 0.9 is applicable for the shear design of corrugated web steel beams. The authors researched the shear design of corrugated web steel beams specifically in accordance with AISC and CSA code philosophies determining applicable steel resistance factors which are shown to be similar.

Kiymaz and Seckin [33] examined the strength and design of slotted and gusset plate welded tubular member connections for stainless steel. The authors explained there is currently no literature in the stainless-steel international specifications which cover the design of slotted tubular-gusset connections, which is a common connection used in steel design. This type of connection could be used to frame into a common node with other steel members or when a full capacity tubular connection isn't required. Slotted tubular-gusset connections are frequently used for bracing, where the member loads are typically tension and compression, and also to simplify the connection welding from a tubular full penetration weld to longitudinal fillet welds on the gusset plate to tubular. Typical slotted tubular-gusset plate connections for a square HSS and round HSS are shown in Figure 7. Kiymaz and Seckin [33] experimentally tested 24 square and round beams with slotted tubular-gusset connections under tension load to develop load-deformation curves. The authors then compared the experimental results to the available design rules for carbon steel following the American AISC 360-05 [15], Canadian CSA S16-01 [14], and European EN1993 [27]. They provide a detailed description comparing the methods between the three codes for calculating the connection resistance including shear lag and weld capacities. It is concluded from the comparison of the experimental resistances to the calculated resistances that CSA clauses are the most applicable and provide the safest design parameters for slotted tubular-gusset plate stainless steel connections. This study was limited to the scope of slotted tubular-gusset plate connections using the above steel codes and the authors did not research torsion loading for the connections.

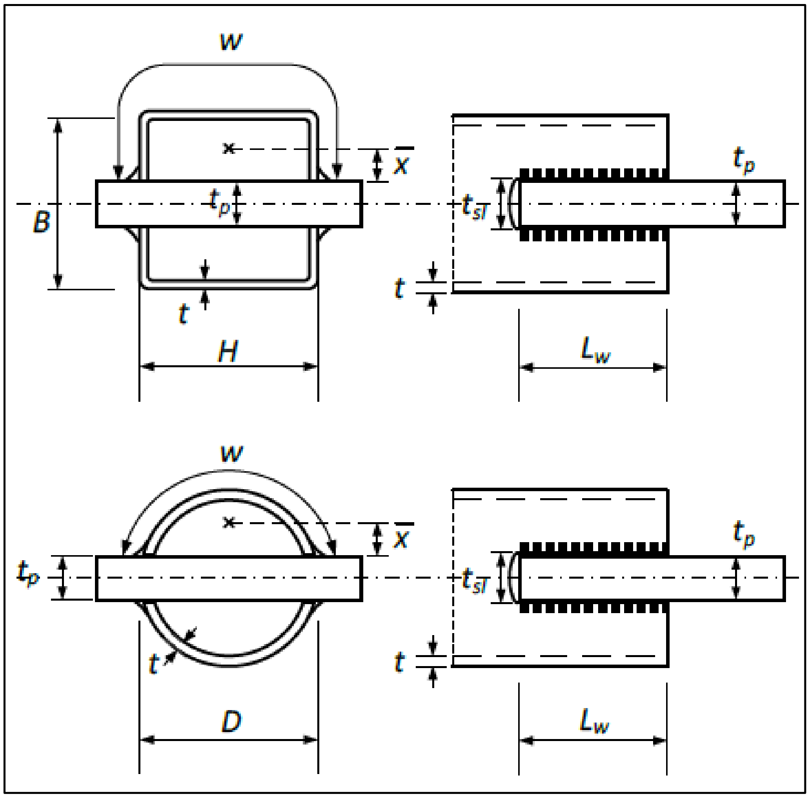

Figure 7: Slotted tubular-gusset plate connections [33]

Willibald et al. [34] completed related research studying the behavior of gusset plates welded to the ends of round and elliptical hollow structural members. The scope of the research was to experimentally study the behavior of 13 plate to round or elliptical HSS connections under tension and compression loadings. The authors included a detailed comparison of clauses to calculate shear lag reductions and block shear strength between the AISC 360-05 [15], CSA S16-01 [14], and Eurocode 3 [27] noting the resemblances. They concluded from comparing the experimental results to the calculated resistances, the equations found in CSA and AISC for determining shear block failure are almost identical and suitable. This study was limited to gusset plate end connection to HSS in tension/ compression and did not include any torsional loading.

The research was conducted by Guravich and Dawe [35] on simple beam connections that are loaded in combined shear and tension. The authors of this study realized there is no design guidance in CSA S16-01 [14] or AISC 360-01 [36] on simple beam connections subject to simultaneous shear and tension. There are clauses that cover bolts and welds in combined shear and tension in both standards, but they do not include the additional connection components. The experimental work performed included various specimens of four typically used shear connections which were loaded in combined shear and tension using the CSA S16-01 [14] factored shear capacity of the welds or bolts. The different shear connections that were experimentally tested are shown in Figure 8, which were two different double angle connections, a single angle connection, and a shear tab connection. It was noted from the test results that the strength of the connection components was provided from shear yielding of the angles or shear tab, bending of the angles, or yielding through bearing at the bolt holes in the angles or shear tabs. The experimental results indicated simple beam connections that are loaded to their factored shear capacity can resist substantial tension load. The authors noted the behavior of a simple connection under combined shear and tension is complicated and aspects such as plastic deformation of the angles/ tabs, prying effects between components, bolt pretension tolerances, and slippage of bolts make them problematic to test systematically. Guravich and Dawe [35] also provide recommended clauses between both CSA S16-01 [14] and AISC 360-01 [36] for designing certain connection components that are loaded in combined shear and tension.

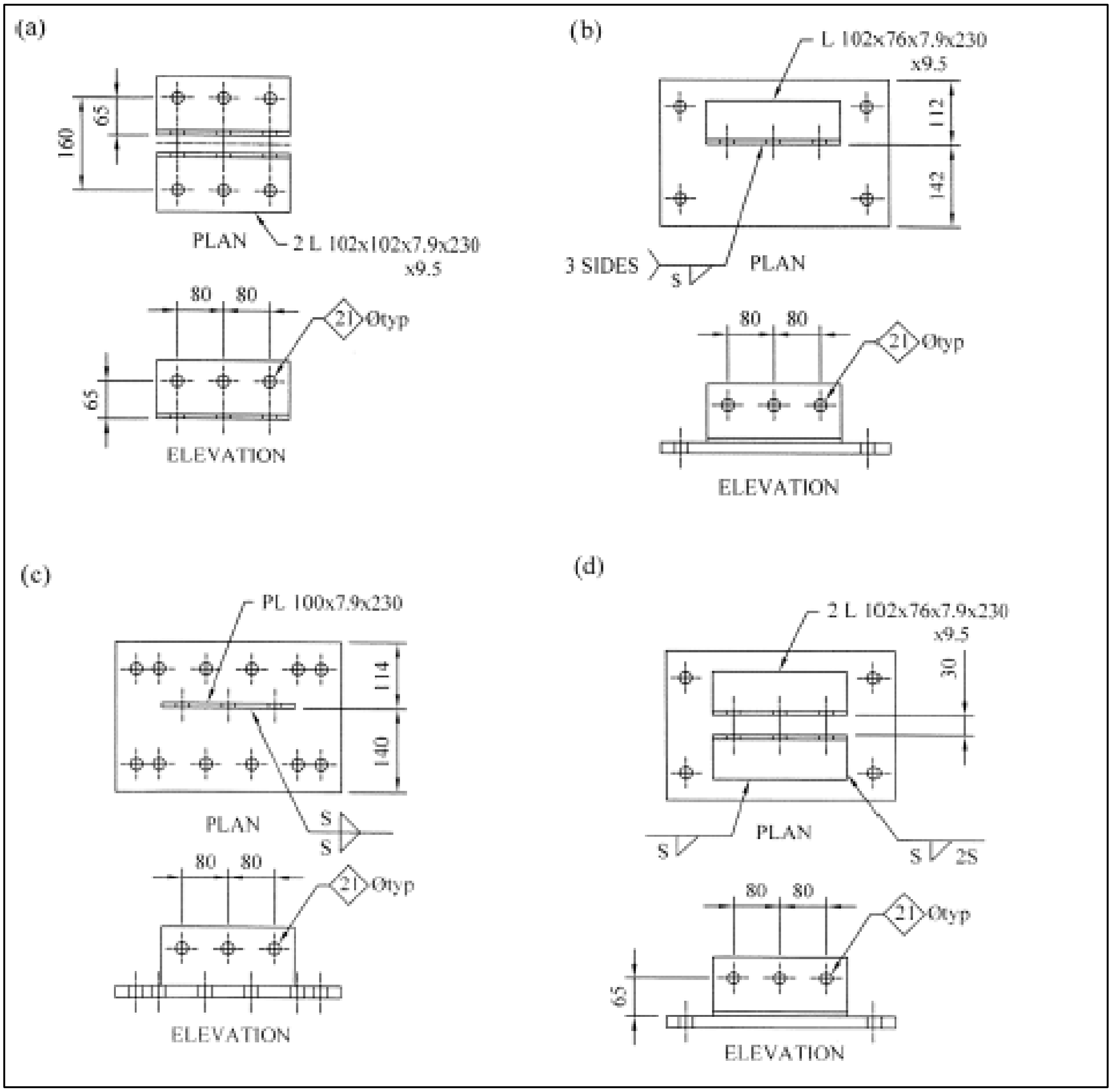


Figure 8: Tested Shear Connections [35]

Carril et al. [37] completed a similar study on tensile and bearing capacities of bolted connections. The scope of the research was to experimentally test seventy-five bolted connections observing the behavior of bearing capacity, tension capacity, and combined bearing and tension capacity. The authors completed a comprehensive review of applicable standards including AISC and Canadian specifications documenting clauses utilized for calculating resistances. The extend of this research was to examine the capacities of the bolted connections and compare them to the calculated values.

Shaback [38] studied the behavior of square HSS braces that were subject to reverse cyclic axial loading. Experiments were completed on various specimens and the results were compared to CSA S16 [39] compression capacities. It was noted by Shaback [38] the key input parameters for the experiments were the end support conditions, width to thickness ratios, and slenderness ratios of the braces. Throughout the research, the author compared the experimentally obtained initial buckling loads to the calculated capacities of CSA S16.1-94 [39] and AISC [40]. A comparison of the CSA and AISC buckling formulae is shown in Figure 9, with the ordinate representing the critical buckling stress and the abscissa representing the slenderness ratio.

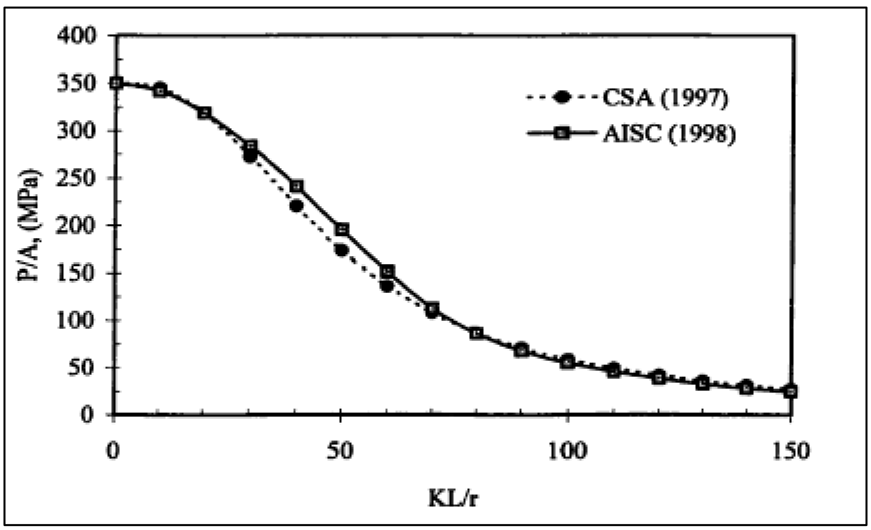


Figure 9: Comparison of CSA and AISC Buckling Formulae [38]

From the graphical representation of the buckling formulae, it can be seen that both codes provide very similar results at different slenderness ratios. Comparison of the experimental and calculated initial buckling loads are shown in Table 2-1, which confirms CSA S16.1-94 [39] provides slightly more conservative compression capacities. This research was focused on the compression capacity of axially loaded HSS braces and did not include any torsional loading.

| Specimen | KL/r | Initial Buckling Loads | | | $P_{exp.}/P_{theo.}$ | |
|---|---|---|---|---|---|---|
| | | CSA (1997) (kN) | AISC (1998) (KN) | Experimental (kN) | CSA (1997) | AISC (1998) |
| 1A | 52.3 | 977 | 1038 | 904 | 0.92 | 0.87 |
| 1B | 53.9 | 1126 | 1200 | 1156 | 1.03 | 0.96 |
| 2A | 53.3 | 1378 | 1453 | 1507 | 1.09 | 1.04 |
| 2B | 52.4 | 1621 | 1709 | 1721 | 1.06 | 0.96 |
| 3A | 64.8 | 813 | 897 | 864 | 1.06 | 0.96 |
| 3B | 65.8 | 924 | 1016 | 927 | 1.00 | 0.91 |
| 3C | 61.6 | 1241 | 1353 | 1011 | 0.82 | 0.75 |
| 4A | 63.5 | 1232 | 1346 | 1381 | 1.12 | 1.03 |
| 4B | 59.7 | 1510 | 1636 | 1435 | 0.95 | 0.88 |

Table 2-1: Comparison of Initial Buckling Loads [38]

## 2.2 CSA S16, AISC 360 and Eurocode 3 HSS Beam Torsion Design

As stated in Section 1.2 above, a detailed gap analysis was completed between CAN S16-19 [1] and AISC 360-16 [2] which resulted in the incentive to research HSS torsion design and how it is evaluated in Canada. Further to this, three international standards CAN S16-19 [1], AISC 360-16 [2], and Eurocode 3 [27] were compared on the basis of HSS beam torsion design. As earlier discussed, CAN S16-19 [1] does not provide theoretical equations to analyze HSS sections that are subject to torsion loads but recommends an elastic analysis for assessment. The Canadian code includes explanations in clause 14.10 – Torsion in four sections with user recommendations on how to assess beams loaded in torsion. Clause 14.10.4 provides the following statement, "For members subject to torsion or to combined flexure and torsion, the maximum combined normal stress, as determined by an elastic analysis, arising from warping torsion and bending due to the specified loads shall not exceed $F_y$." [1]. In CAN S16-19 [1] the variable $F_y$ is defined as the specified minimum yield stress, yield point or yield strength. The Canadian code commentary provides more information on torsion, referring the user to the Driver & Kennedy [41] moment-torque interaction diagrams for I-beams, for in-elastic torsion I-beam design to Pi & Trahair [42], and for elastic design methods to Seaburg & Carter [43] and Brockenbrough & Johnson [44]. Lastly, the commentary refers the user to Englekirk [45] for methodology on I-beams and analyzing the angle of rotation under torsion load.

When comparing AISC 360-16 [2] to the Canadian code, it offers simple formulas to determine the resistance of HSS sections in torsion and combined loading. Specifically, under clause H3-1: Round and Rectangular HSS Subject to Torsion and clause H3-2: HSS Subject to Combined Torsion, Shear, Flexure and Axial Force [2]. Refer to Appendix A for the full description of clauses H3-1 and H3-2. Outside of HSS for open sections such as I-beams, channels and angles the recommendation is similar to the Canadian code where a separate stress analysis is required. The American code also references work completed by Seaburg & Carter [43] for torsional analysis which is the published steel design guide – Torsion Analysis of Structural Steel Members.

Eurocode 3 [27] provides guidance in clause 6.2.7 - Torsion on how to check I-beams, channels, and HSS sections in torsion. Eurocode 3 [27] clause 6.2.7 – Torsion, parts (1) and (2) are shown in Table 2-2 below. In part (5) of this clause it is generally stated for an elastic check of the section, equation 6.1 can be applied, which is similar to the direction offered in the Canadian code. Equation 6.1 from Eurocode 3 [27] clause 6.2.1 – General, for performing elastic analysis is shown in Table 2-2.

| **Eurocode 3 Clause** [27] | **Torsion Design Guidance** |
|---|---|
| Clause 6.2.7 – Torsion, Parts (1) & (2) | (1) For members subject to torsion for which distortional deformations maybe disregarded the design value of the torsional moment $T_{Ed}$ at each cross-section should satisfy: $$\frac{T_{Ed}}{T_{Rd}} \leq 1.0$$ Where $T_{Rd}$ is the design torsional resistance of the cross section. (2) The total torsional moment $T_{Ed}$ at any cross-section should be considered as the sum of two internal effects: $$T_{Ed} = T_{t,Ed} + T_{w,Ed}$$ Where: $T_{Rd}$ is the design torsional resistance of the cross section. $T_{t,Ed}$ is the design value of the internal St. Venant torsion moment. $T_{w,Ed}$ is the design value of the internal warping torsional moment. |
| Clause 6.2.1 – General, Part (5) | (5) For the elastic verification the following yield criterion for a critical point of the cross section may be used unless other interaction formulae apply, see 6.2.8 to 6.2.10. $$\left(\frac{\sigma_{x,Ed}}{f_y/\gamma_{M0}}\right)^2 + \left(\frac{\sigma_{z,Ed}}{f_y/\gamma_{M0}}\right)^2 - \left(\frac{\sigma_{x,Ed}}{f_y/\gamma_{M0}}\right)\left(\frac{\sigma_{z,Ed}}{f_y/\gamma_{M0}}\right) + 3\left(\frac{\tau_{Ed}}{f_y/\gamma_{M0}}\right)^2 \leq 1.0$$ Where: $\sigma_{x,Ed}$ is the design value of the longitudinal stress at the point of consideration. $\sigma_{z,Ed}$ is the design value of the transverse stress at the point of consideration. $\tau_{Ed}$ is the design value of the shear stress at the point of consideration. $f_y$ is the yield strength. $\gamma_{M0}$ is the partial factor for resistance of cross-sections whatever the class is. |

Table 2-2: Eurocode 3 Torsion Design Guidance [27]

## 2.3 FEA Model Results Compared to Experimental Results

This section of the literature review documents research that particularly demonstrates how accurate FEA model results can be when compared to experimental. Mashaly et al. [46] completed a research study where they created a finite element analysis of a beam-to-column joint to compare the results to experimental cases. The complex extended-end-plate beam-to-column connection was selected and modeled with shell elements in ANSYS software which is shown in Figure 10. Symmetry was used to reduce the model geometric size and node-to-node contact elements CONTAC52 were used between bodies. Two load cases were analyzed to study the joint's non-linear behavior, the first was a simple lateral load, and the second a cyclically lateral load was applied. Both the load cases and joint geometry were identical to experimental tests which were chosen in the literature.

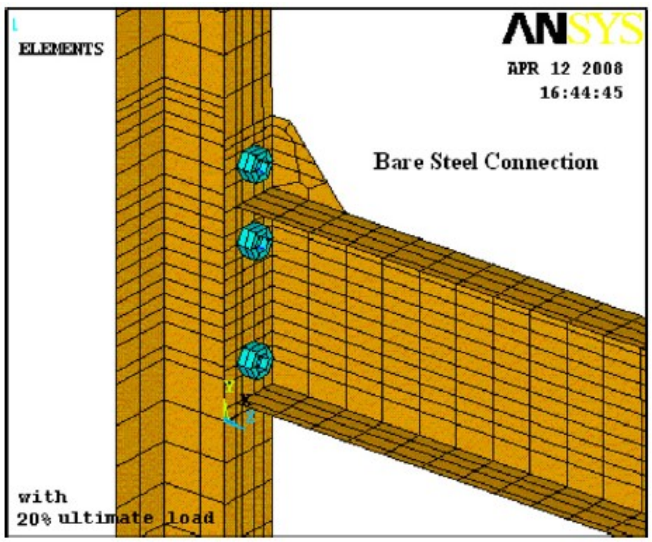

Figure 10: Studied Beam-to-Column Joint Connection [46]

When the finite element results were compared to the experimental results, it was determined they were very similar at different stages of the loading within 4.9% [46]. The plot of experimental results for plastic rotation and moment at the column centerline are shown in Figure 11. The plot of FE results for plastic rotation and moment at the column centerline are shown in Figure 12. Their research displayed that when finite element modeling techniques are properly applied, these models can [46] be used to predict the actual behavior of steel sections.

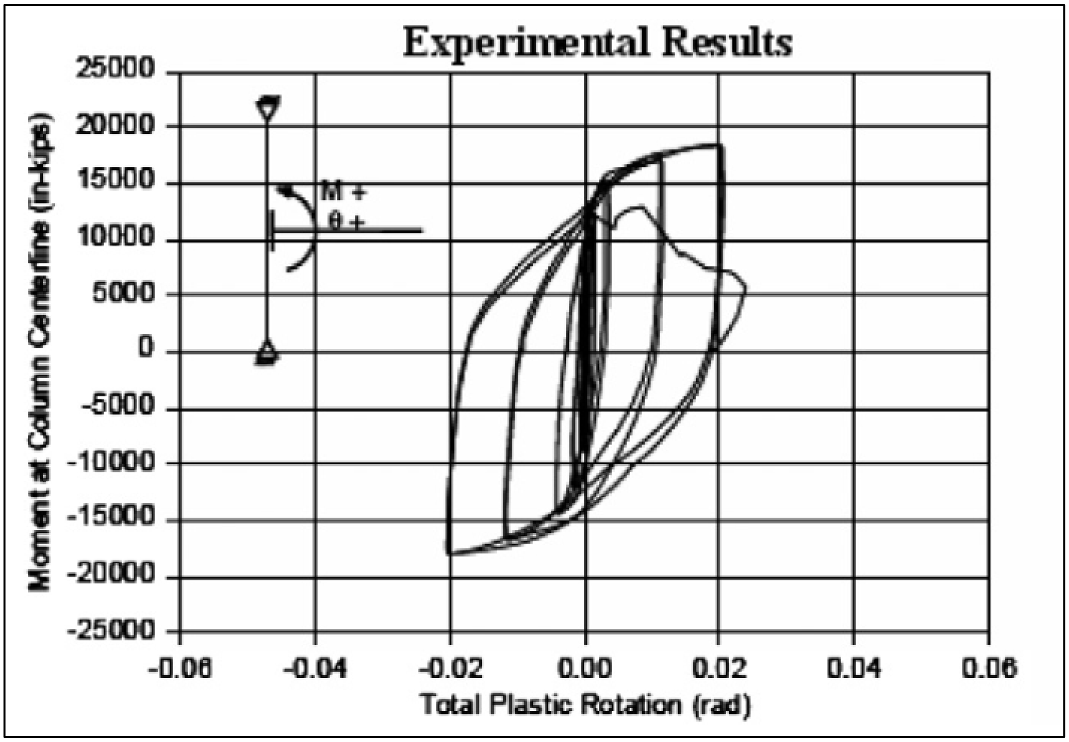


Figure 11: Plot of Experimental Results - Plastic Rotation and Moment at Column Centerline [46]

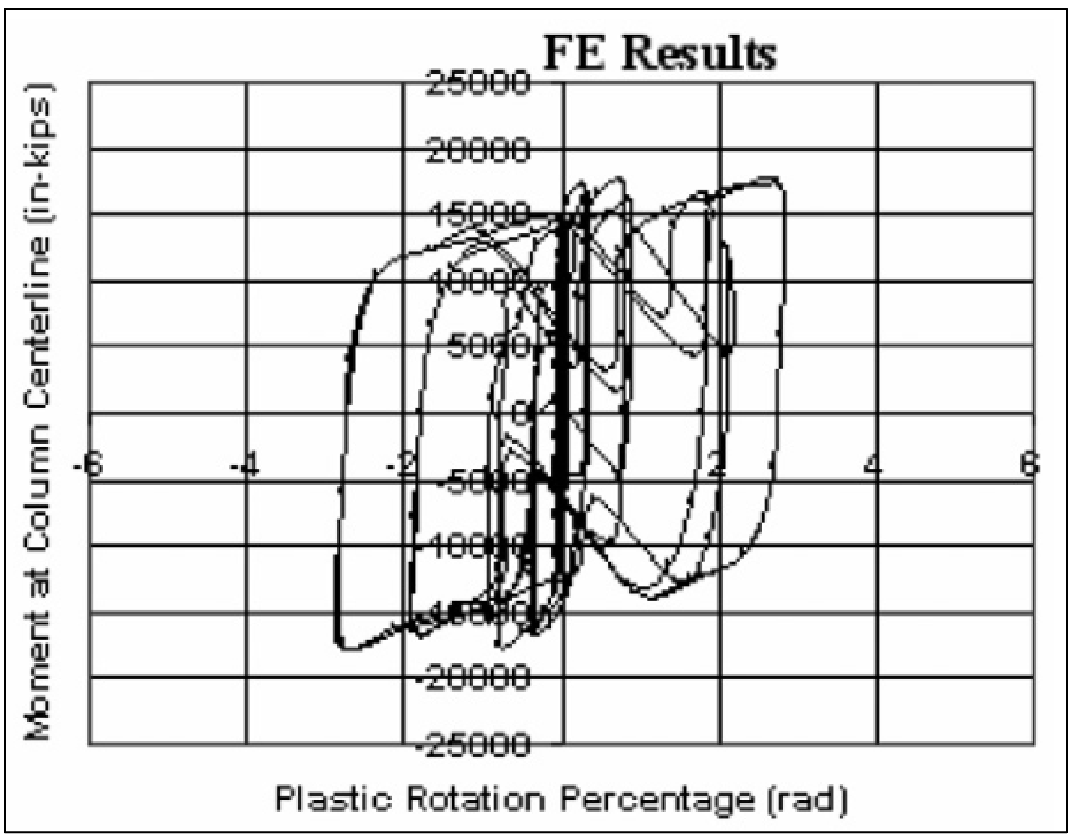


Figure 12: Plot of FE Results - Plastic Rotation and Moment at Column Centerline [46]

Laurendeau [47] completed research on live load testing and finite element analysis of a steel cantilevered Pratt truss bridge. Laurendeau [47] attached strain gauges on a truss bridge and recorded its behavior under live load conditions. Then he modeled the bridge in a finite element model using SAP2000 and applied the same loads for comparison to the experimental results. It was concluded once the FE model was calibrated, the strain values obtained were very comparable to the experimental values for every load path [47]. For some of the beams, the FE predictions and the actual data were within 2.0% [47]. For example, one of the beam strain cross-section comparisons is shown in Figure 13. It is presented in the plot how similar the experimentally recorded stains were compared with the FE model strains.

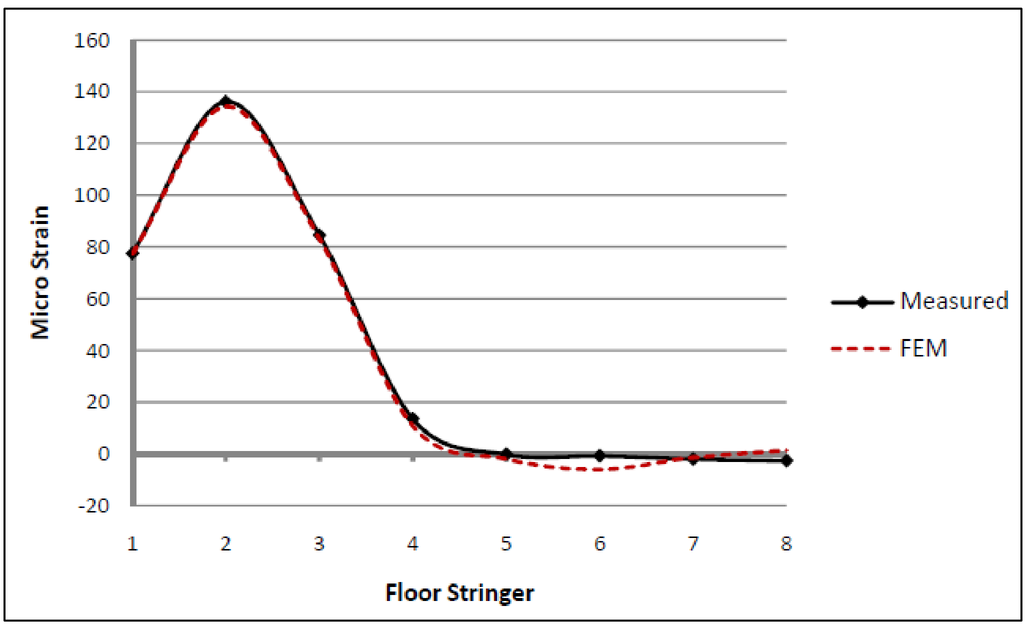


Figure 13: Beam Strain Cross-Section Comparison [47]

Zhao et al. [48] performed a study that utilized parametric FEA on slotted rectangular and square HSS subject to tension loads. The FE models were validated by direct comparison to extensive test data to ensure the output results were accurate. For this research, the equivalent plastic strain was utilized for the rupture limit of the material, which was also used in FEA studies of slotted round HSS by Cheng et al. [49] and Martinez-Saucedo et al. [50]. This is the same approach adopted for the analysis in this thesis, using the equivalent plastic strain as the basis of evaluation. The authors compared the FEA results to the calculated connection resistance values in accordance with CSA S16-01 [14] and AISC 360-05 [15] along with providing recommendations for code improvements.

## 2.4 Steel Beams Loaded in Torsion

This section of the literature review details some past research and studies that were completed specifically on steel beams loaded in torsion. To date, there has been significant research completed for steel beams loaded in torsion and combined loading that has been documented in steel design guide books. Two primary design guides have been published in line with commonly used standards, one in accordance with AISC 360 by Seaburg & Carter [43] and one in accordance with Eurocode 3 by Hughes et al. [51]. Both references are complete design guides that offer equations to check all section types for torsion and combined loading. The scope of this thesis is focused on HSS sections, therefore the initial formulas for calculating torsional shear stress from both design guides are presented in Table 2-3 for high-level comparison. Another well-known steel design guideline was written by Blodgett [52] which offers formulas to evaluate beam torsion, which has also been included in the table. The referenced documents need to be referred to for full methods of torsional analysis.

| Researcher | HSS Torsion Equations |
|---|---|
| [43] | Shear stress equation: (note this equation varies depending on HSS section)<br>$$\tau_t = \frac{T}{2tA_o}$$<br>$$T = GJ\theta' - EC_w\theta'''$$<br>Where:<br>$A_o$ = area enclosed by shape, measured to centerline of thickness of bounding elements, in$^2$.<br>$t_t$ = thickness of bounding element, in.<br>$T$ = torque<br>$G$ = shear modulus of elasticity of steel, 11,200 ksi.<br>J = torsional constant of cross-section, in$^4$.<br>E = modulus of elasticity of steel, 29,000 ksi.<br>$C_w$ = warping constant of cross-section, in$^6$. |
| [51] | Shear stress equation:<br>$$\tau = Gt\emptyset'$$<br>$$\emptyset' = \frac{T}{GI_T}$$<br>Where:<br>$t$ = $t_f$ or $t_w$ as appropriate<br>T = applied torque<br>G = shear modulus<br>$I_T$ = St Venant torsional constant |
| [52] | Shear stress equation:<br>$$\tau = \frac{T * c}{J}$$<br>Where,<br>T = Torque<br>c = distance from centre of the section to outer fibre<br>J = polar moment of inertia of section |

Table 2-3: Design Guide Torsion Shear Stress Equations

De’nan et al. [53] performed research focusing on the torsional resistance of an I-beam with cut-outs in the web of different shapes and sizes. The geometries were modeled in the finite element software LUSUS and the torsion behavior was analyzed to compare to the results of the I-beam with no web cut-out. The authors determined that the angle of rotation of a beam without the cut-out is lower compared to a beam with any type of cut-out, but noted the difference was small [53]. This indicated that an I-beam loaded in torsion with a web cut-out would be suitable in many design cases to reduce costs [53]. De’nan et al. [53] concluded the optimal size for a web cut-out of an I-beam is an opening size half the depth of the section as the results from these models were essentially identical to the beam without a cut out. It was concluded from this study that an I-beam with a cut out of optimal size can have close torsional resistance to an I-beam without a cut out [53].

Another study was performed by De’nan et al. [54] on finite element analysis of an angled web profile beam loaded in torsion compared to a standard I-beam. Various models were created for the angular web beam and the standard I-beam varying in length, web thickness, depth, and width. Comparing the results of the angular web models and the standard web models, it was concluded the angular web models had a higher torsional resistance due to the angle of the web increasing the torsional constant of the section [54]. It was also observed the angle of twist of the angled web section was decreased as well [54].

Nandhakumar et al. [55] completed a recent study focused on cold-formed steel sections and their resistance to torsion loads. The main objective of the research was to determine if lighter cold-formed beams of specific shapes could potentially replace heavier sections in a structure, as cold-formed sections are typically thinner members made from cold working sheets. The authors concentrated on analyzing cold-formed sections of Z-shapes in FEA ABAQUS models. The models were cantilever sections fixed at one end with the applied torsion load at the opposite end. Nandhakumar et al. [55] studied the behavior of the z shapes under torsion looking at the stress patterns and what changes increase the rotational stiffness.

Lin and Trahair [56] investigated the nonlinear behavior of steel I-beams subject to combined flexure and torsion, due to the lack of guidance available at the time for members under this loading condition. Three different support conditions were analyzed for combined bending and torsion using FEA. The varying boundary conditions studied were continuously braced, centrally braced, and unbraced beams. The authors stated in the case of a continuously braced beam that prevents flexure torsional buckling, torsional buckling can still happen. They further explained, "torsional buckling effects may increase the interaction between in-plane bending and torsion, and reduce the strength of a beam, even when flexural torsional buckling is prevented." [56]. Using the nonlinear FEA modeling results and the load-deformation behavior observed, the authors proposed design equations to represent bending and torsion, flexural-torsional buckling, and destabilizing torsion. It was noted models that produced the highest flexure and torque at midspan of the beam were directly associated with the slenderness ratio, lateral bracing arrangement utilized and percentage of torque and moment applied [56].

Similar research was completed by Estabrooks [57] on combined bending and torsion of steel I-beams. In this study, he experimentally tested six different simply supported I-beams under combined bending and torsion loads. In addition, the author developed FEA models which were used to simulate the behavior of the simply support I-beam subject to bending and torsion. From the results, Estabrooks [57] concluded current interaction equations for combined bending and torsion may not be conservative enough for high moment to torque ratios. It is noted in the paper, Driver & Kennedy [41] preformed research on I-beams loaded in combined bending and torsion from which they proposed interaction diagrams to predict the resistance, which is user recommended in the Canadian code commentary. The author summarized the Driver & Kennedy [41] interaction diagrams were comparable to the experimental results obtained which are shown in Figure 14. The study also describes that Pi and Trahair [58] completed significant research in combined bending and torsion utilizing a plastic large deformation FE model to obtain I-beam capacities. Estabrooks [57] also concluded from his research, the FE results plotted by Pi and Trahair [58] are similar to the obtained experimental results as shown in Figure 15.

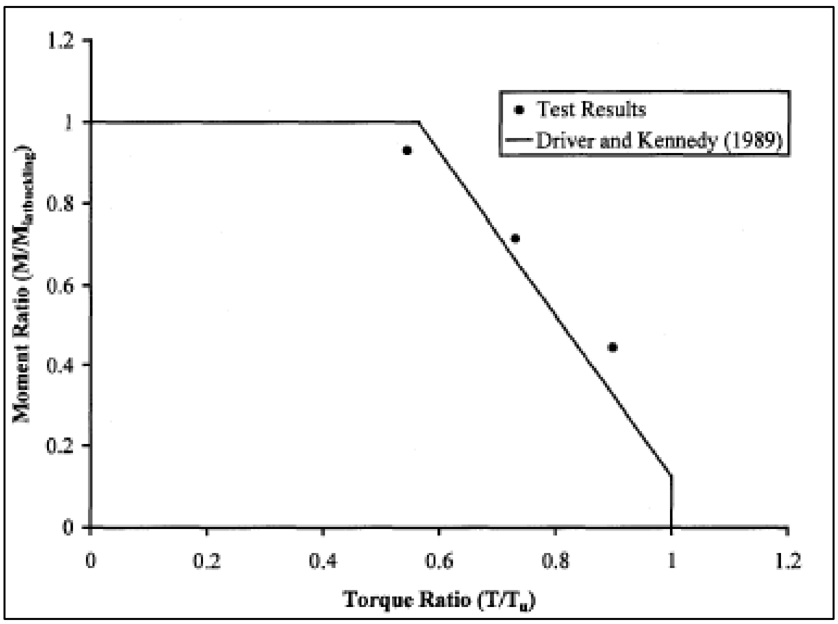


Figure 14: Comparison of Test Results to Driver and Kennedy Interaction Diagram Results for Class 1 Sections [57]

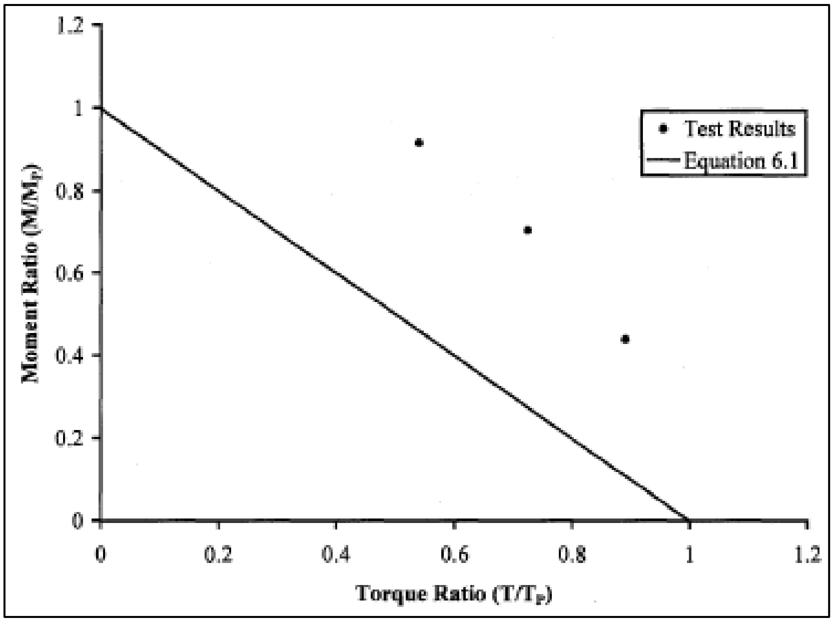

Figure 15: Comparison of Test Results to Pi and Trahair's FE Model Capacities for Class 1 Sections [57]

Another related study completed by Ashkinadze [7] was focused on limit states torsional design for wide-flange steel I-beams. The author noted the limitations of the user recommendations in the area of I-beams in torsion and combined loading in the Canadian steel design code. In the paper, the author explained how there is a necessity for a design methodology that would allow engineers to practically check I-beams loaded into torsion without having to complete a complex finite element analysis. The author researched the literature on I-beam moment-torque interaction diagrams, noting the diagrams developed by Driver & Kennedy [41] and recent work by Trahair & Pi [59]. The paper includes a for information only I-beam limit states design moment-torque interaction diagram, which is shown for comparison to Driver & Kennedy [41] and Trahair & Pi [59] diagrams in Figure 16. The author concludes the proposed moment-torque interaction diagram was developed for visual purposes only and not recommended for use in accordance with Canadian limit states design due to various limitations. The author also concludes further research is required for validation of the results through experimentation and second-order nonlinear analysis [7].

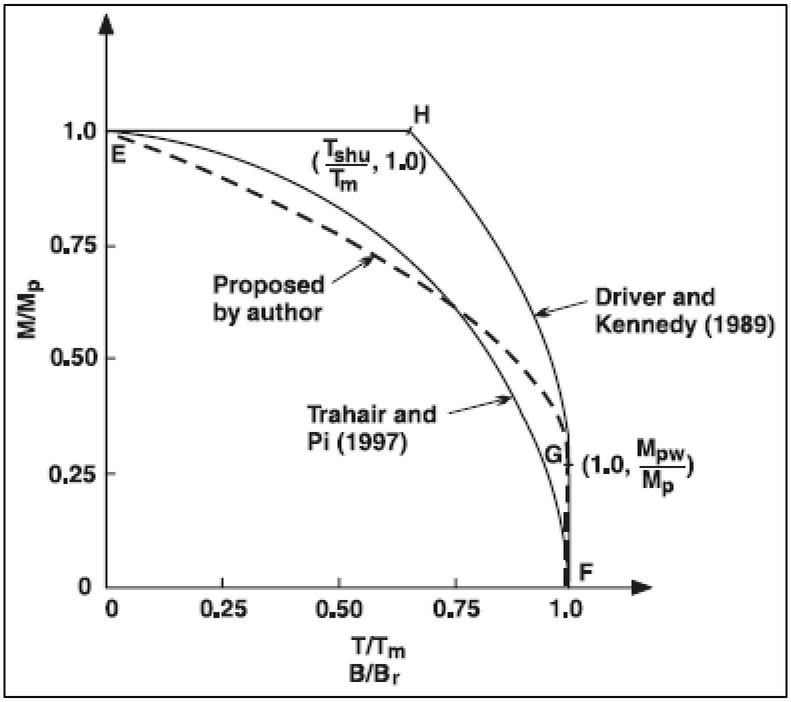


Figure 16: Moment-Torque Interaction Diagrams [7]

Kim and Yoo [60] did a study using FEA to determine the ultimate strengths of steel rectangle box beams that are loaded in combined bending and torsion. They compared their FE model results to other researcher's experimental test data. Initial imperfections in the box beams were taking into account and the effects of residual stresses were incorporated. From the FEA results and comparison to existing interaction equations, Kim and Yoo [60] proposed ultimate strength interaction equations for combined bending and tension and also combined bending, tension, and shear loading. They concluded the proposed interaction equations provide comparable results to other researcher's data while including resistance reductions for initial imperfections and combined interactions. Konate [61] completed similar experimental research on square HSS beam-columns with additional torsion load applied. In this study, numerous square HSS sections subject to axial, bending, and torsion loads were experimental tested and the behavior investigated. The author noted even though the international primary steel design codes include interaction formulas for beam-columns loaded in strong and weak axis, if an additional torsion load was present, it could not be accounted for in the combined check. From the results, the author developed new strength and yield limits for the beams that include the effects of applied torsion. Konate [61] also proposes original moment-torsion interaction equations for beam-column design for potential adoption into the international steel design standards.

## 2.5 Literature Review Summary

Through the literature review of this thesis topic, numerous relevant studies and research papers were identified. The key findings are summarized below:

- Most of these studies included comparisons of specific clauses and particular topics from both Canadian and American steel design codes.
- There were not any studies identified that were purely a full gap analysis between the two codes identifying if significant design assessment gaps exist.
- It has been determined that significant research, both theoretical and experimental, has been completed on the topic of steel beams in torsion.
- Substantial literature has been documented on lateral-torsional buckling of steel I-beams and I-beams subject to combined loadings including torsion.
- Numerous researchers have developed similar first principal equations to verify torsion interaction and check combined loading stresses.
- These interaction equations have been published in international design guides to be used by practicing structural engineers.
- No studies were identified that researched the American code HSS torsion/ combined loading clauses for potential design applicability in Canada.

The review conducted, demonstrated the available literature is devoid of research in the field of HSS torsion and combined loading for use in Canada. It was determined if the American code

HSS torsion clauses are examined on the basis for application in Canada, there could be substantial benefits to practicing engineers. The literature review has shown torsion and combined loading are principal methods of beam failure. If a structure is code checked with a structural design software program to the current Canadian code, HSS torsion or combined loading would not be checked. A separate stress analysis is required if these loadings are present when using CAN S16-19 [1]. Researching HSS torsion and combined loading also has the potential to add clarity on the subject or efficiencies to the design processes presently available.

# Chapter 3 Design Data and Principles

## 3.1 General

This chapter describes the design data/ principles used for the analysis of HSS sections in torsion and combined loading using finite element techniques. The approach is broadly illustrated in Figure 3 of Section 1.2 and the analysis methodology is described in detail in the following sections.

## 3.2 Material Properties

The following material properties were used in the analysis:

| | |
|---|---|
| Steel Specified Minimum Yield Strength: | $F_y = 350$ MPa |
| Steel Tensile Strength: | $F_u = 450$ MPa |
| Density of Steel: | $\rho = 7850$ kg/m$^3$ |
| Modulus of Elasticity: | E = 200 GPa |
| Shear Modulus: | G = 80 GPa |
| Poisson Ratio: | $\nu = 0.3$ |

## 3.3 Finite Element Analysis Methodology

Finite element analysis methodology was used as the primary tool for the structural assessment of the sections as it provides a refined and precise analysis of the structure. The sections were modeled and analyzed for all the applicable load cases using ANSYS 2020 R1 [62]. A non-linear material model was used to assess the stress and strain values of the sections under applied loads. The sections that were investigated were modeled completely using shell elements as they provide more accurate and consistent stress results when compared to solid elements where multiple elements through the thickness are required. Shell elements are also less prone to negative jacobian errors when meshing geometries.

For the non-linear analysis, a bilinear kinematic hardening material model was selected. The true stress-true strain curve from DNVGL-RP-C208 [63] applicable for S355 plate up to 40mm thick was used and a tangent modulus of 573.2 MPa was calculated. The tangent modulus is equal to the slope of the true stress-true strain curve on the first section after yield of the material. The true stress-true strain curve is shown in Figure 17. The evaluation of the strain will be completed according to DNVGL-RP-C208 [63] where the limit for linearized averaged plastic strain is 0.04 (4%) for S355 material.

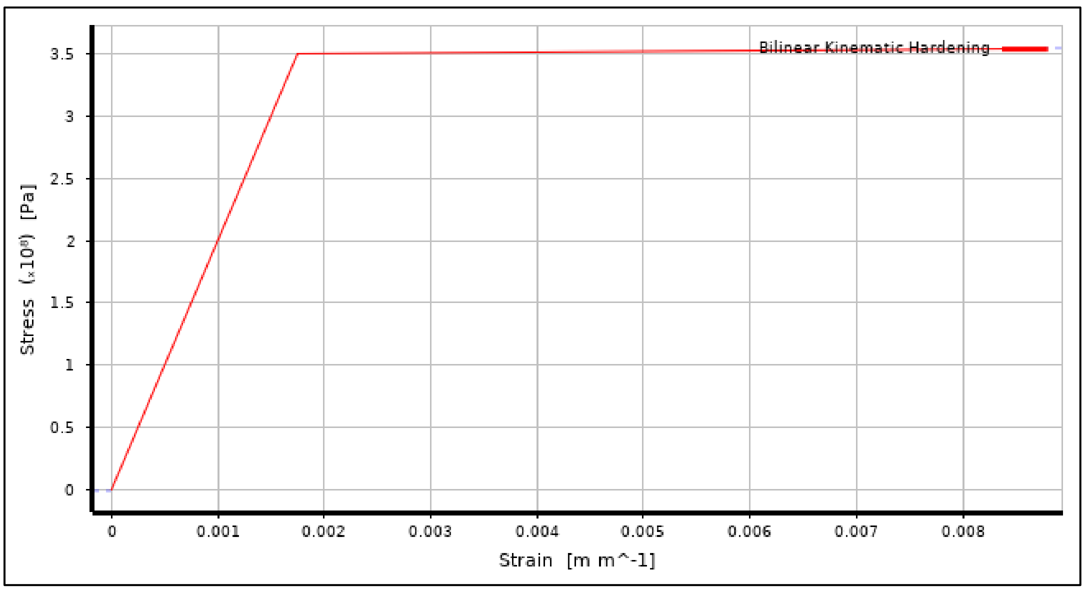


Figure 17: ANSYS Stress-Strain Curve

The design principles for this analysis are based on Ultimate Limit States (ULS), in accordance with CAN/CSA S16-19 [1]. According to this design standard, the steel sections shall be designed such that:

$$\text{factored resistance} \geq \text{effect of factored loads} \tag{3-1}$$

According to CAN/CSA S16-19 [1], the von Mises equivalent stress ($f_y$) for steel shall not exceed the resistance ($\phi \cdot F_y$).

$$f_y \leq \phi \cdot F_y \tag{3-2}$$

Where:

$f_y$ = Stress

$\phi$ = Resistance Factor

$F_y$ = Yield Strength

The resistance factor, $\phi$, to be applied for the yield check is 0.9 in accordance with CAN/CSA S16-19 [1]. The von Mises equivalent stress can be obtained directly from the finite element models. Results of the FEA analysis will be evaluated under all loading conditions. Beam deflections are checked to ensure they are within reasonable limits for deflection at failure and acceptable based on sound engineering judgment.

# Chapter 4 Analysis Method and Modeling

## 4.1 General

This chapter outlines the analysis method/ modeling techniques used for the assessment of HSS sections in torsion and combined loading in the finite element program ANSYS [62]. The purpose of this analysis is to verify the sections under the specific load magnitudes which allow for verification in accordance with predetermined stress and strain limits. The finite element techniques and modeling parameters are detailed in the following sections.

## 4.2 Geometric Models

The steel sections were analyzed using ANSYS 2020 R1 [62]. Two round, two square, and two rectangular structural sections of various sizes with ½" and 1" wall thicknesses were modeled as cantilever beams. A total of six different geometries (½" and 1" WT) 1 m in length were checked for torsion loading only and three of these geometries (½" WT) with end caps were additionally checked for combined torsion, flexure, shear, and axial force. The sizes of the steel sections analyzed are shown in Table 4-1. Cantilever beams were focused on in this study as they produce worst-case results in comparison to fixed-fixed beam models. Also note simply supported beam models will not converge under torsion due to instabilities as the beam is free to rotate.

| Section Type | Designation (mm) |
|---|---|
| Round | HSS 168x13 |
| | HSS 324x25 |
| Square | HSS 152x152x13 |
| | HSS 305x305x25 |
| Rectangular | HSS 203x152x13 |
| | HSS 356x254x25 |

Table 4-1: Steel Sections

The geometric models for round, square, and rectangular HSS in torsion loading are presented in Figure 18 to Figure 23.

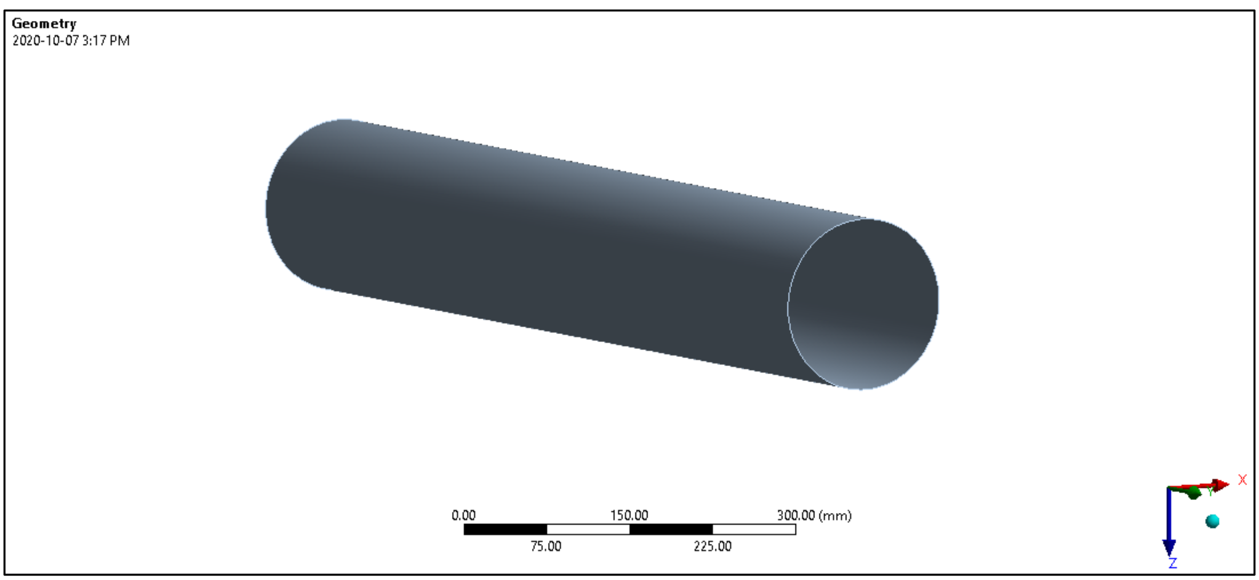


Figure 18: Round HSS 168x13 Geometry (Torsion Loading)

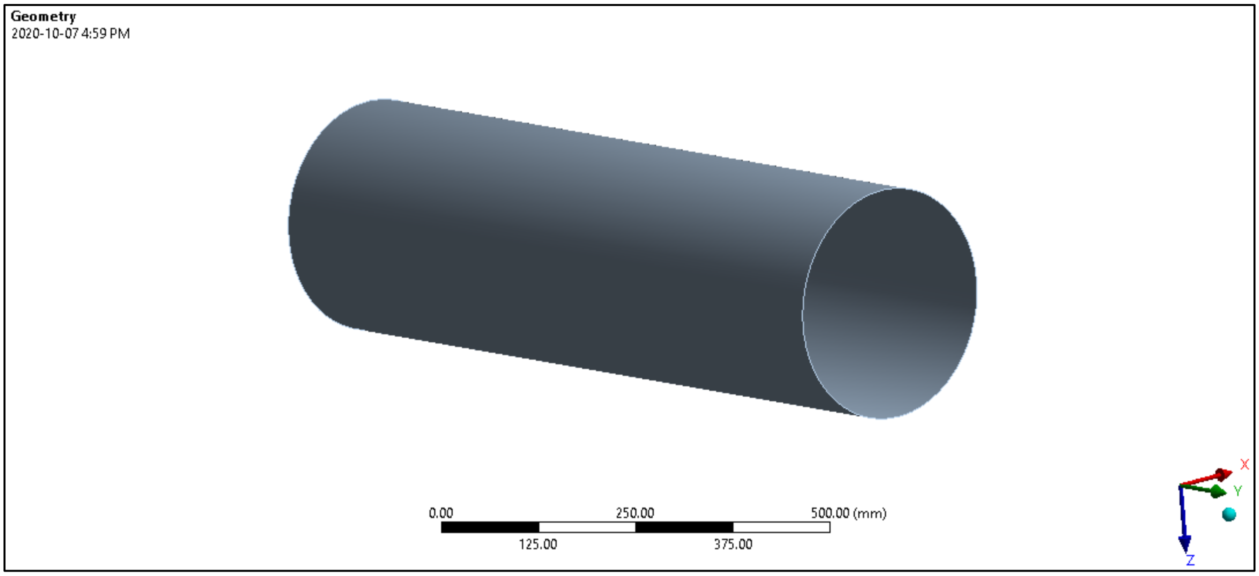

Figure 19: Round HSS 324x25 Geometry (Torsion Loading)

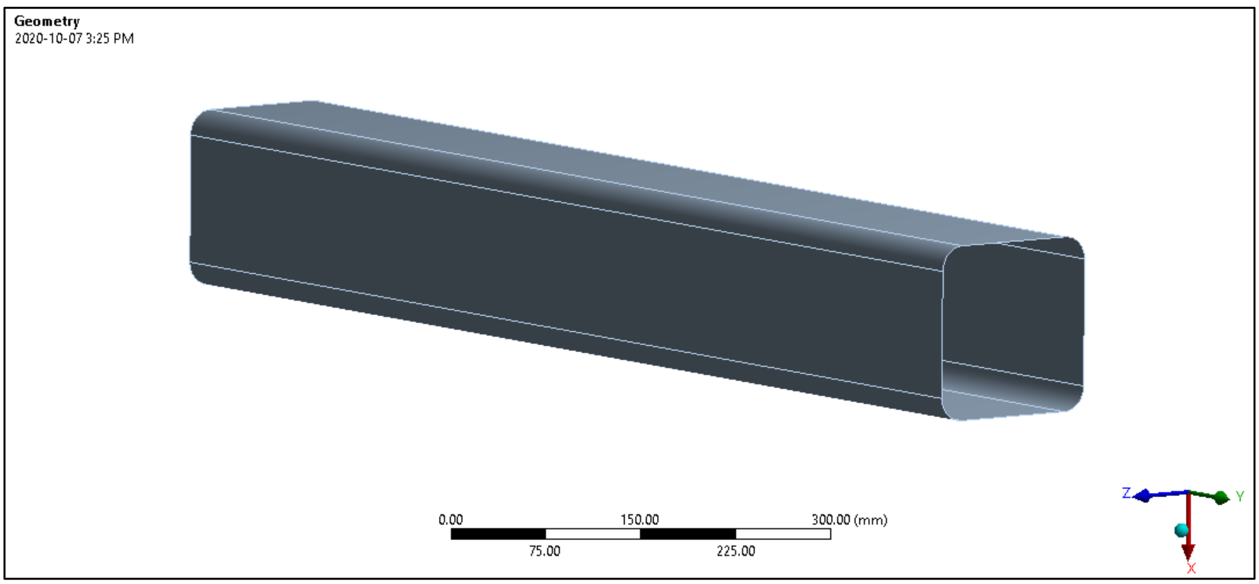

Figure 20: Square HSS 152x152x13 Geometry (Torsion Loading)

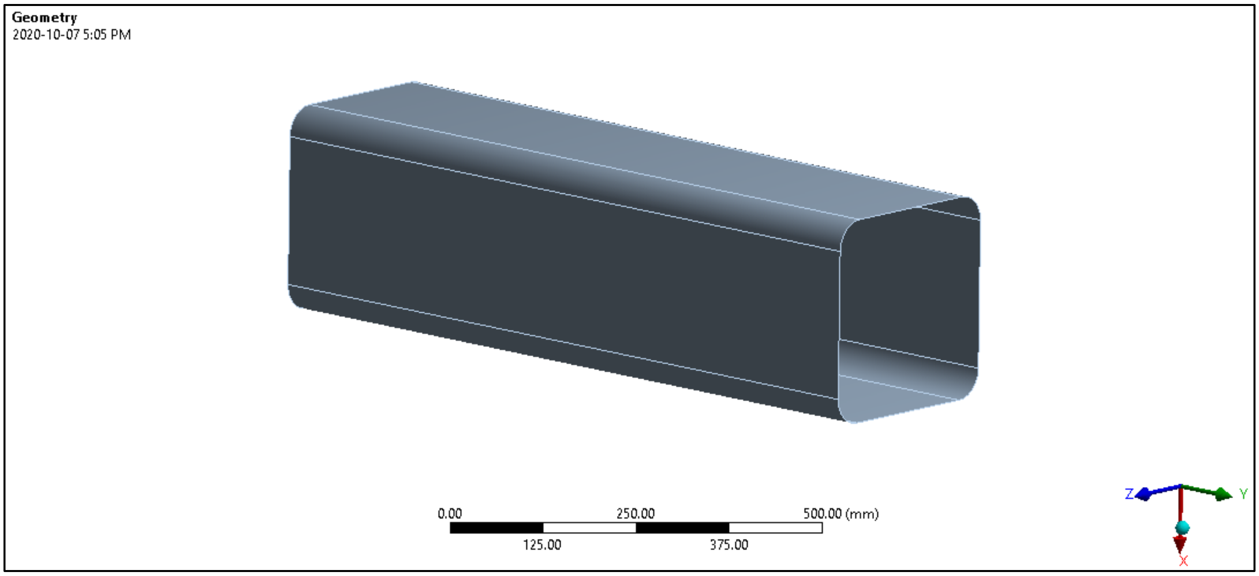

Figure 21: Square HSS 305x305x25 Geometry (Torsion Loading)

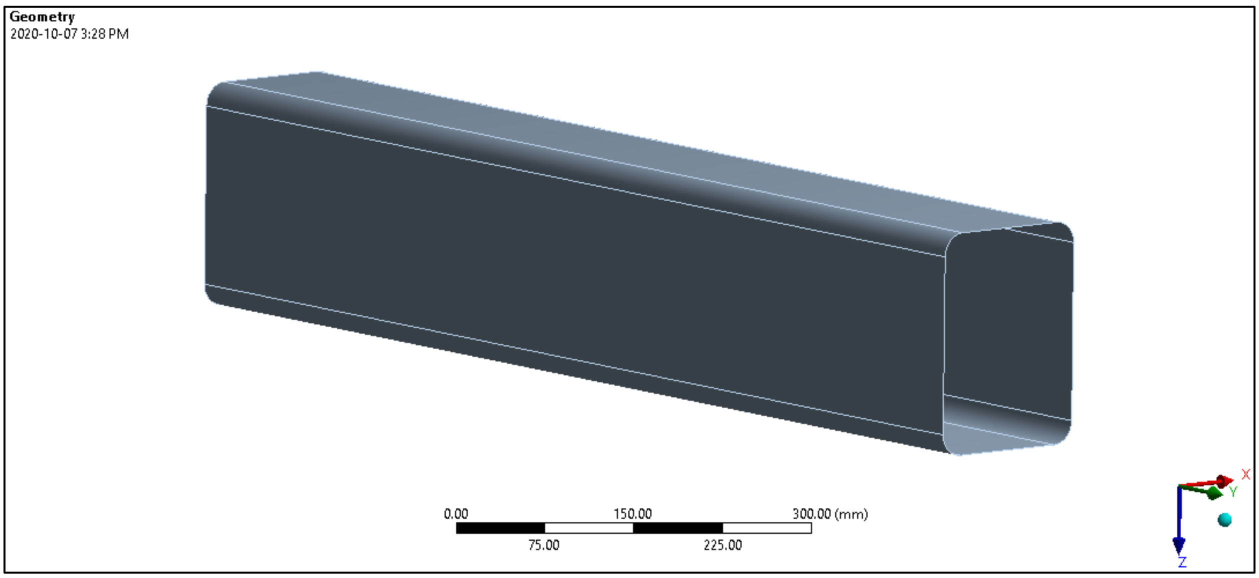

Figure 22: Rectangular HSS 203x152x13 Geometry (Torsion Loading)

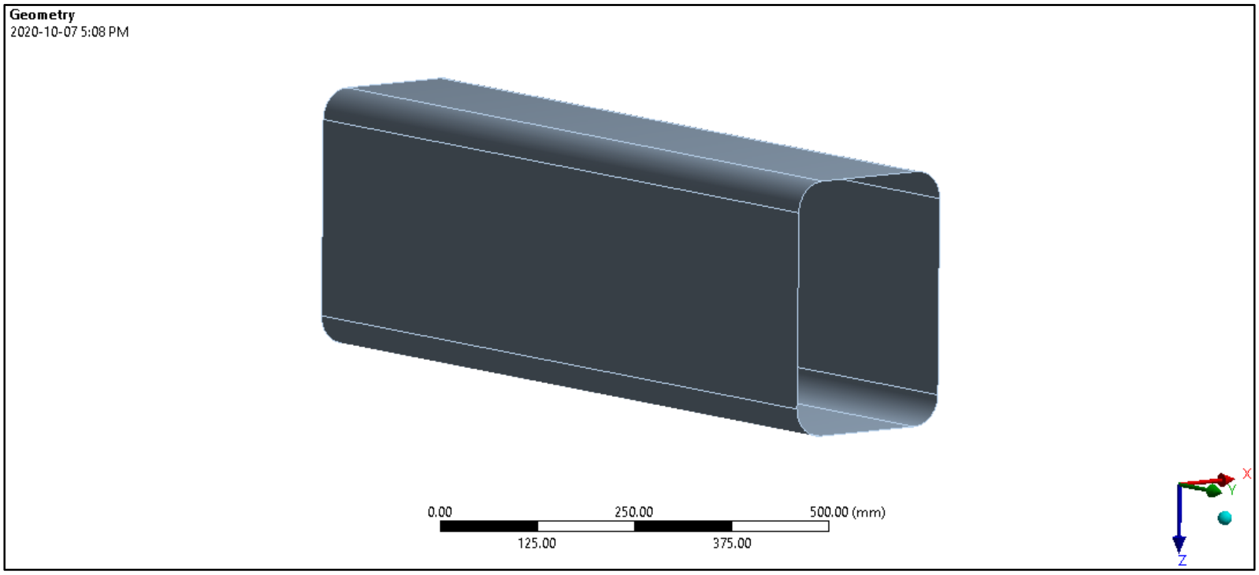

Figure 23: Rectangular HSS 356x254x25 Geometry (Torsion Loading)

The geometric models for round, square, and rectangular HSS in combined loading are presented in Figure 24 to Figure 26. The combined loading models are similar to the ½" wall thickness torsion models but with an end cap modeled to locally stiffen the open ends of the beams for load application purposes. The models also have an additional imprinted face at 0.1m from the support for the shear application.

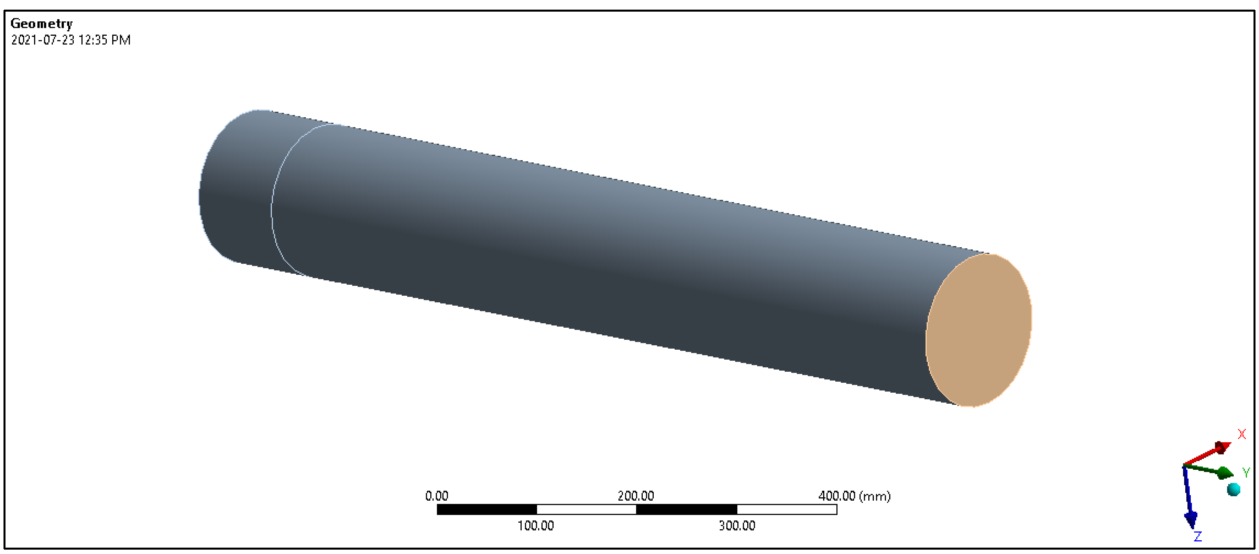

Figure 24: Round HSS 168x13 Geometry (Combined Loading)

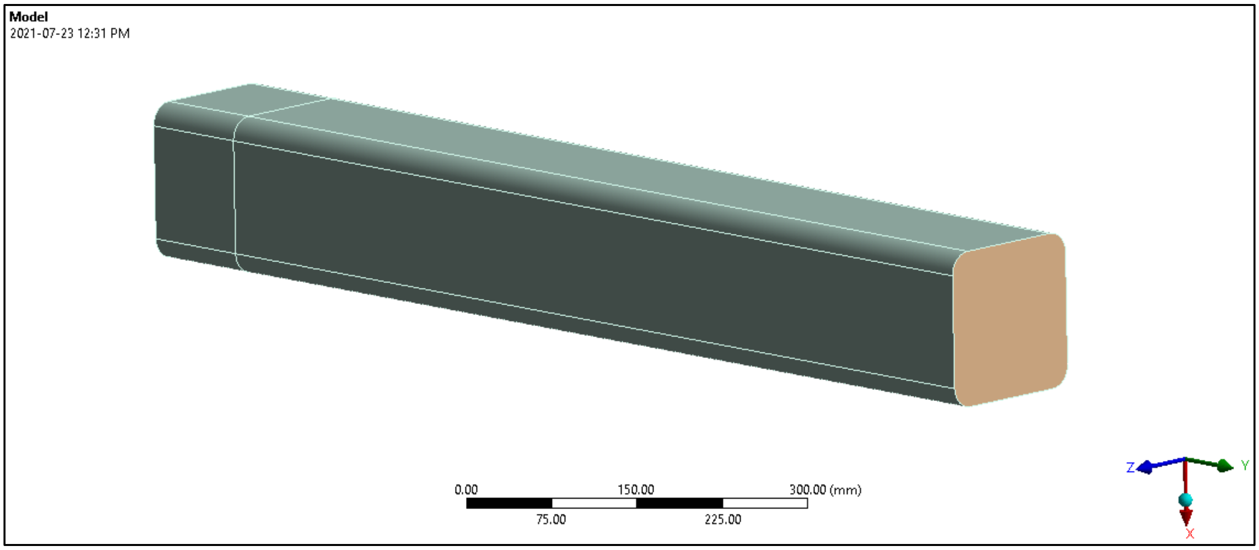


Figure 25: Square HSS 152x152x13 Geometry (Combined Loading)

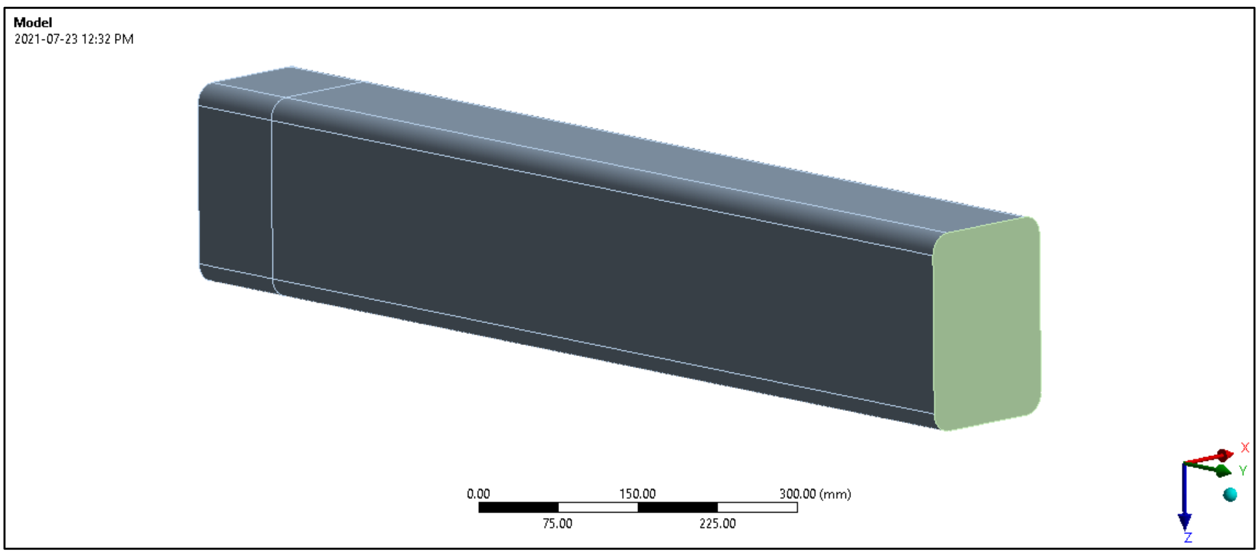


Figure 26: Rectangular HSS 203x152x13 Geometry (Combined Loading)

## 4.3 Mesh

All model meshes are constructed using SHELL181 elements using automatic method. SHELL181 is a 4-node structural shell element that is "well suited for linear, large rotation and/or large strain nonlinear applications" [64]. Body sizing in each model is set to the wall thickness depending on the steel section being analyzed. For the shell element's 5 through-thickness integration points were applied, which is the ANSYS automatic default for SHELL181 elements when plasticity is present and a single layer shell is defined [64]. Mesh quality of all models was checked to ensure acceptance criteria were achieved based on good engineering judgment for finite element analysis. Mesh convergence analyses were not required for the models because the shell element edge lengths are on the order of their thicknesses. For an example of the typical mesh quality checks, information from one model was included. Refer to Table 4-2 for round HSS 168x13 mesh quality checked in ANSYS mesh metric. The model meshes are shown in Figure 27 to Figure 35.

| Mesh Quality Check | |
|---|---|
| **Acceptance Criteria** | **FEA Output** |
| Element Count/ Node Count | 3081/ 3120 |
| Element Quality: >0.3 | 0 elements fail |
| Warpage: <0.05 | 0 elements fail |
| Skew: <0.6 | 0 elements fail |
| Quad Element Max Angle: <120° | 0 elements fail |
| Quad Element Min Angle: >60° | 0 elements fail |
| Trias Element Max Angle: <140° | N/A |
| Trias Element Min Angle: >20° | N/A |
| Jacobian Check: | Ok, there are no elements with negative Jacobian in the model. |
| Mesh Sensitivity Check: | Averaged and unaveraged equivalent stress results were confirmed to show the same stress distribution. |

Table 4-2: Round HSS 168x13 Mesh Quality Check

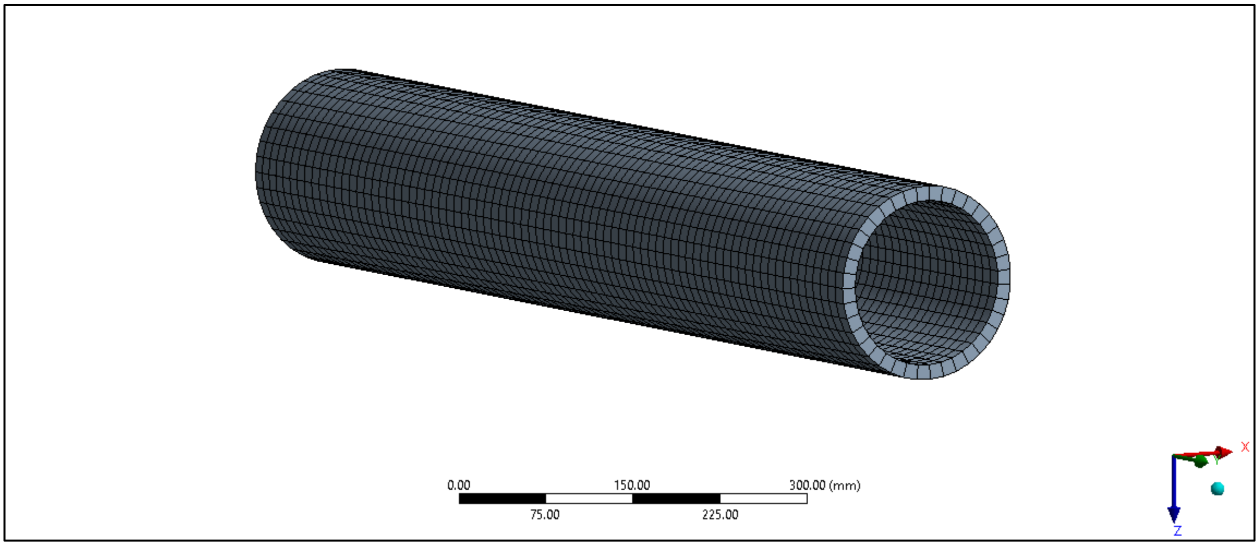

Figure 27: Round HSS 168x13 Mesh (Torsion Loading)

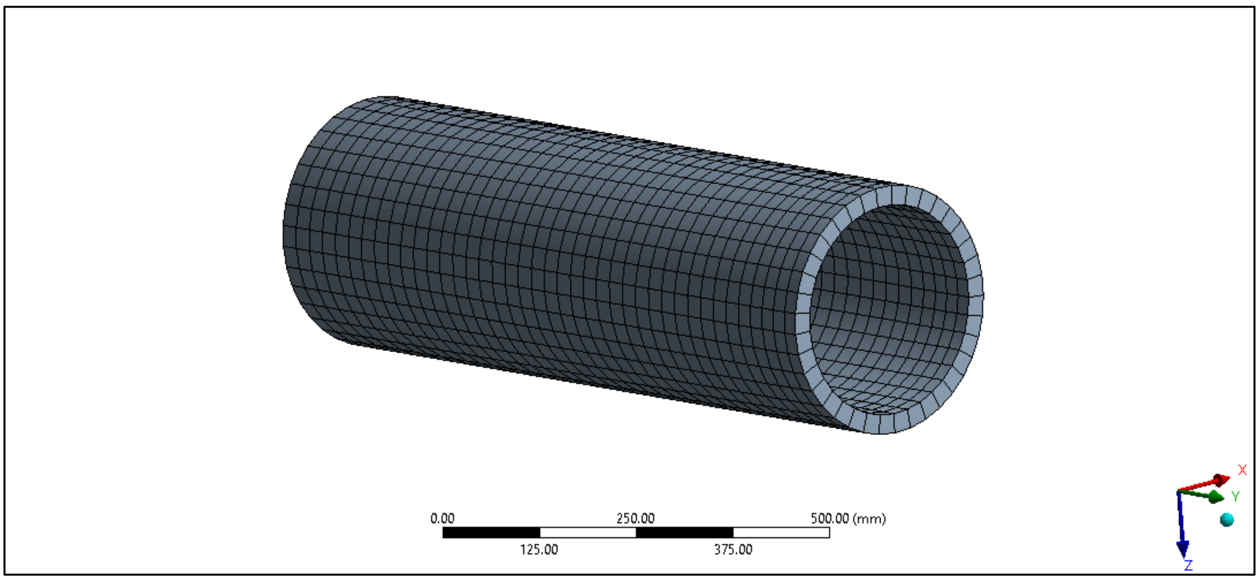

Figure 28: Round HSS 324x25 Mesh (Torsion Loading)

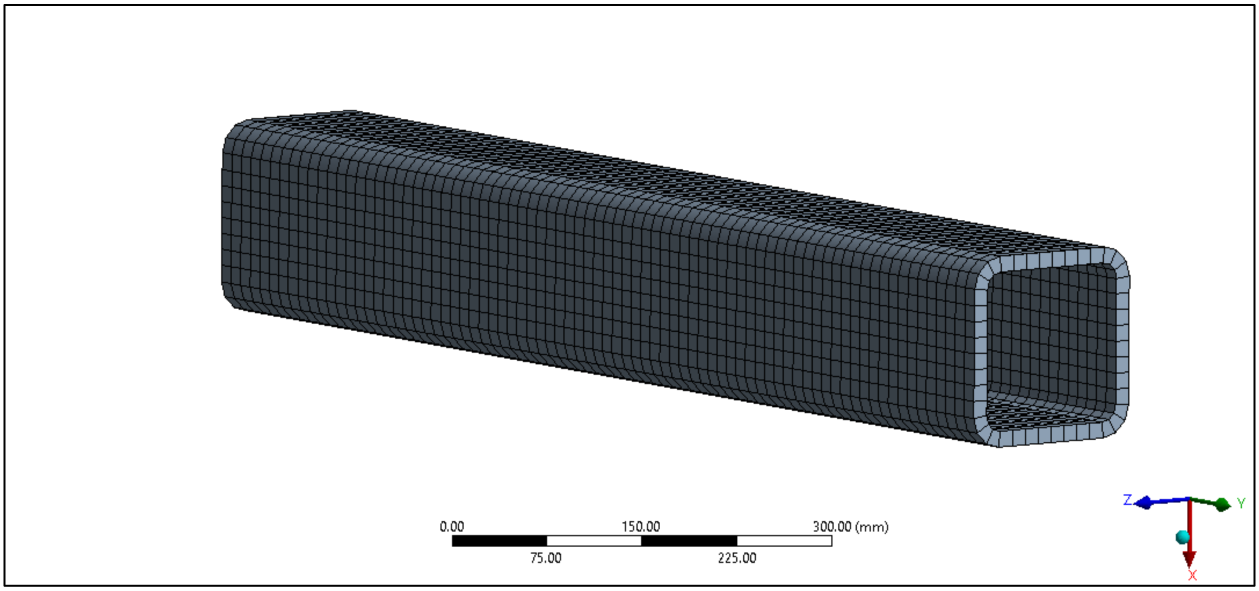

Figure 29: Square HSS 152x152x13 Mesh (Torsion Loading)

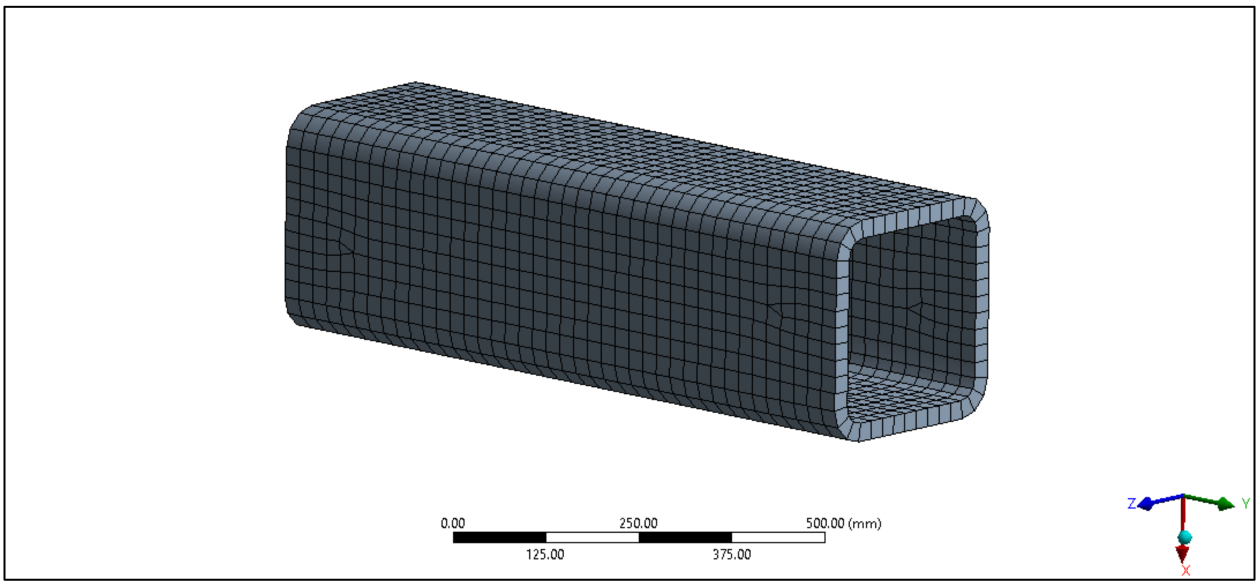

Figure 30: Square HSS 305x305x25 Mesh (Torsion Loading)

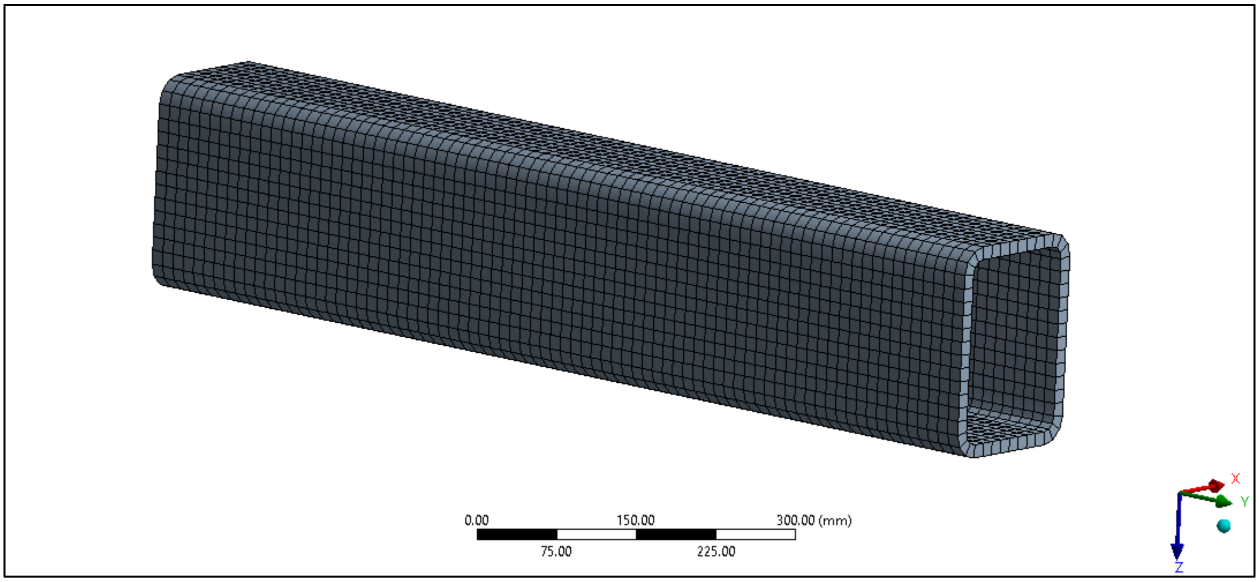


Figure 31: Rectangular HSS 203x152x13 Mesh (Torsion Loading)

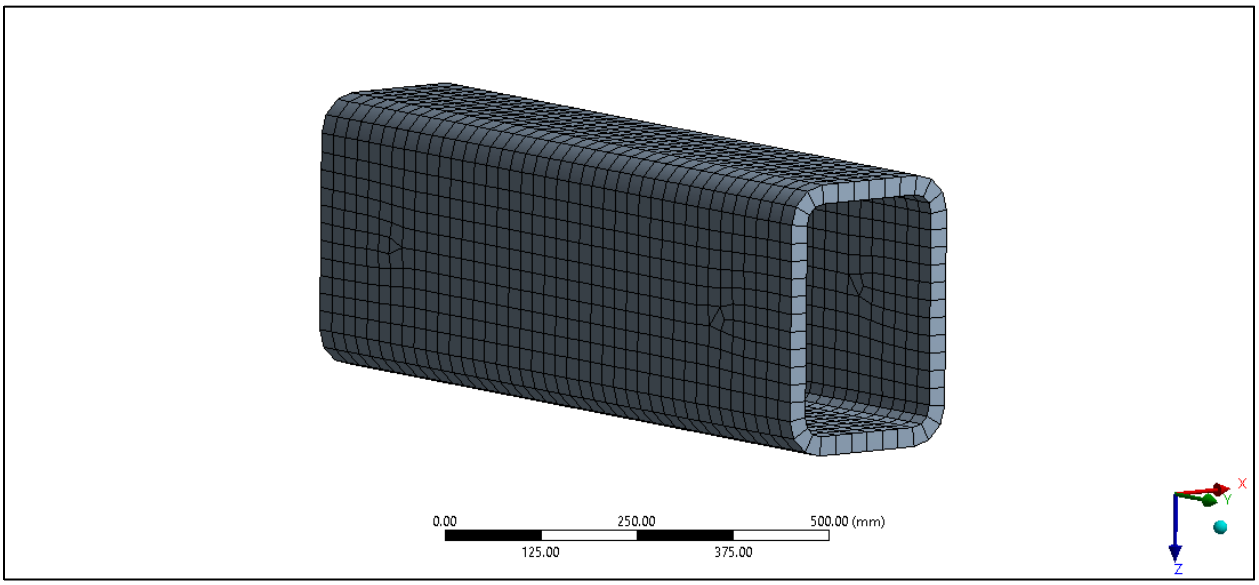


Figure 32: Rectangular HSS 356x254x25 Mesh (Torsion Loading)

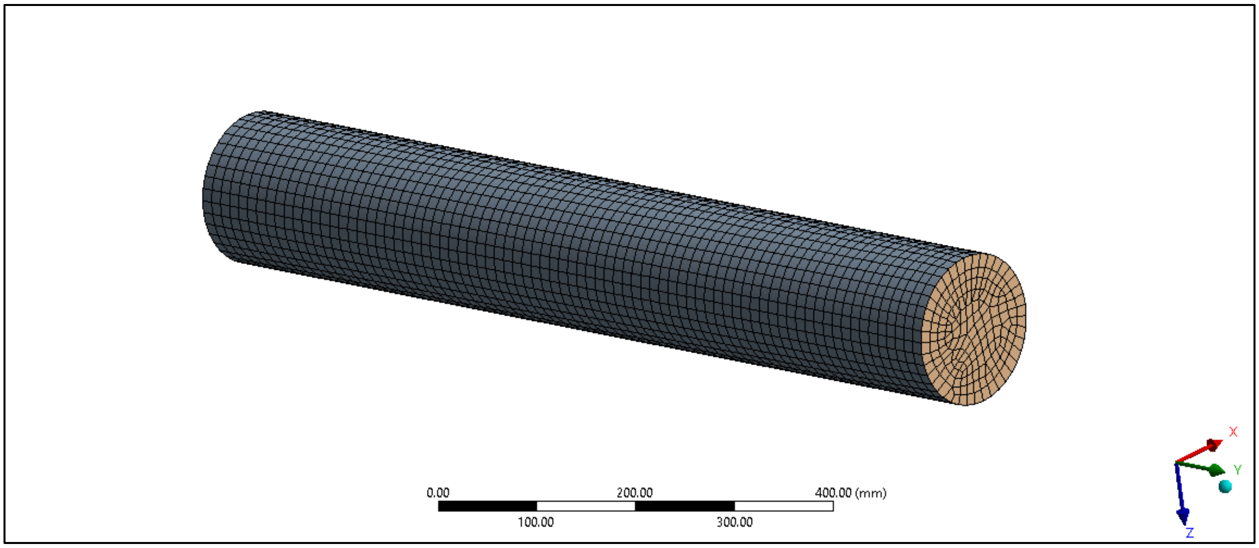

Figure 33: Round HSS 168x13 Mesh (Combined Loading)

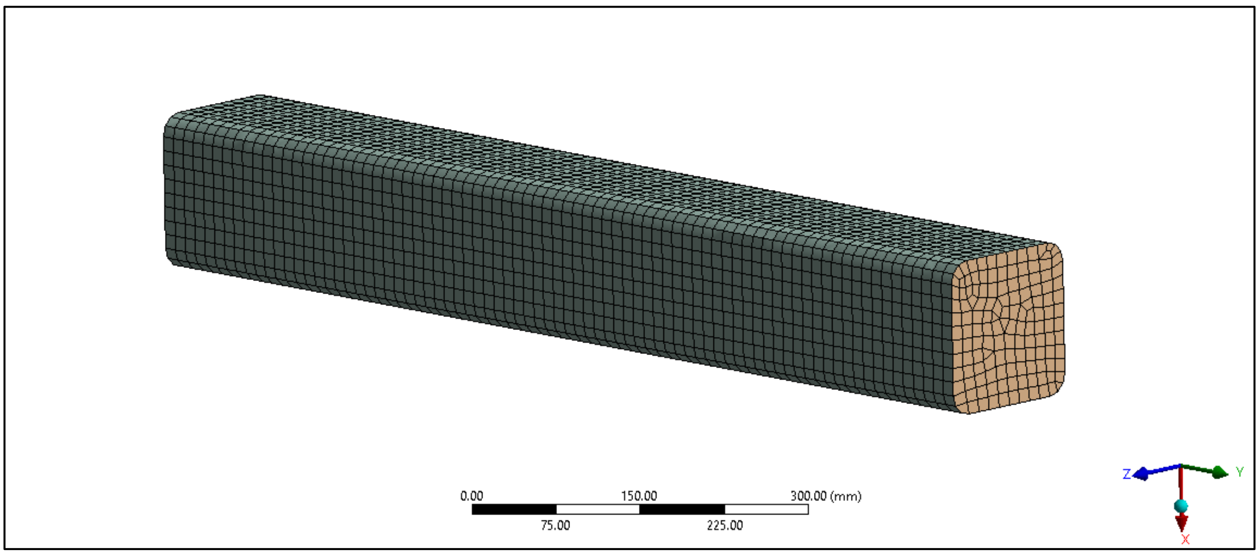

Figure 34: Square HSS 152x152x13 Mesh (Combined Loading)

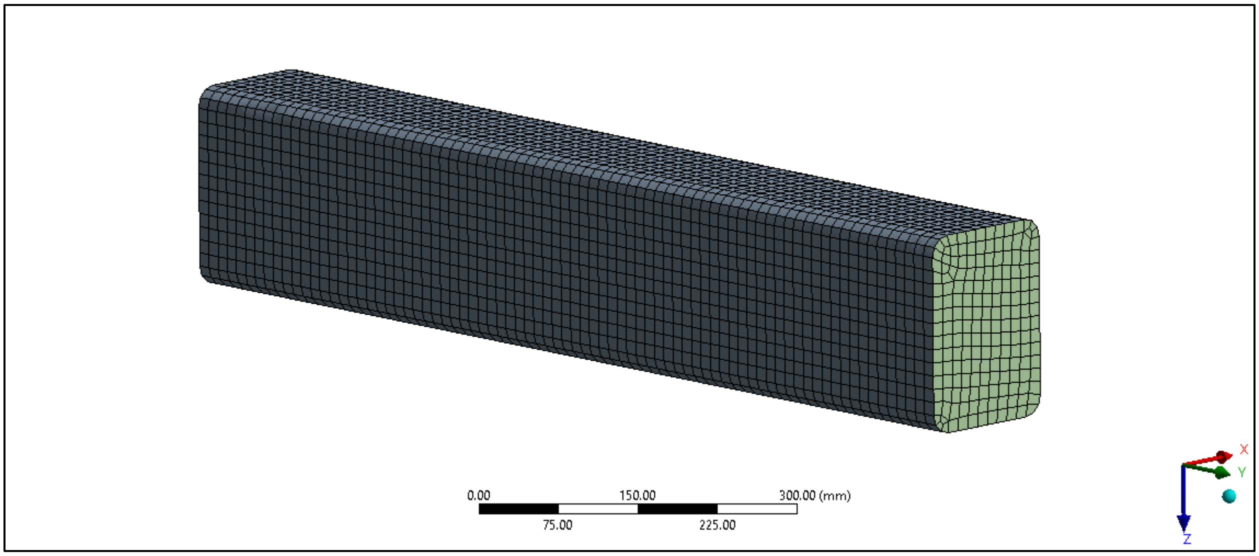

Figure 35: Rectangular HSS 203x152x13 Mesh (Combined Loading)

## 4.4 Boundary Conditions

All models utilize a fixed boundary support at one end of the beam to simulate a cantilever section. The model boundary conditions are shown in Figure 36 to Figure 44. All intersections between components are modeled with shared topology where surfaces are connected in all six degrees of freedom.

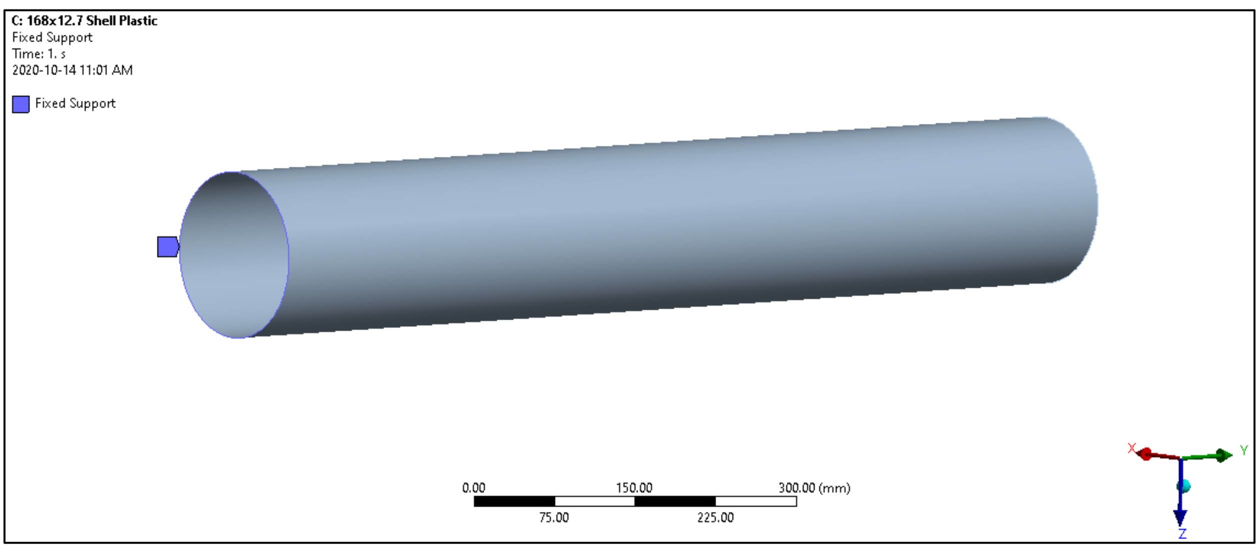

Figure 36: Round HSS 168x13 Boundary Condition (Torsion Loading)

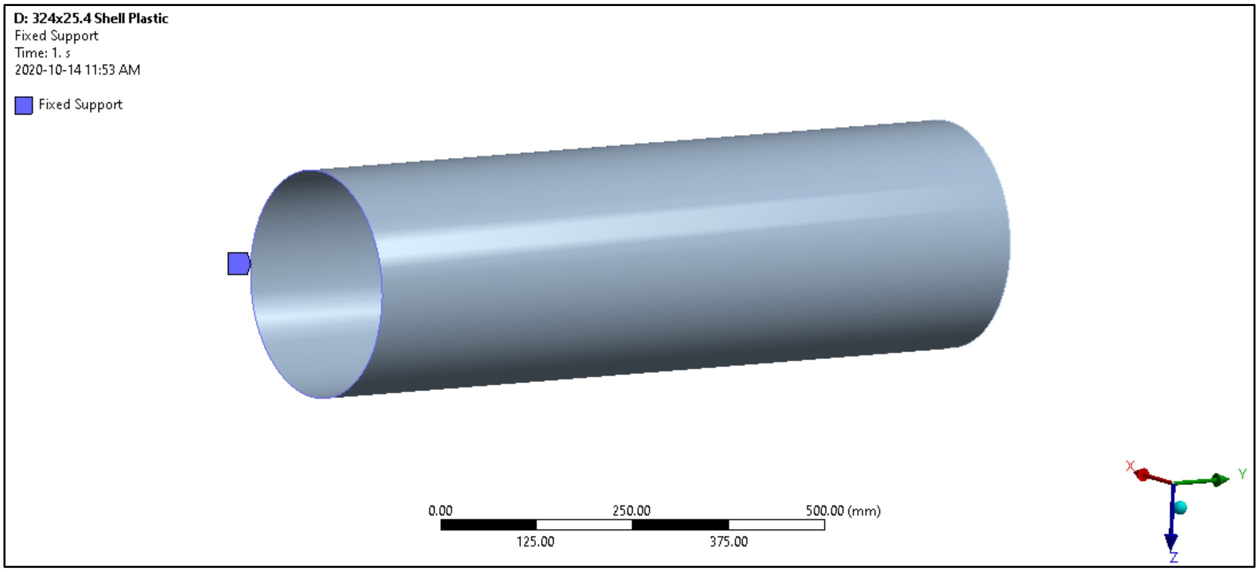

Figure 37: Round HSS 324x25 Boundary Condition (Torsion Loading)

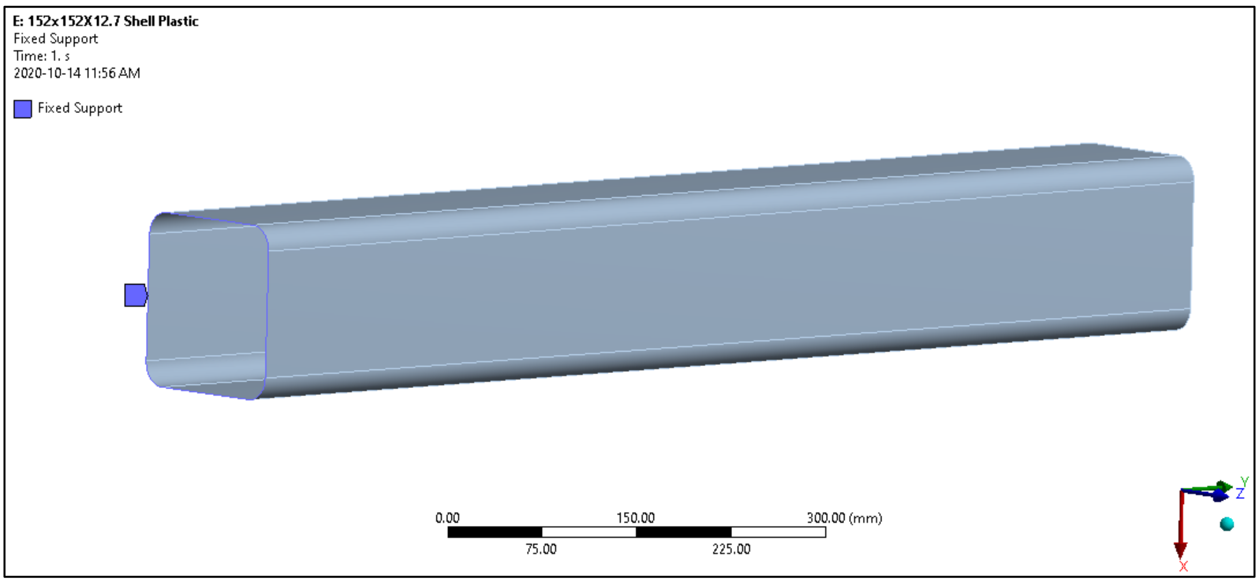

Figure 38: Square HSS 152x152x13 Boundary Condition (Torsion Loading)

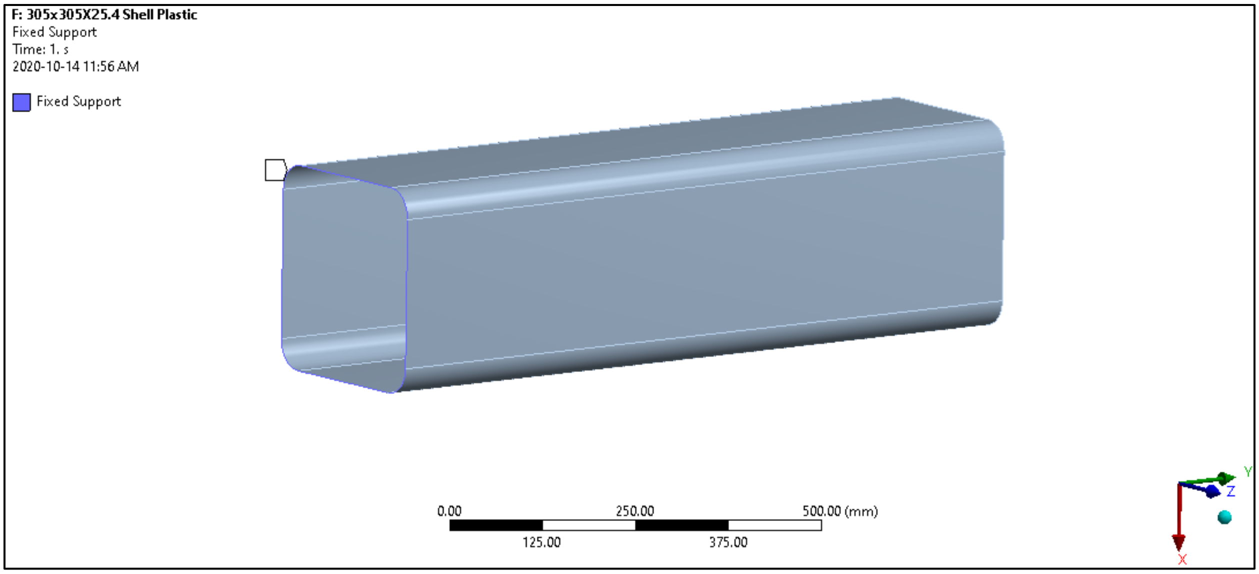

Figure 39: Square HSS 305x305x25 Boundary Condition (Torsion Loading)

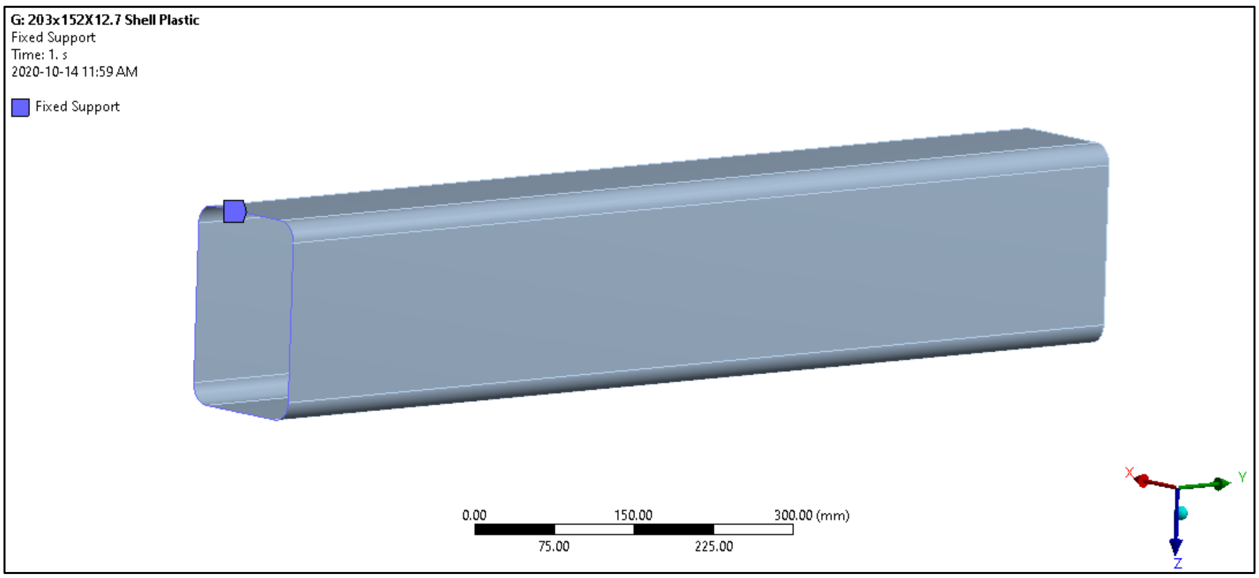

Figure 40: Rectangular HSS 203x152x13 Boundary Condition (Torsion Loading)

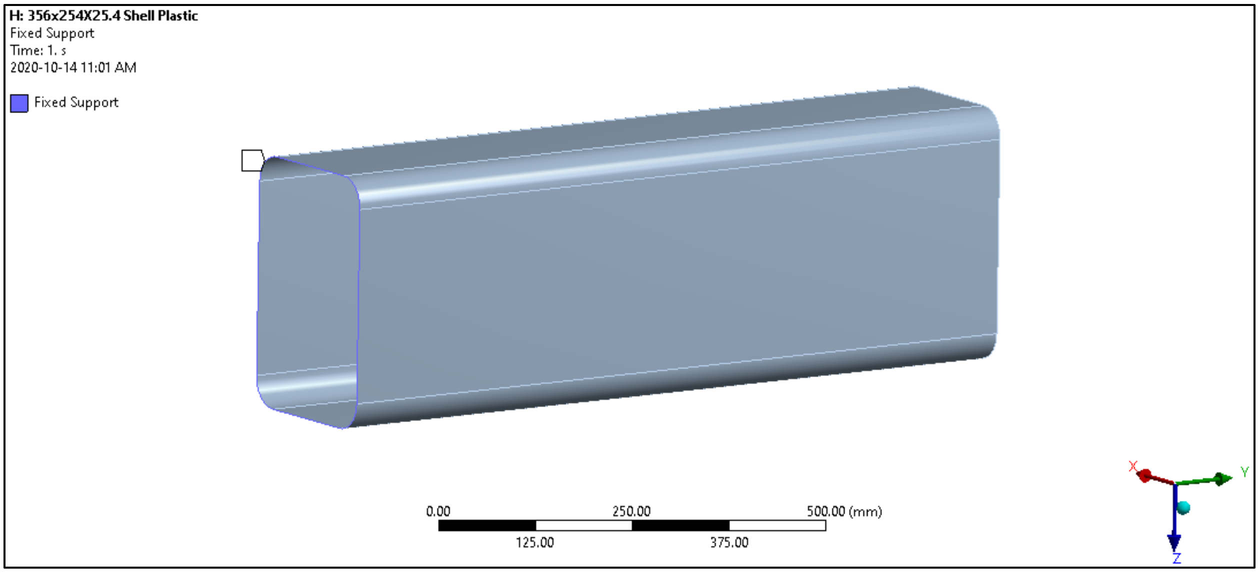


Figure 41: Rectangular HSS 356x254x25 Boundary Condition (Torsion Loading)

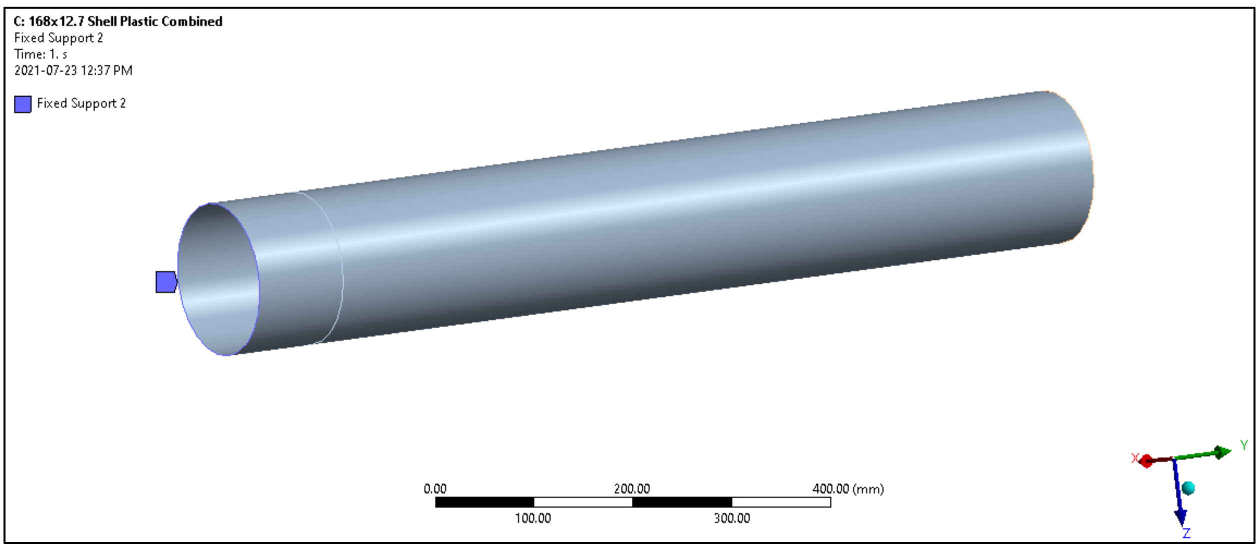


Figure 42: Round HSS 168x13 Boundary Condition (Combined Loading)

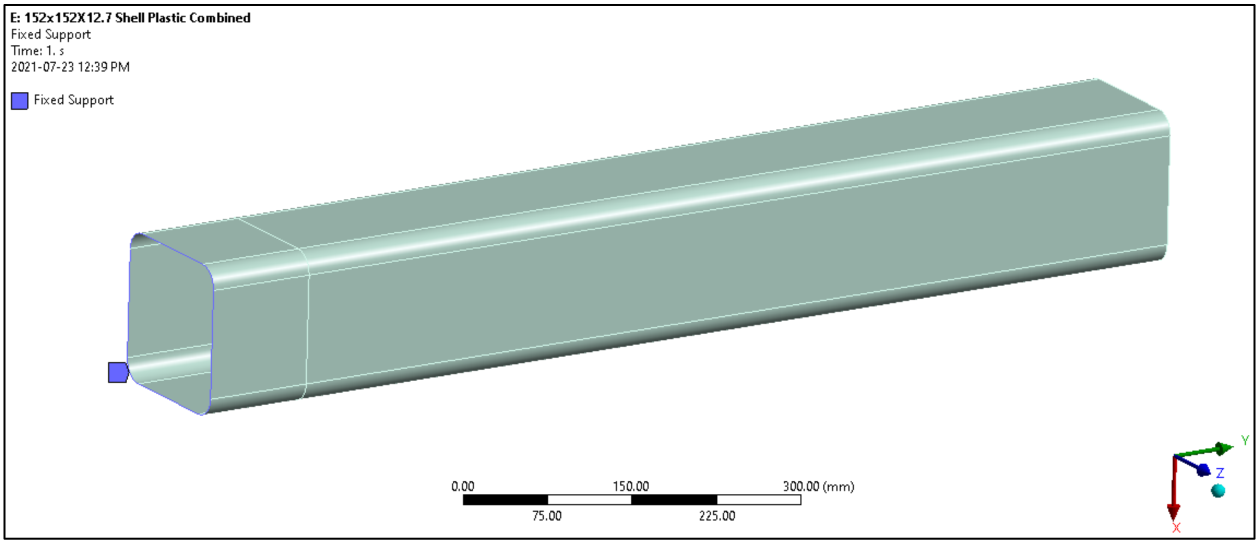


Figure 43: Square HSS 152x152x13 Boundary Condition (Combined Loading)

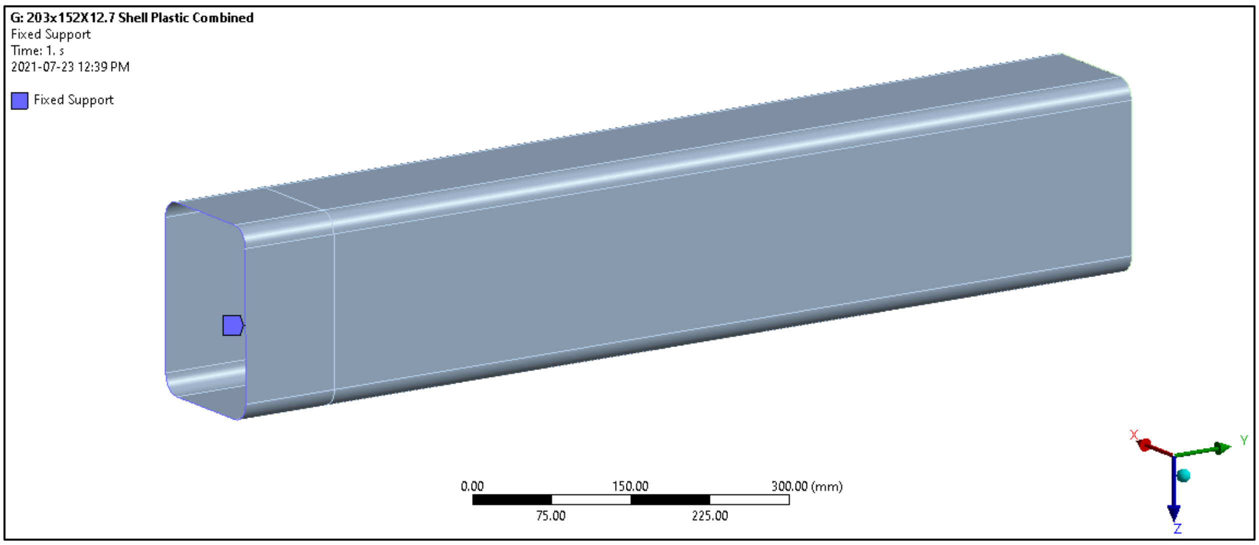


Figure 44: Rectangular HSS 203x152x13 Boundary Condition (Combined Loading)

## 4.5 Load Cases

External loads are applied to the models in one-time step. Torsion and combined loading section capacities were determined in accordance with ANSI/AISC 360-16 [2] as calculated in Appendix A. These capacities were then applied to the models to check the validity of the results for potential design application in Canada in line with CAN/CSA S16-19 [1].

The ANSI/AISC 360-16 [2] capacity values used in the combined loading models for flexure, shear, and axial force were additionally calculated using CAN/CSA S16-19 [1] for comparison to ensure they were less than or equal to the AISC values as shown in Appendix A. This assessment ensures the combined loading analyses completed in this study produce the worst-case possible results for a design application in Canada in accordance with CAN/CSA S16-19 standards [1]. It was determined all the CSA section capacities were equal to or less than the AISC capacities used in this study except for the shear capacity of the round HSS 168x13 section. See Results Section 5.11 for more information on the separate check using the CSA shear value for the round HSS 168x13 combined loading analysis.

For the combined model loads, percentages of the total section capacities were calculated to yield a utilization ratio of 1.0 based on the ANSI/AISC 360-16 [2] H3-2 clause. For the combined load cases 25% of the axial, bending, shear, and torsion capacities were applied. A load factor of 1.0 was used on the external loads as the section capacities were applied in the models to produce maximum utilization. For the combined load cases, a first run of the analysis was completed applying all the loads at the end of the sections. This produces a conservative check as the shear applied at the end is creating additional moment in the beams. Based on the results it was determined the sections were overutilized applying the shear load at the end. Therefore, for the combined load cases the shear is applied 0.1m from the support. The additional moment created from the shear is subtracted from the calculated moment section capacity as shown in the table below. The torsion model load cases are presented in Table 4-3 and combined model load cases are shown in Table 4-4. The section capacity calculations are shown in Appendix A.

| Load Case | Section Type | Designation (mm) | Torsion (kN*m) |
|---|---|---|---|
| 1 | Round | HSS 168x13 | 90.9 |
| 2 | Round | HSS 324x25 | 672.4 |
| 3 | Square | HSS 152x152x13 | 36.1 |
| 4 | Square | HSS 305x305x25 | 292.2 |
| 5 | Rectangular | HSS 203x152x13 | 57.8 |
| 6 | Rectangular | HSS 356x254x25 | 267.3 |

Table 4-3: Torsional Model Load Cases

| Load Case | Section Type | Designation (mm) | Torsion (kN·m) | Bending (kN·m) | Shear (kN) | Axial (kN) |
|---|---|---|---|---|---|---|
| 7 | Round | HSS 168x13 | 32.2 | 24.3kN·m – (207.5kN·0.1m) = 3.5kN·m | 207.5 | 489.0 |
| 8 | Square | HSS 152x152x13 | 12.8 | 26.9kN·m – (171.8kN·0.1m) = 9.8kN·m | 171.8 | 526.1 |
| 9 | Rectangular | HSS 203x152x13 | 20.4 | 41.6kN·m – (258.3kN·0.1m) = 15.7kN·m | 258.3 | 627.6 |

Table 4-4: Combined Model Load Cases

For the torsion models, the load was applied to the end of the shell section in the first load step. The maximum torsional capacities applied to the sections are shown in Figure 45 to Figure 50.

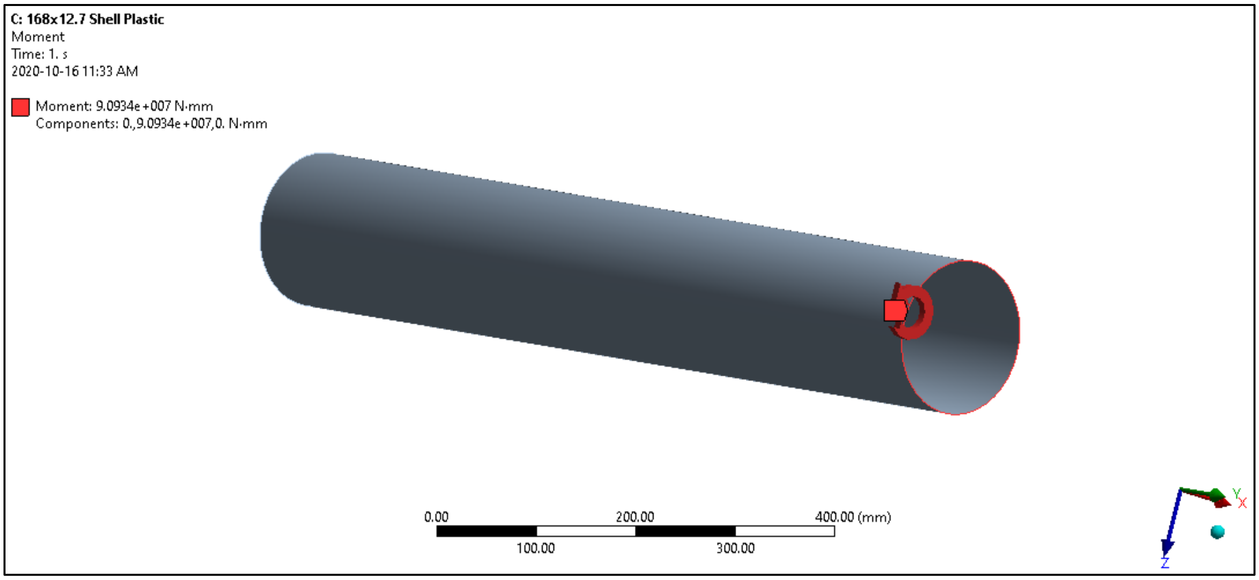


Figure 45: Load Case 1 - Round HSS 168x13 (Torsion Loading)

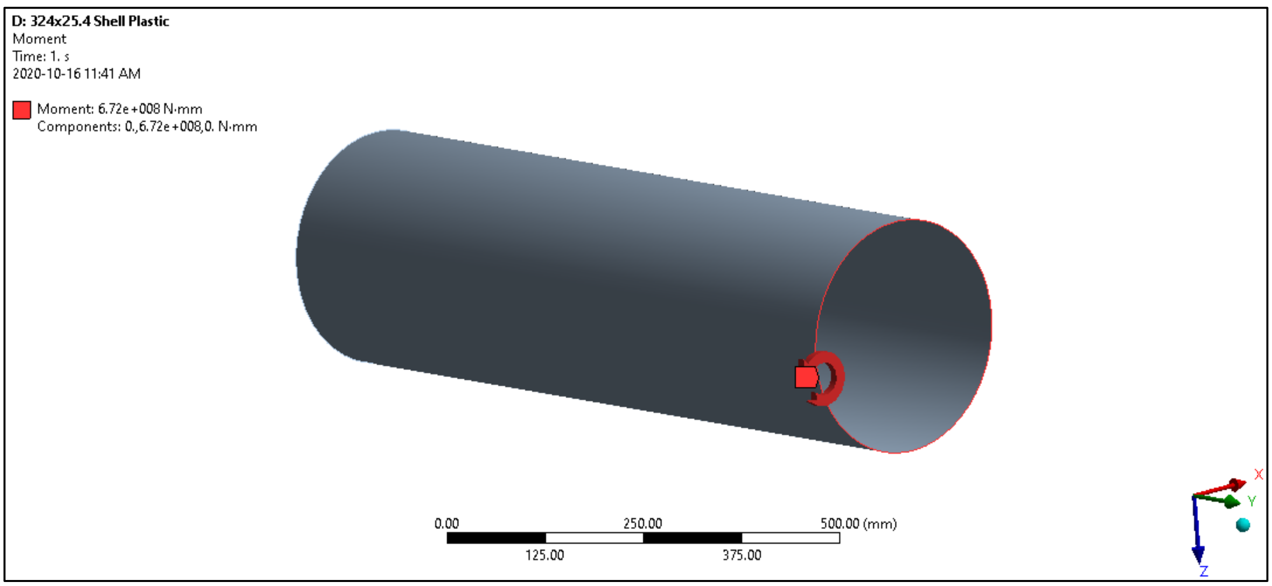


Figure 46: Load Case 2 - Round HSS 324x25 (Torsion Loading)

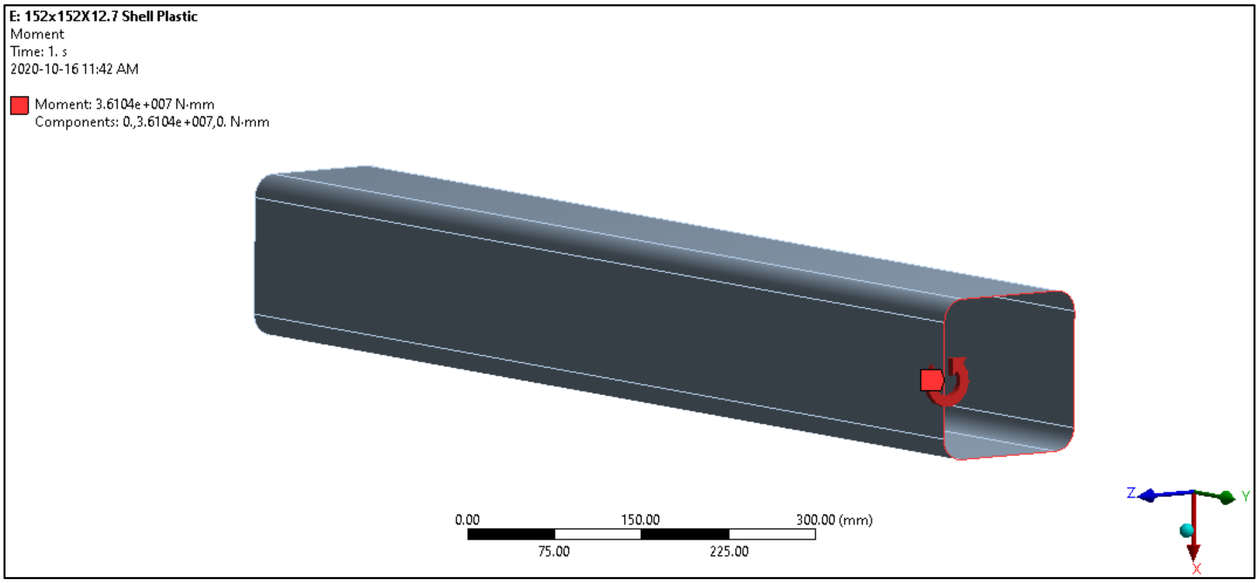


Figure 47: Load Case 3 - Square HSS 152x152x13 (Torsion Loading)

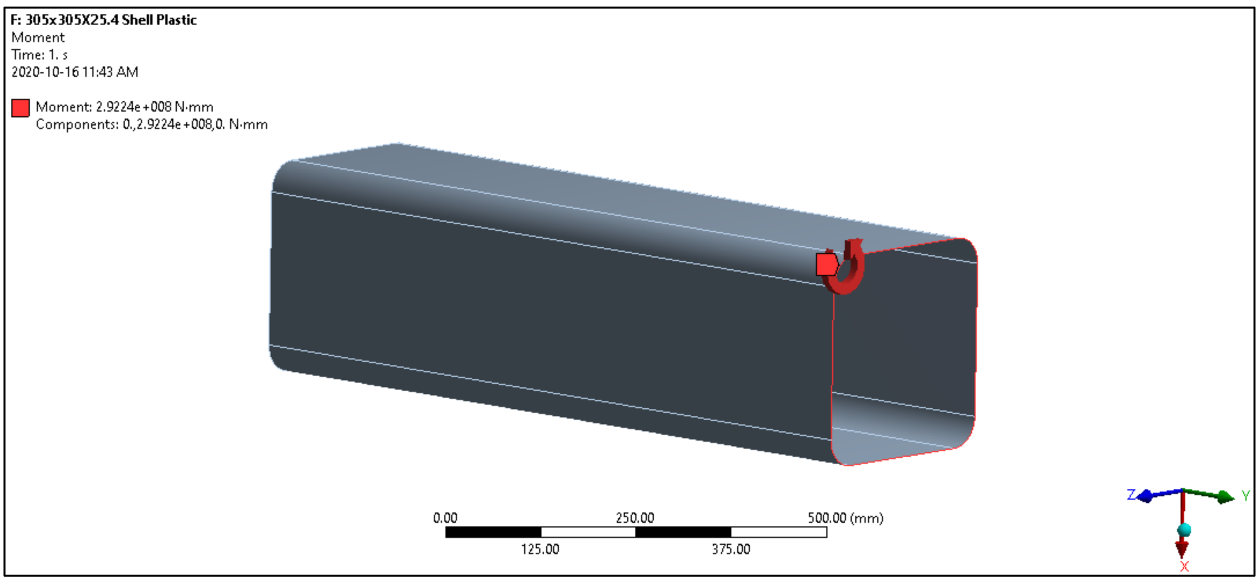


Figure 48: Load Case 4 - Square HSS 305x305x25 (Torsion Loading)

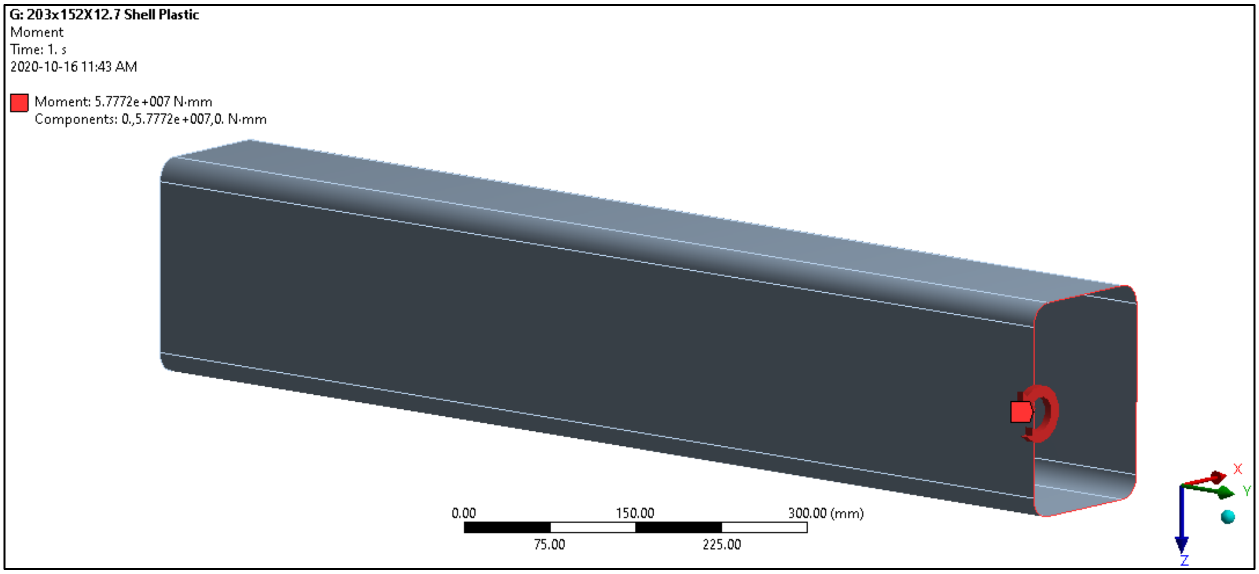


Figure 49: Load Case 5 - Rectangular HSS 203x152x13 (Torsion Loading)

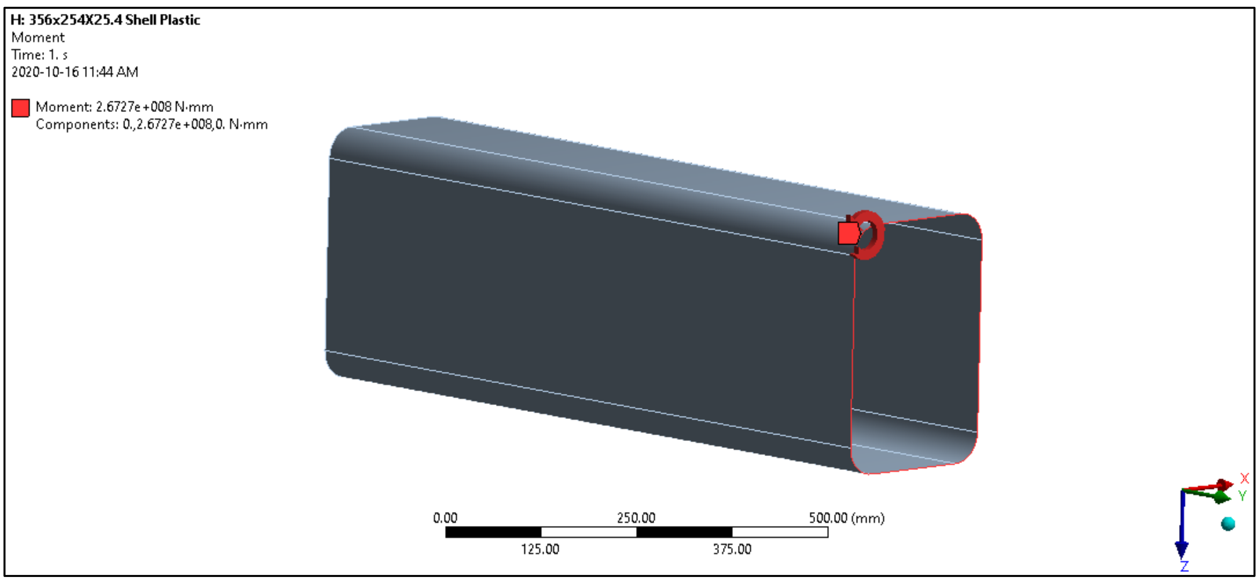


Figure 50: Load Case 6 - Rectangular HSS 356x254x25 Load Case (Torsion Loading)

For the combined models the loads were applied to the end of the shell section in the first load step, except the shear loads which were applied 0.1m from the support. End caps were included for the combined load cases to locally stiffen the open ends of the beams. When the combined loads were applied to the open end, the sections were failing in local buckling before reaching their combined capacity. It is noted if a HSS is subject to combined loading at the end of the section an end cap is required for local stiffening. The maximum combined capacities applied to the sections are shown in Figure 51 to Figure 53.

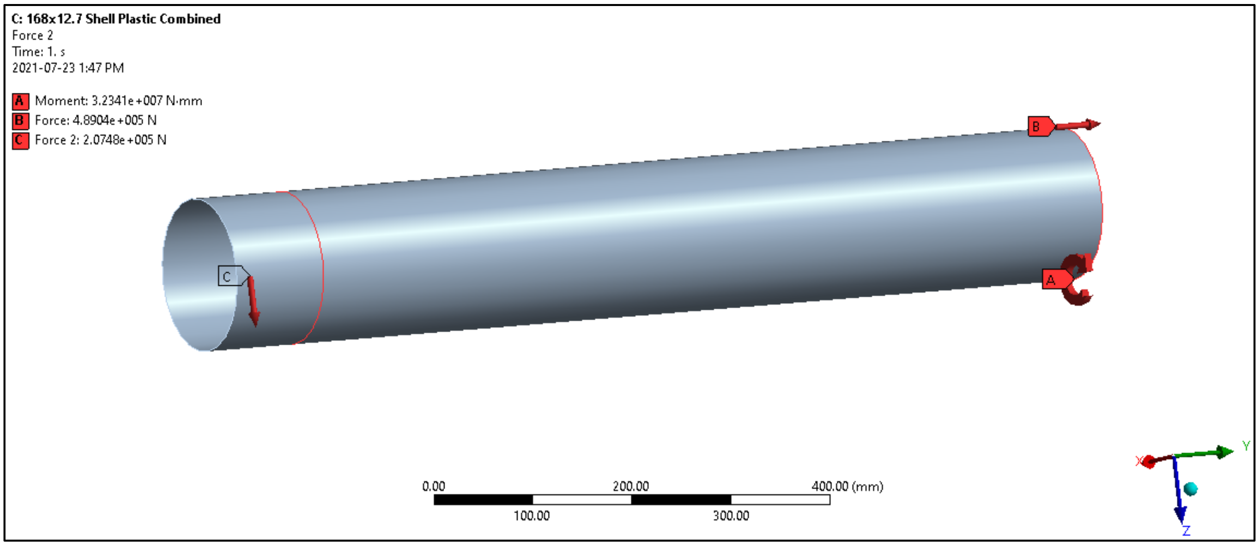


Figure 51: Load Case 7 - Round HSS 168x13 (Combined Loading)

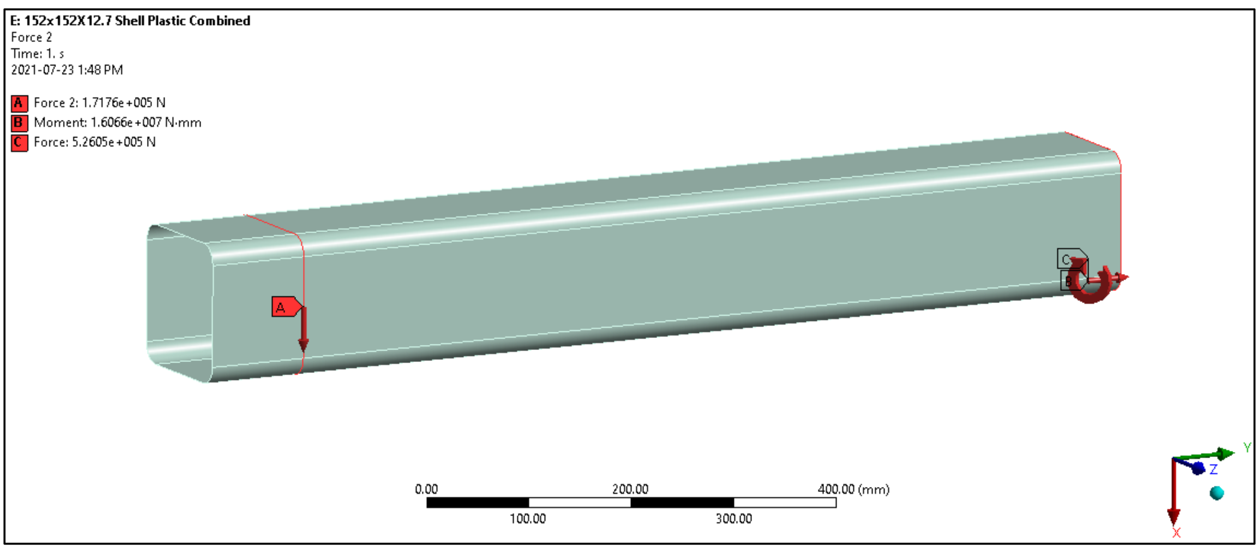


Figure 52: Load Case 8 - Square HSS 152x152x13 (Combined Loading)

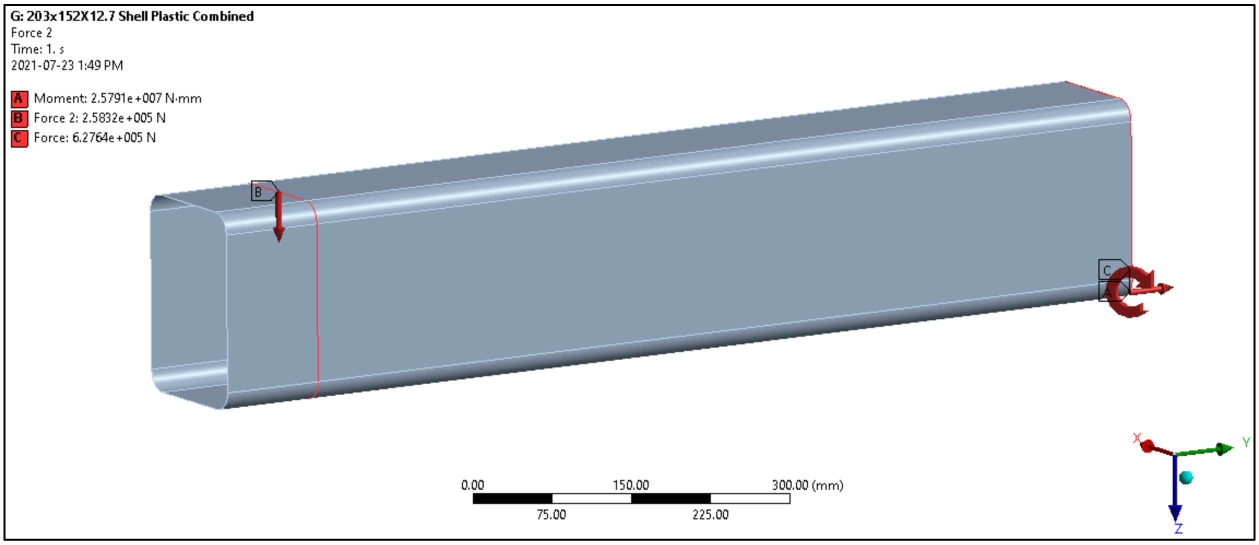


Figure 53: Load Case 9 - Rectangular HSS 203x152x13 (Combined Loading)

# Chapter 5 Discussion of Results

## 5.1 Finite Element Analysis Results

Equivalent Von-Mises Stress plots are shown below with stresses higher than allowable (315 MPa) but lower than the material yield (350 MPa) in red and higher than yield in grey. Equivalent plastic strain and deflection plots are also reported below for each load case. Local stresses over allowable and yield presented in the analysis will be discussed. Often finite element analysis results show local peak stress that has resulted from a mathematical discontinuity at sharp edges in the geometry rather than the actual deformation of the section.

The stresses are documented, however where a non-linear analysis has been completed the equivalent plastic strain will be evaluated to determine if the results are considered acceptable as previously discussed in Section 3.2. The equivalent plastic strain results provide the accurate basis for the evaluation of non-linear material models. The equivalent plastic strain is defined as the total strain energy that occurs in the plastic deformation of a material [65]. ANSYS redistributes the stress in areas above material yield in non-linear models utilizing strain hardening.

## 5.2 Finite Element Model Validation

To check the validation of the finite element (FE) cantilever models used in this thesis, two STAAD.Pro [66] models were developed for the round HSS 168x13 section. STAAD.Pro [66] is a different finite analysis software than ANSYS which is commonly used for beam element structural analysis. In one model the calculated AISC torsion capacity was applied to the beam which provided a utilization ratio of 0.996 as shown in Appendix B. In another model, the calculated AISC combined torsion, shear, flexure, and axial capacities were applied to the beam which provided a utilization ratio of 0.998 which is also shown in Appendix B. The STAAD model results are in alignment with FE model stress results presented in Sections 5.3 and 5.9, validating the FE model. The STAAD beam utilization ratios are basically at max capacity of the section which is expected confirming the section capacities are calculated/ applied correctly in the FE and STAAD models.

## 5.3 Load Case 1 – Round HSS 168x13 Torsion Loading

Equivalent stresses for load case 1 – round HSS 168x13 torsion loading, are shown in Figure 54 with a maximum stress of 348.9 MPa. The max stress occurs in the outer wall of the tubular close to the load application point as shown in Figure 55. The high-stress area is present on the extreme fibers of the material and not through the full thickness. The maximum stress is higher than allowable stress in accordance with CAN/CSA S16-19 [1] but lower than material yield stress which is expected due to the torsion capacity load applied.

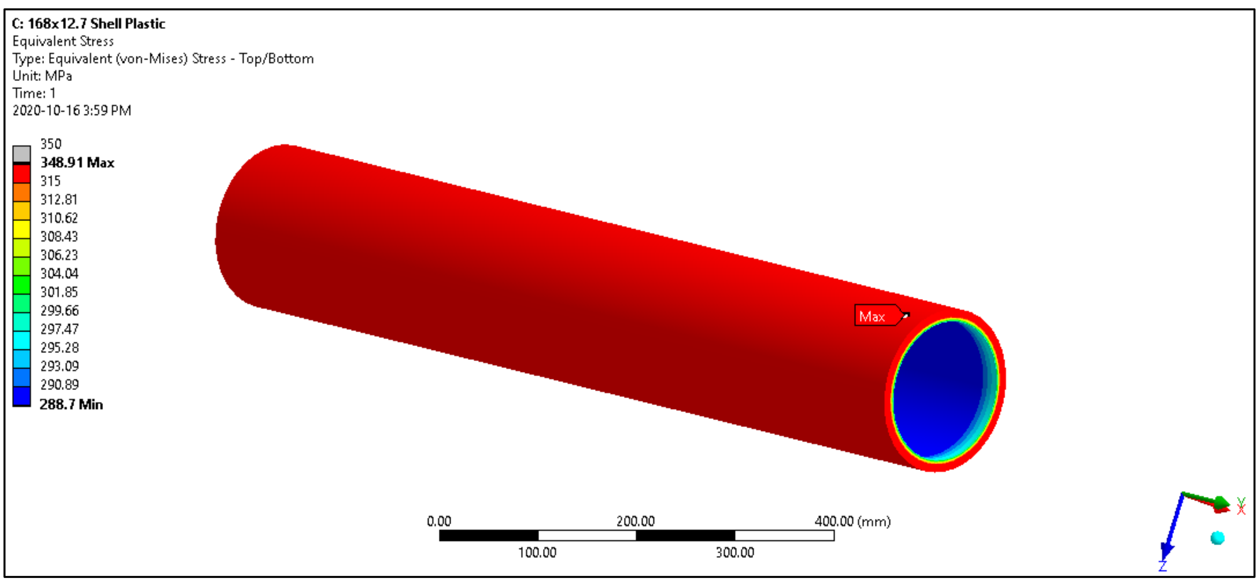

Figure 54: Load Case 1 - Round HSS 168x13 Torsion Loading Stress

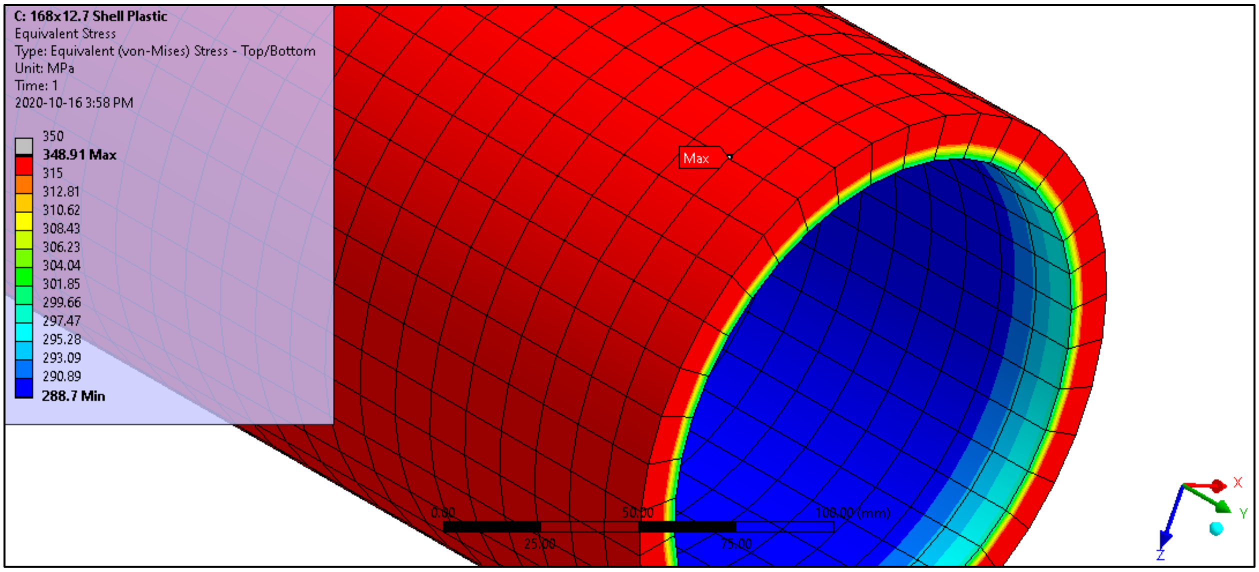


Figure 55: Load Case 1 - Round HSS 168x13 Torsion Loading Stress

Equivalent plastic strains for load case 1 – round HSS 168x13 torsion loading, are presented in Figure 56 with a maximum plastic strain of 0.00007 (0.007%). The max plastic strain occurs in the outer wall of the tubular close to the load application point as shown in Figure 57. The peak nodal strain value is sufficiently below the allowable linearized averaged plastic strain of 0.04 (4%) in accordance with DNVGL-RP-C208 [63], therefore the strain results are considered acceptable.

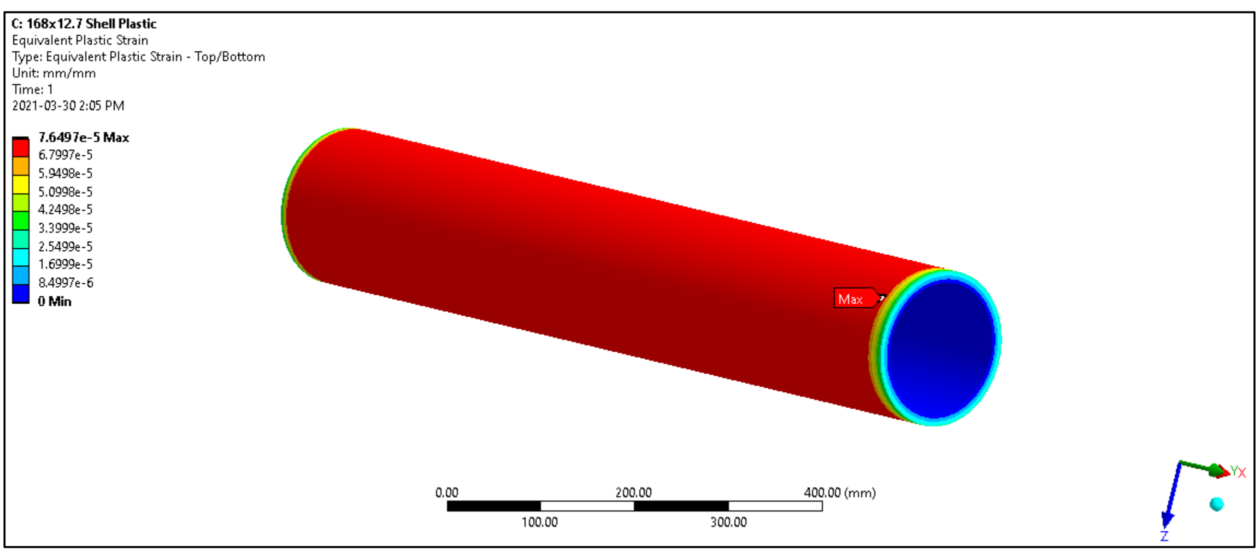


Figure 56: Load Case 1 - Round HSS 168x13 Torsion Loading Plastic Strain

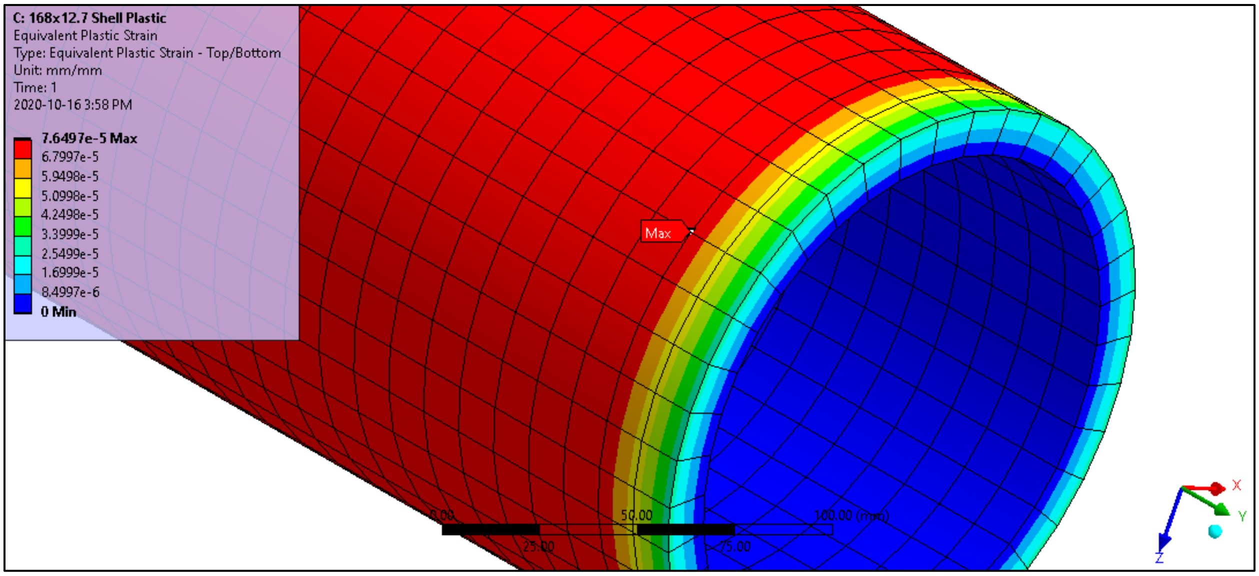


Figure 57: Load Case 1 - Round HSS 168x13 Torsion Loading Plastic Strain

The total deflection under load case 1 is shown in Figure 58. The maximum deflection value of 2.48 mm is acceptable for defection at failure magnitude.

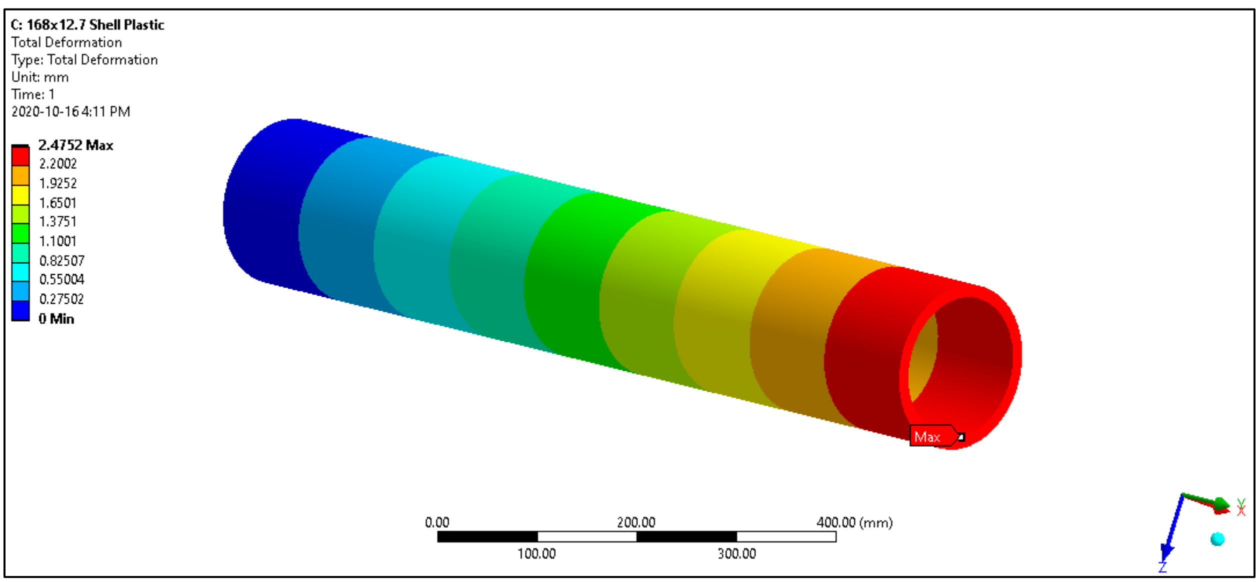


Figure 58: Load Case 1 - Round HSS 168x13 Torsion Loading Deflection

## 5.4 Load Case 2 – Round HSS 324x25 Torsion Loading

Equivalent stresses for load case 2 – round HSS 324x25 torsion loading, are shown in Figure 59 with a maximum stress of 348.8 MPa. The max stress occurs in the outer wall of the tubular close to the load application point as shown in Figure 60. The high-stress area is present on the extreme fibers of the material and not through the full thickness. The maximum stress is higher than allowable stress in accordance with CAN/CSA S16-19 [1] but lower than material yield stress which is expected due to the torsion capacity load applied. Note, the maximum stress is of a similar magnitude as determined in the previous round HSS load case.

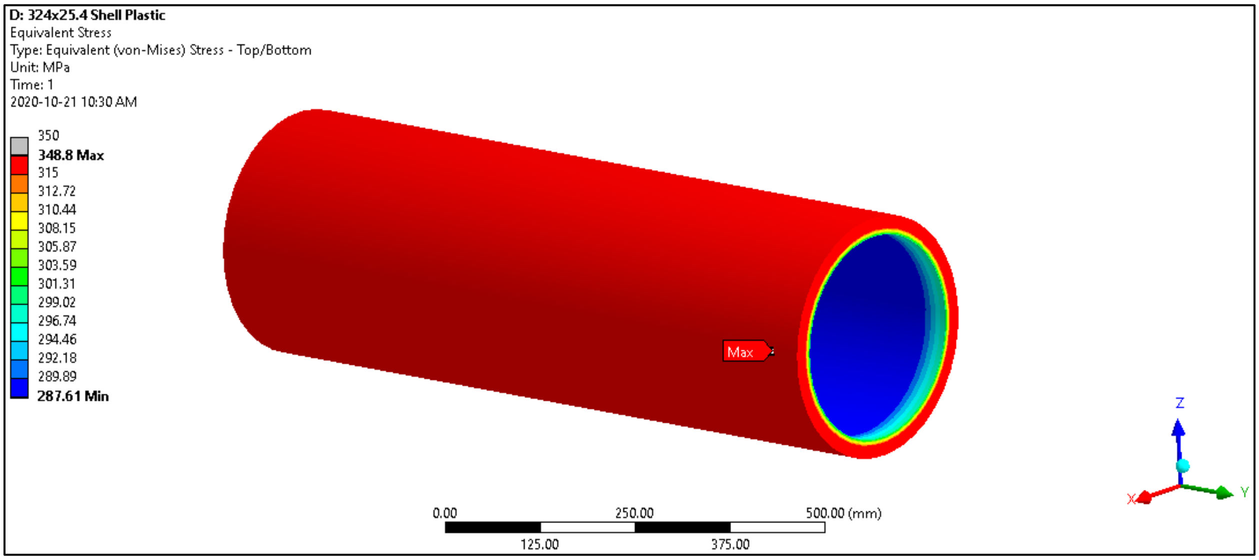


Figure 59: Load Case 2 - Round HSS 324x25 Torsion Loading Stress

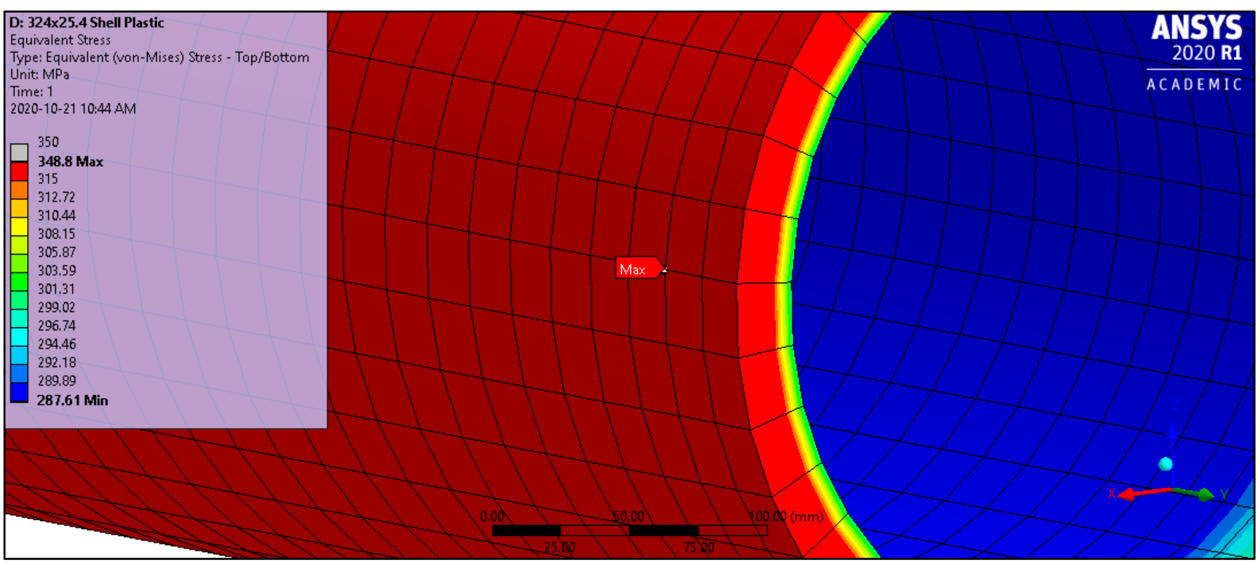


Figure 60: Load Case 2 - Round HSS 324x25 Torsion Loading Stress

Equivalent plastic strains for load case 2 – round HSS 324x25 torsion loading, are presented in Figure 61 with a maximum plastic strain of 0.00009 (0.009%). The max plastic strain occurs in the outer wall of the tubular close to the load application point as shown in Figure 62. The peak nodal strain value is sufficiently below the allowable linearized averaged plastic strain of 0.04 (4%) in accordance with DNVGL-RP-C208 [63], therefore the strain results are considered acceptable. Note, the maximum plastic strain is of a similar magnitude as determined in the previous round HSS load case.

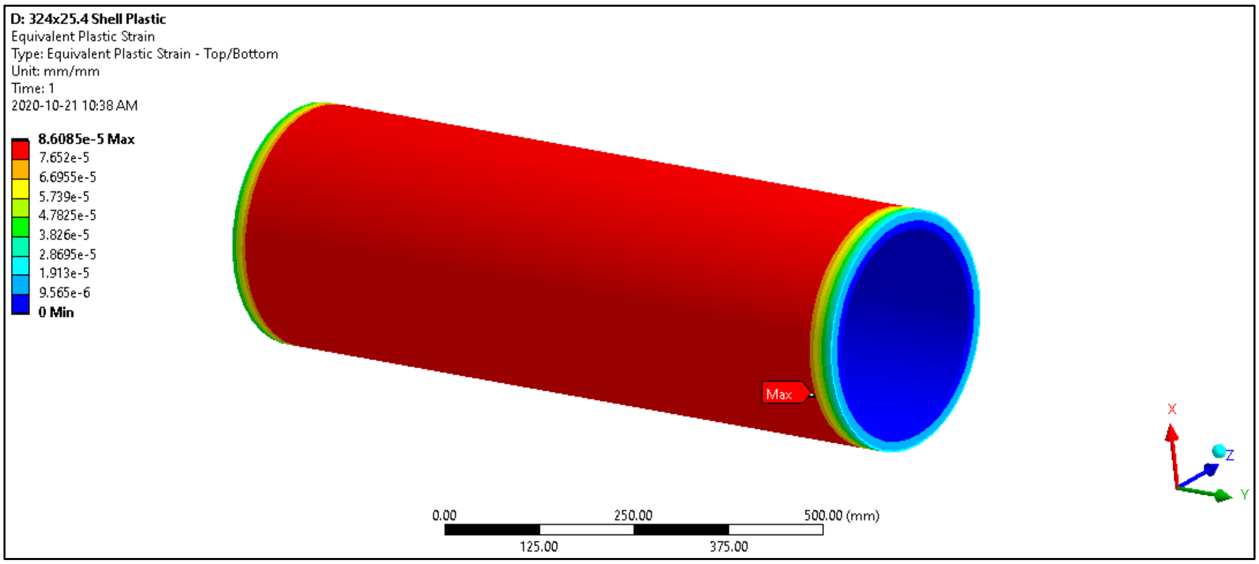


Figure 61: Load Case 2 - Round HSS 324x25 Torsion Loading Plastic Strain

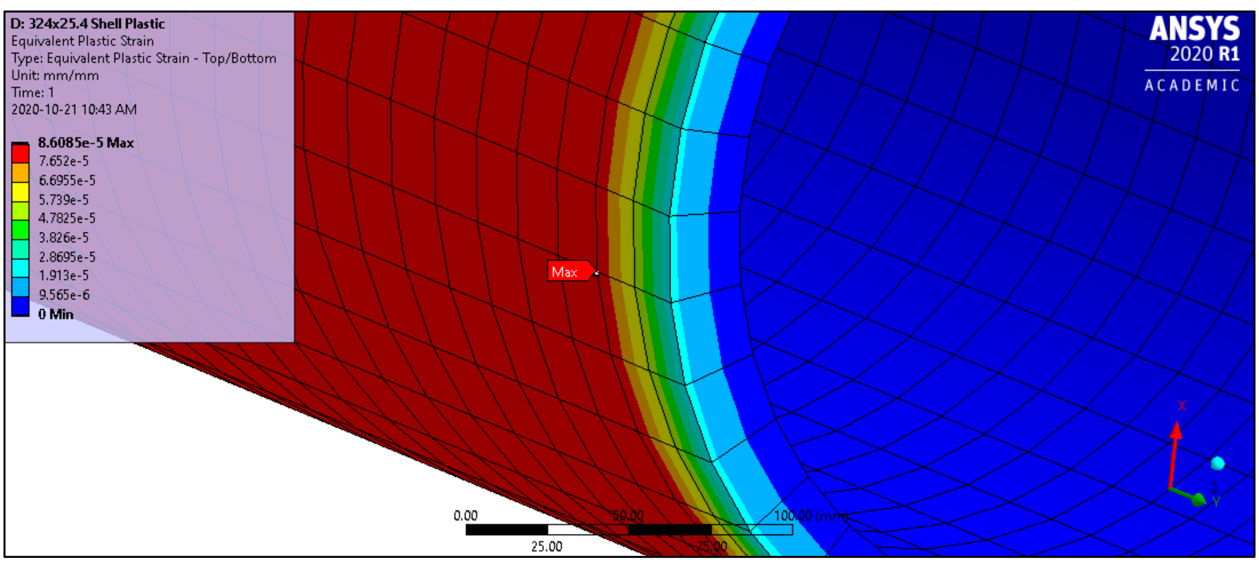


Figure 62: Load Case 2 - Round HSS 324x25 Torsion Loading Plastic Strain

The total deflection under load case 2 is shown in Figure 63. The maximum deflection value of 2.48 mm is acceptable for a defection at failure magnitude.

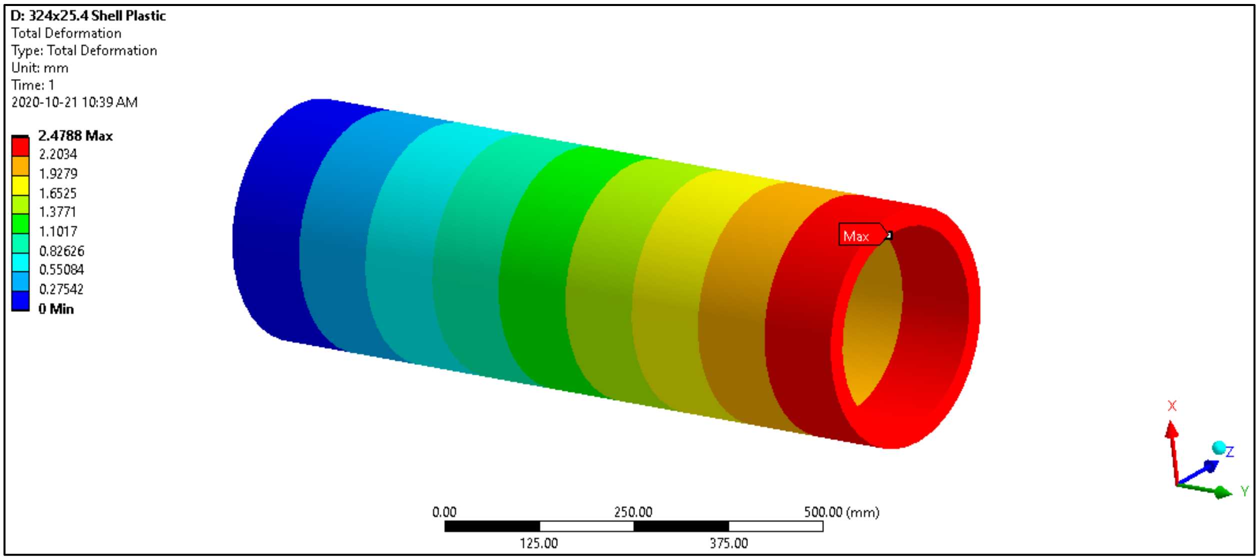

Figure 63: Load Case 2 - Round HSS 324x25 Torsion Loading Deflection

## 5.5 Load Case 3 – Square HSS 152x152x13 Torsion Loading

Equivalent stresses for load case 3 – square HSS 152x152x13 torsion loading, are shown in Figure 64 with a maximum stress of 332.7 MPa. The max stress occurs at the edge of the section at the load application point as shown in Figure 65. The maximum stress value is only present on the edge of the element and not through the thickness, this is a mathematical discontinuity due to the load application rather than a representation of actual stress and is not considered an issue. The maximum stress is higher than allowable stress in accordance with CAN/CSA S16-19 [1] but lower than material yield stress which is expected due to the torsion capacity load applied.

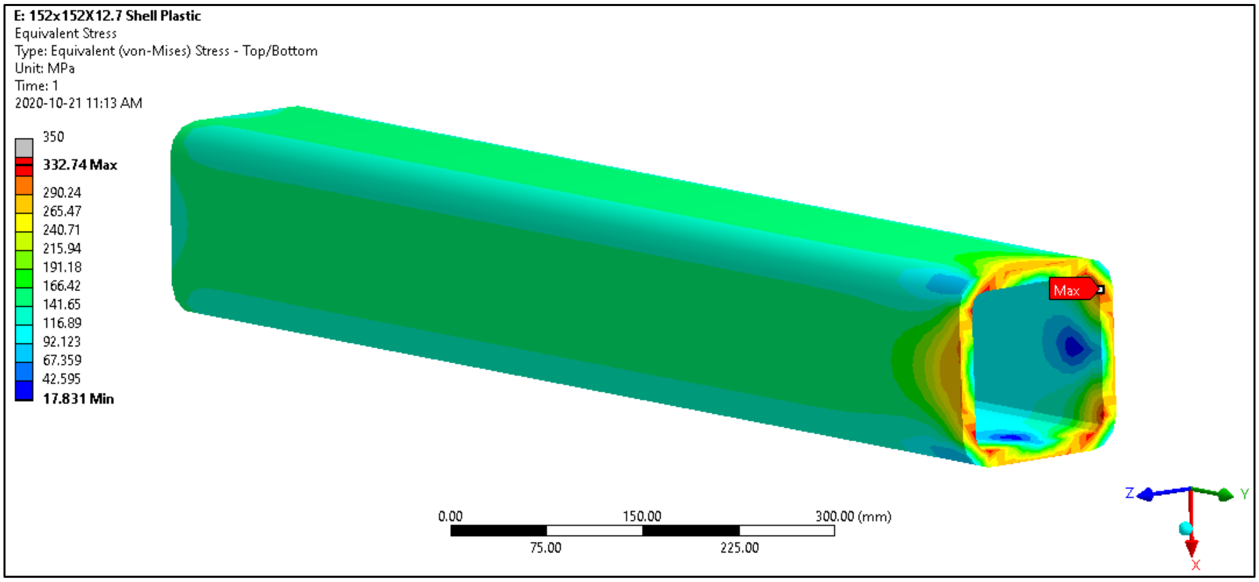


Figure 64: Load Case 3 - Square HSS 152x152x13 Torsion Loading Stress

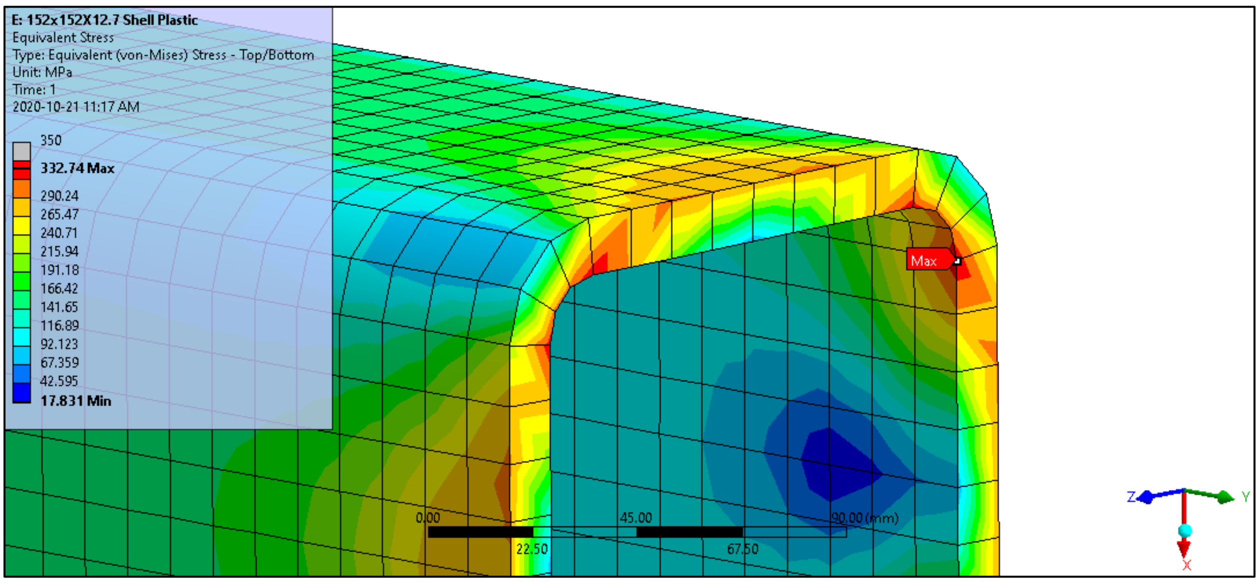


Figure 65: Load Case 3 - Square HSS 152x152x13 Torsion Loading Stress

Equivalent plastic strains for load case 3 – square HSS 152x152x13 torsion loading, are presented in Figure 65 with a maximum plastic strain of 0 (0%). Although the applied torsion magnitude was the calculated section capacity, it was not large enough to cause the square HSS to plastically strain to produce a strain value. The peak nodal strain value is sufficiently below the allowable linearized averaged plastic strain of 0.04 (4%) in accordance with DNVGL-RP-C208 [63], therefore the strain results are considered acceptable.

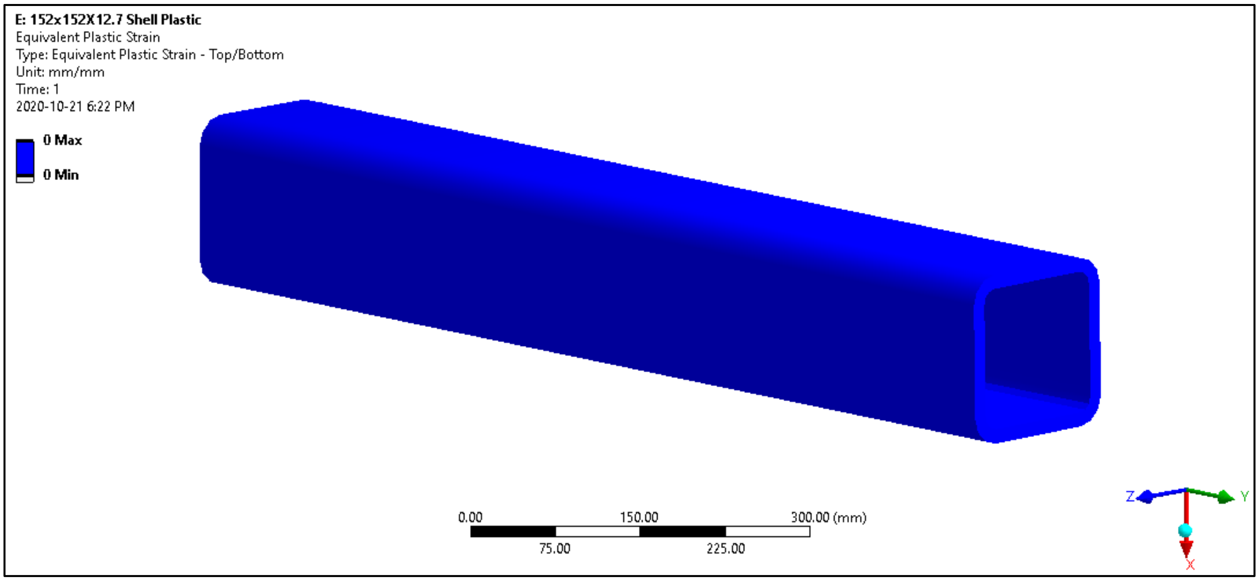


Figure 66: Load Case 3 - Square HSS 152x152x13 Torsion Loading Plastic Strain

The total deflection under load case 3 is shown in Figure 67. The maximum deflection value of 1.23 mm is acceptable for a defection at failure magnitude.

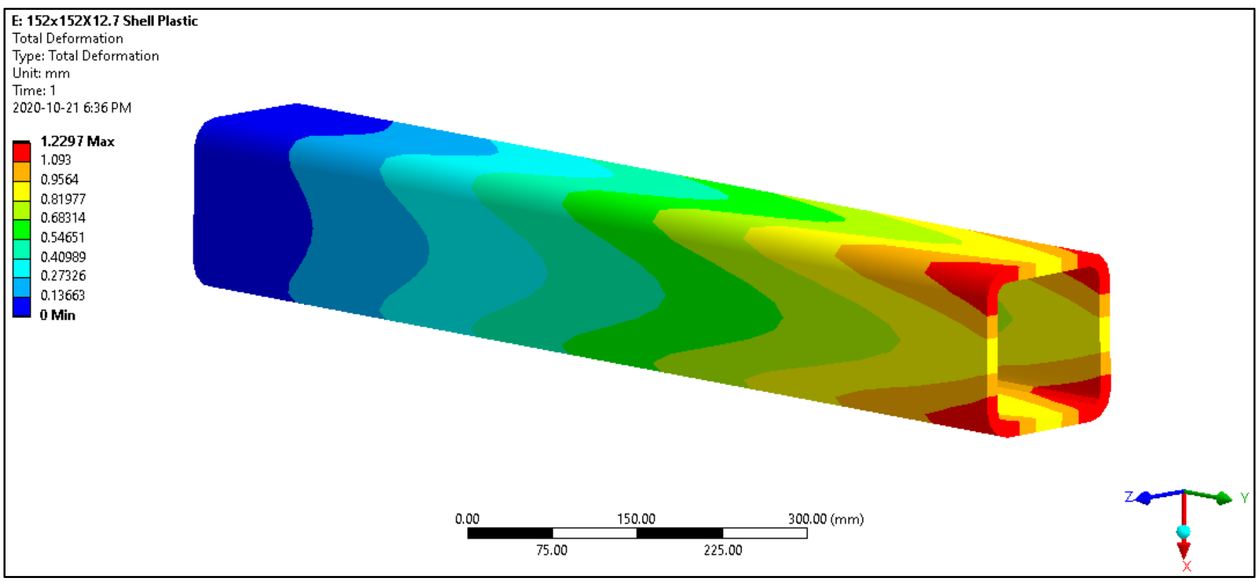


Figure 67: Load Case 3 - Square HSS 152x152x13 Torsion Loading Deflection

## 5.6 Load Case 4 – Square HSS 305x305x25 Torsion Loading

Equivalent stresses for load case 4 – square HSS 305x305x25 torsion loading, are shown in Figure 68 with a maximum stress of 337.7 MPa. The max stress occurs at the edge of the section at the load application point as shown in Figure 69. The maximum stress value is only present on the edge of the element and not through the thickness, this is a mathematical discontinuity due to the load application rather than a representation of actual stress and is not considered an issue. The maximum stress is higher than allowable stress in accordance with CAN/CSA S16-19 [1] but lower than material yield stress which is expected due to the torsion capacity load applied. Note, the maximum stress is of a similar magnitude as determined in the previous square HSS load case.

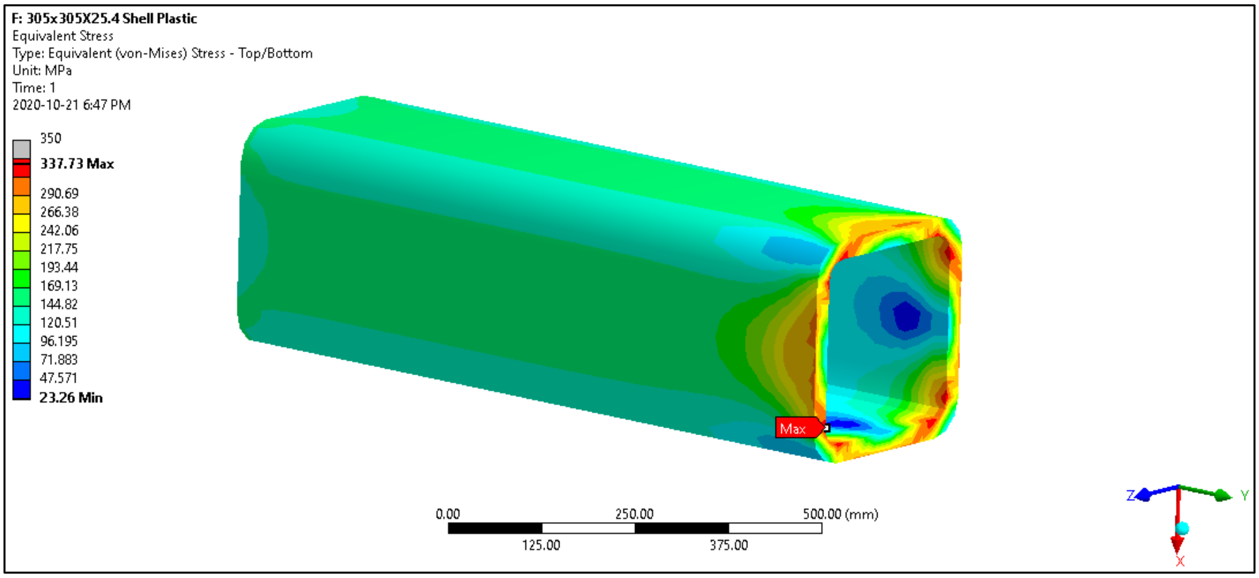


Figure 68: Load Case 4 - Square HSS 305x305x25 Torsion Loading Stress

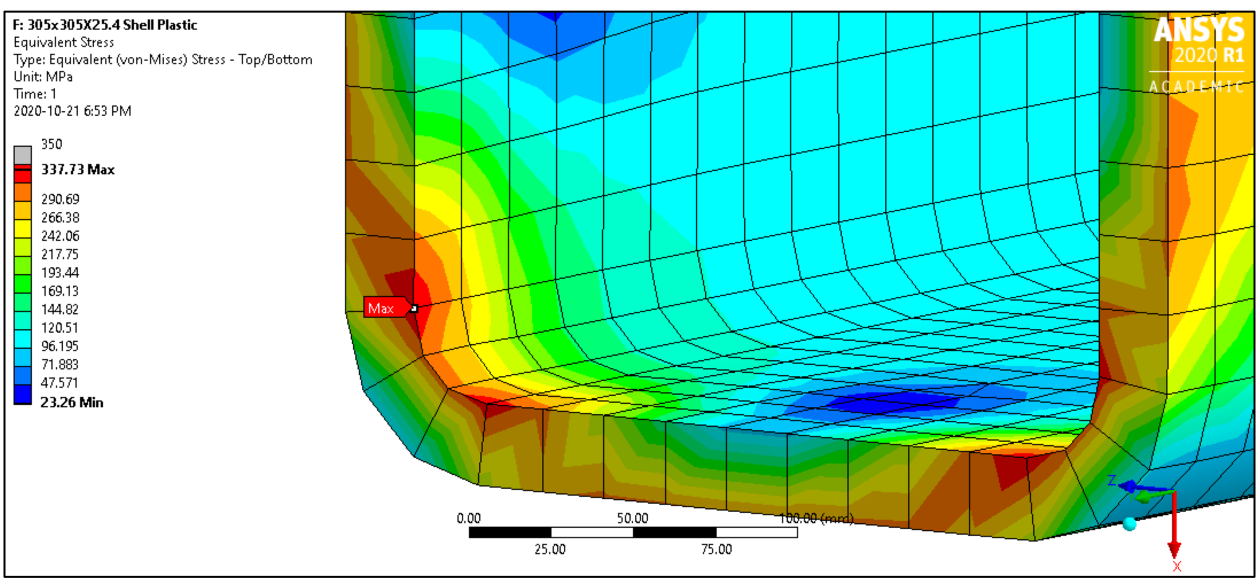


Figure 69: Load Case 4 - Square HSS 305x305x25 Torsion Loading Stress

Equivalent plastic strains for load case 4 – square HSS 305x305x25 torsion loading, are presented in Figure 70 with a maximum plastic strain of 0 (0%). Although the applied torsion magnitude was the calculated section capacity, it was not large enough to cause the square HSS to plastically strain to produce a strain value. The peak nodal strain value is sufficiently below the allowable linearized averaged plastic strain of 0.04 (4%) in accordance with DNVGL-RP-C208 [63], therefore the strain results are considered acceptable. Note, the maximum plastic strain is the same value as determined in the previous square HSS load case.

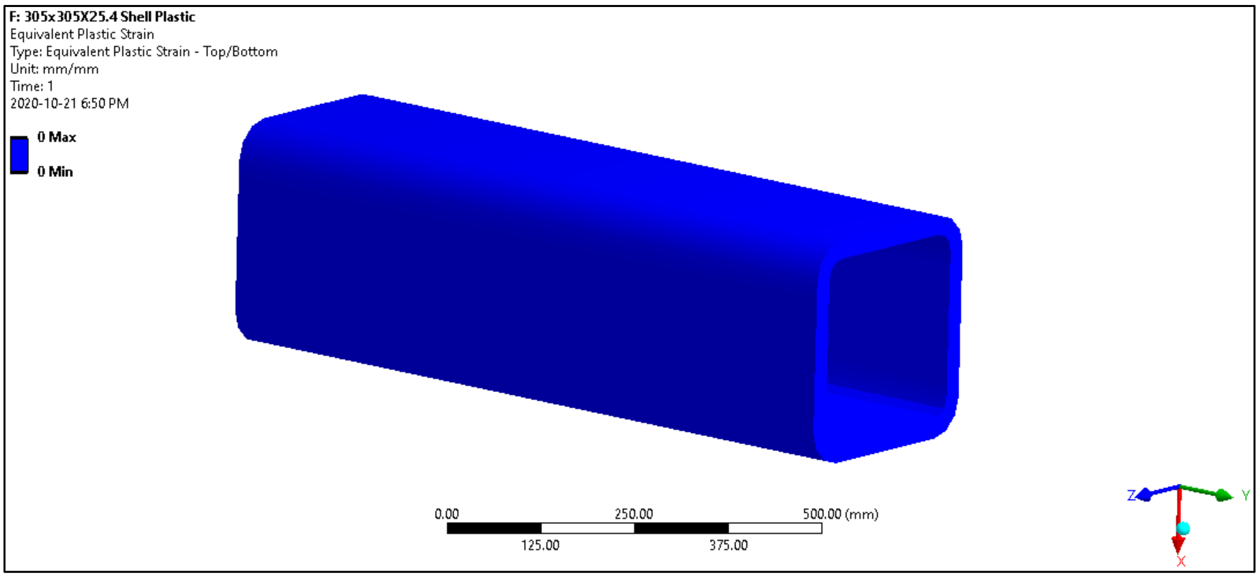


Figure 70: Load Case 4 - Square HSS 305x305x25 Torsion Loading Plastic Strain

The total deflection under load case 4 is shown in Figure 71. The maximum deflection value of 1.28 mm is acceptable for a defection at failure magnitude.

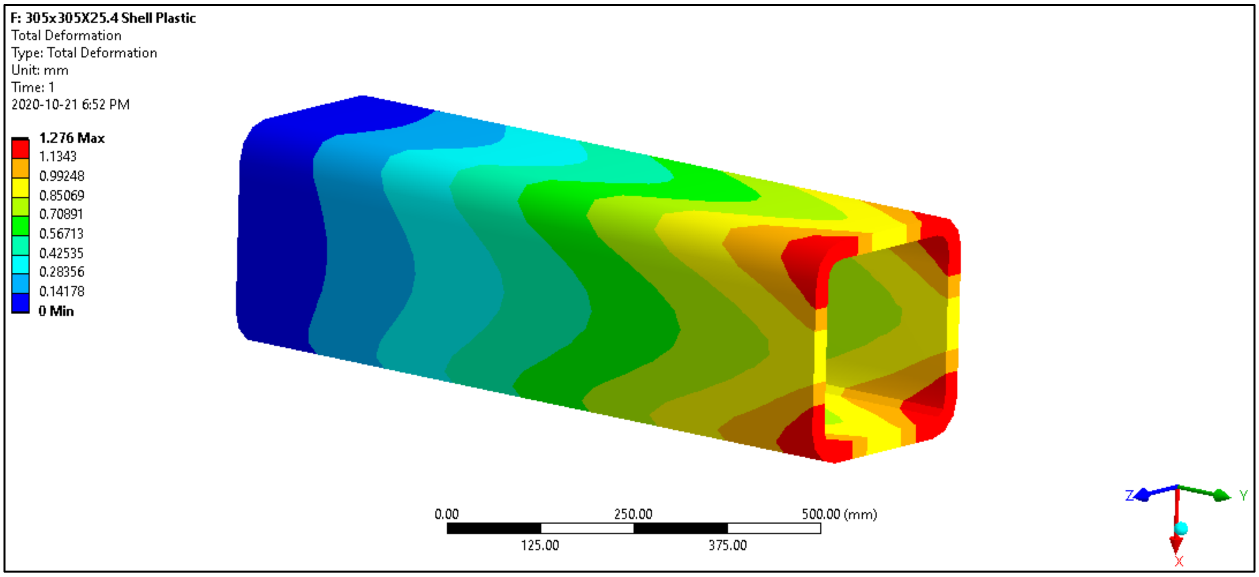


Figure 71: Load Case 4 - Square HSS 305x305x25 Torsion Loading Deflection

## 5.7 Load Case 5 – Rectangular HSS 203x152x13 Torsion Loading

Equivalent stresses for load case 5 – rectangular HSS 203x152x13 torsion loading, are shown in Figure 72 with a maximum stress of 349.0 MPa. The max stress occurs in the outer wall thickness of the tubular close to the load application point as shown in Figure 73. The maximum stress is higher than allowable stress in accordance with CAN/CSA S16-19 [1] but lower than material yield stress which is expected due to the torsion capacity load applied.

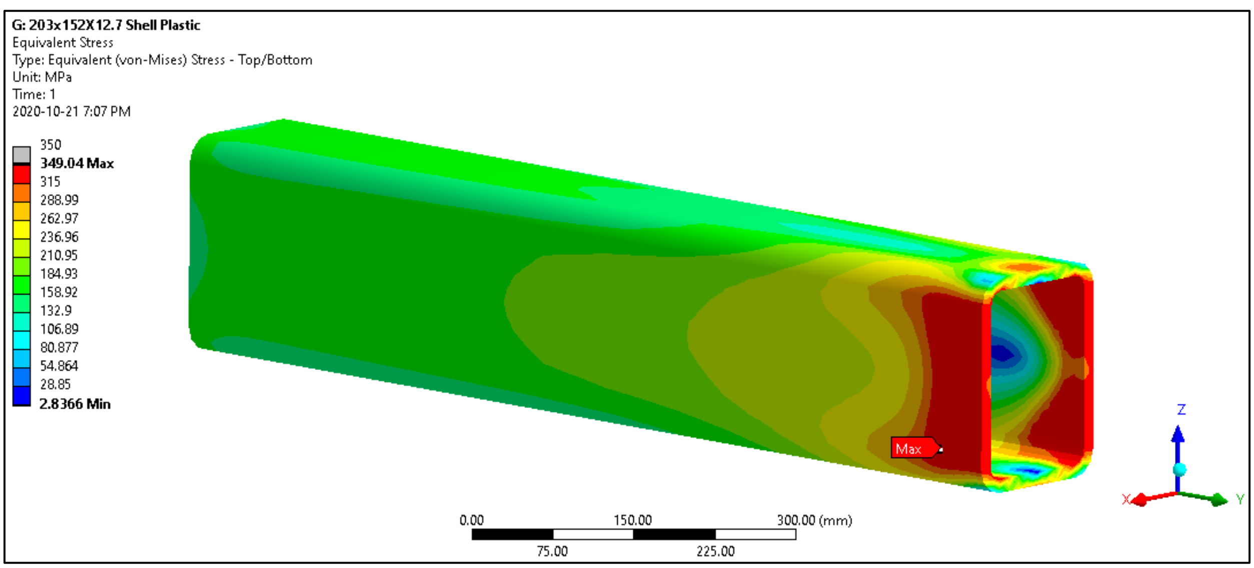


Figure 72: Load Case 5 - Rectangular HSS 203x152x13 Torsion Loading Stress

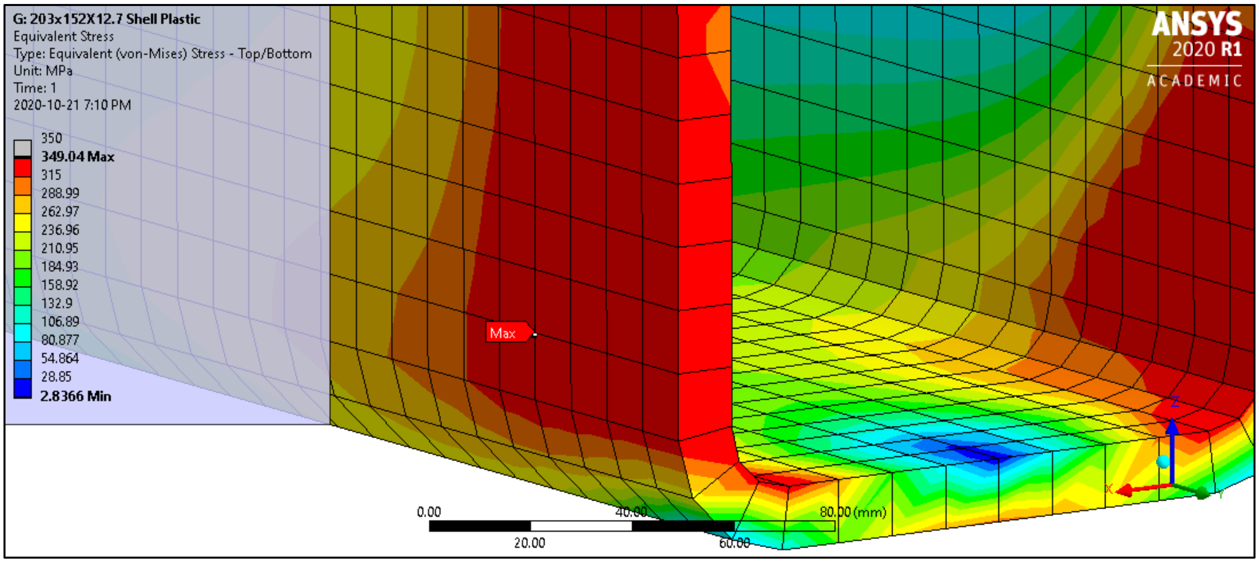


Figure 73: Load Case 5 - Rectangular HSS 203x152x13 Torsion Loading Stress

Equivalent plastic strains for load case 5 – rectangular HSS 203x152x13 torsion loading, are presented in Figure 74 with a maximum plastic strain of 0.0032 (0.32%). The max plastic strain occurs in the outer wall thickness of the tubular close to the load application point as shown in Figure 75. The peak nodal strain value is below the allowable linearized averaged plastic strain of 0.04 (4%) in accordance with DNVGL-RP-C208 [63], therefore the strain results are considered acceptable.

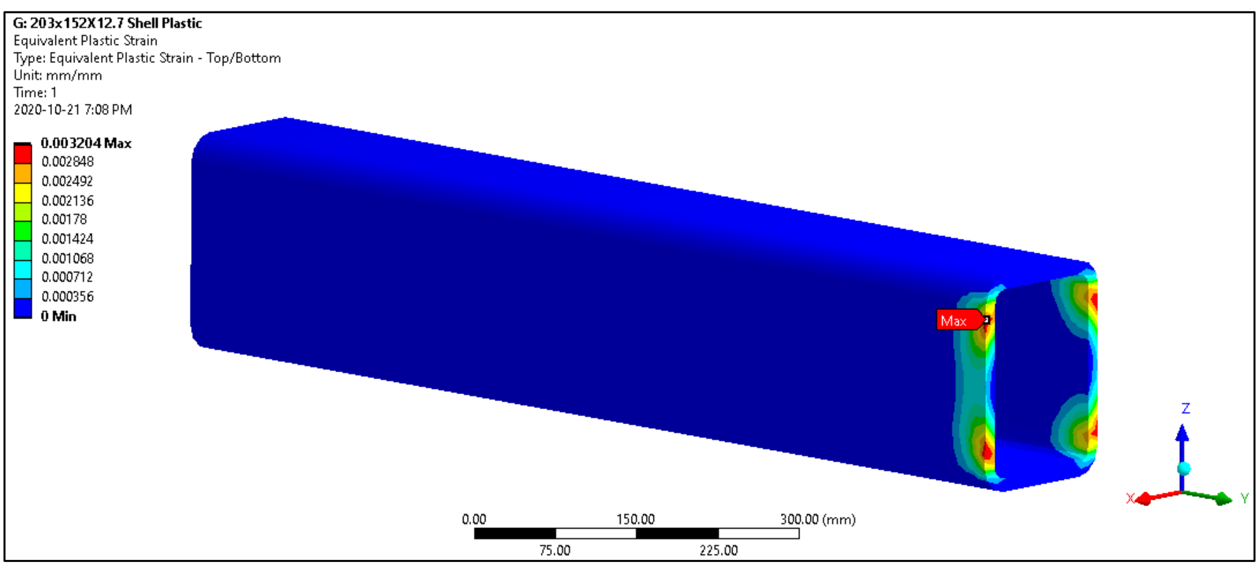


Figure 74: Load Case 5 - Rectangular HSS 203x152x13 Torsion Loading Plastic Strain

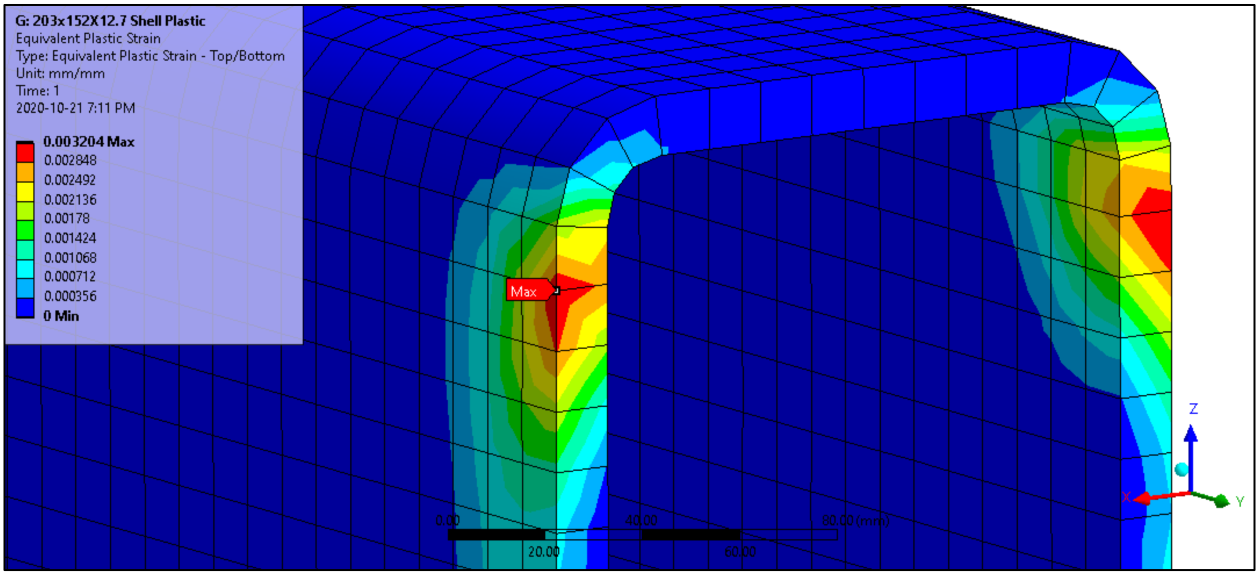


Figure 75: Load Case 5 - Rectangular HSS 203x152x13 Torsion Loading Plastic Strain

The total deflection under load case 5 is shown in Figure 76. The maximum deflection value of 2.15 mm is acceptable for a defection at failure magnitude.

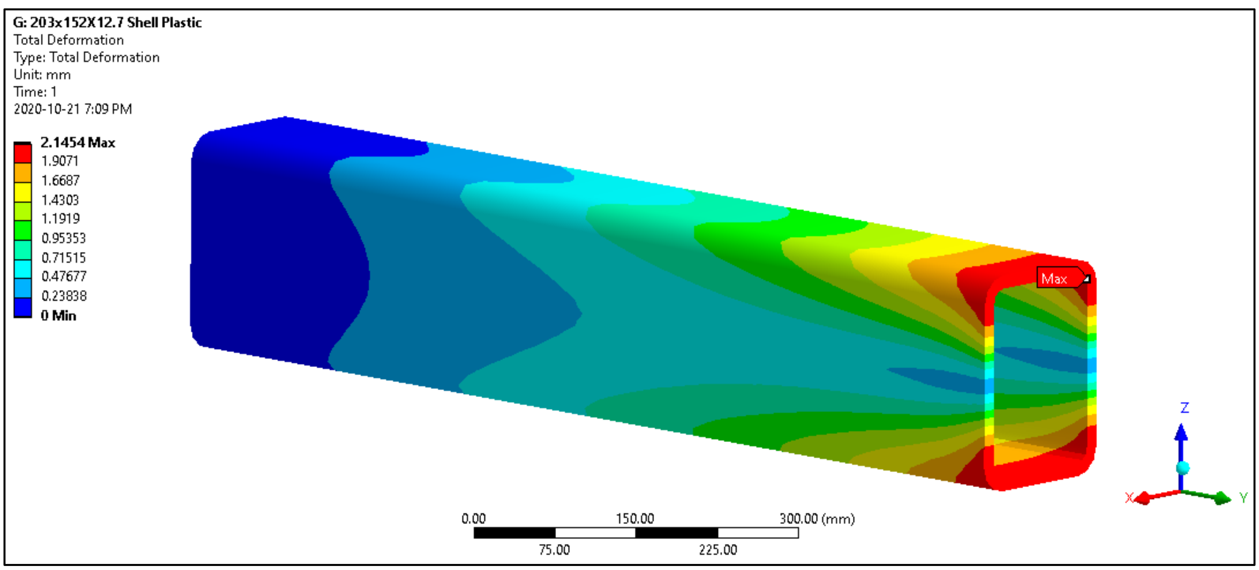


Figure 76: Load Case 5 - Rectangular HSS 203x152x13 Torsion Loading Deflection

## 5.8 Load Case 6 – Rectangular HSS 356x254x25 Torsion Loading

Equivalent stresses for load case 6 – rectangular HSS 356x254x25 torsion loading, are shown in Figure 77 with a maximum stress of 349.0 MPa. The max stress occurs in the outer wall thickness of the tubular close to the load application point as shown in Figure 78. The maximum stress is higher than allowable stress in accordance with CAN/CSA S16-19 [1] but lower than material yield stress which is expected due to the torsion capacity load applied. Note, the maximum stress is of a similar magnitude as determined in the previous rectangular HSS load case.

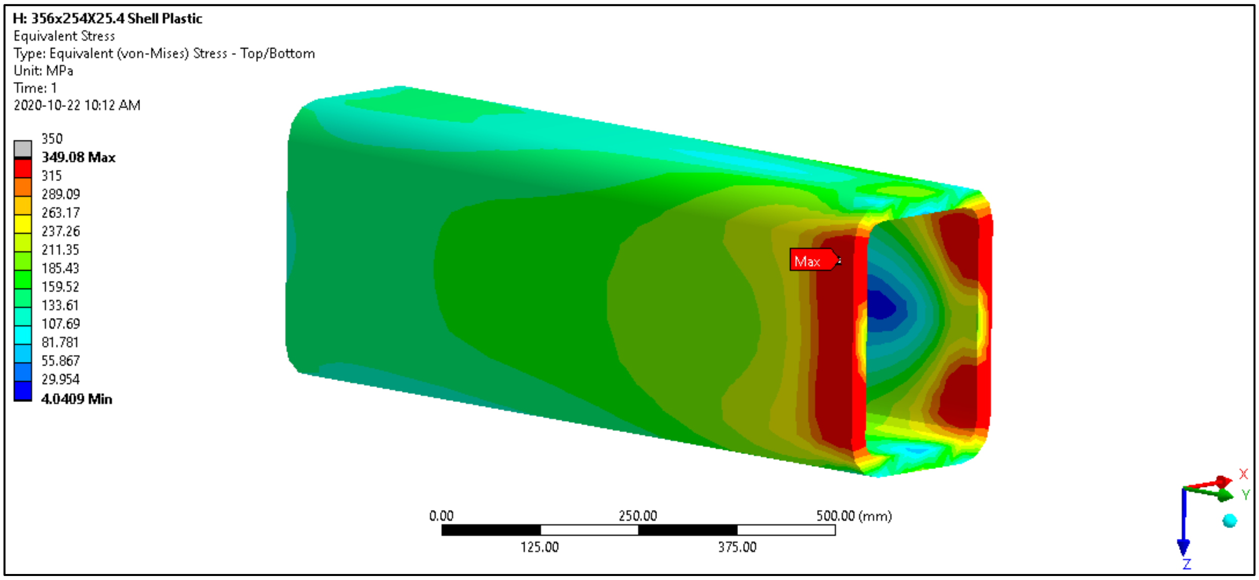


Figure 77: Load Case 6 - Rectangular HSS 356x254x25 Torsion Loading Stress

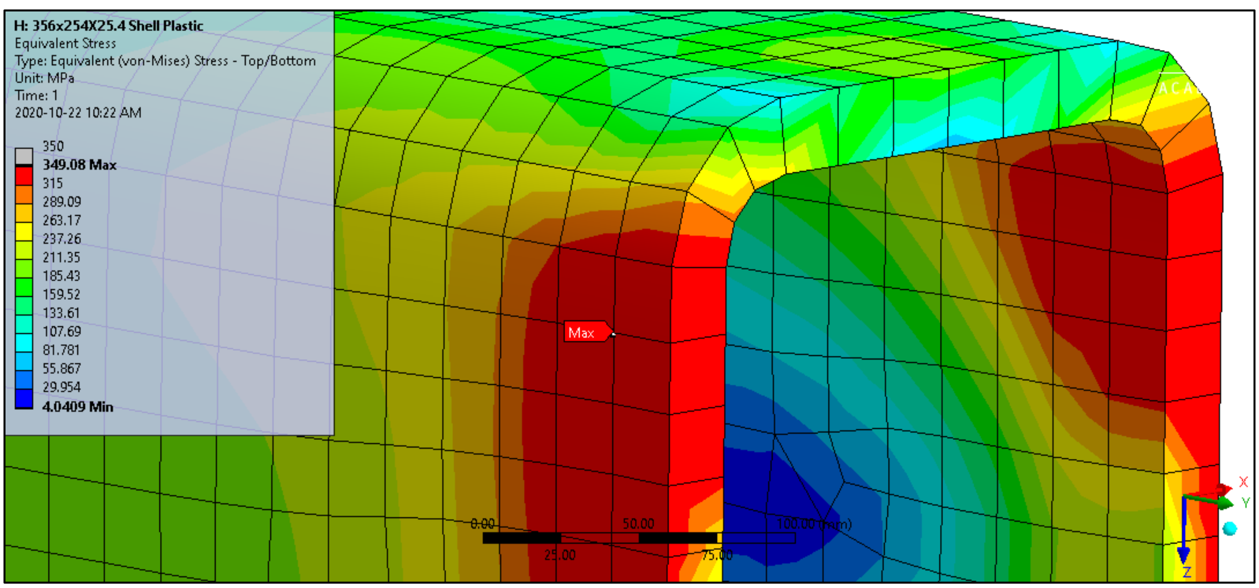


Figure 78: Load Case 6 - Rectangular HSS 356x254x25 Torsion Loading Stress

Equivalent plastic strains for load case 6 – rectangular HSS 356x254x25 torsion loading, are presented in Figure 79 with a maximum plastic strain of 0.0011 (0.11%). The max plastic strain occurs in the outer wall thickness of the tubular close to the load application point as shown in

Figure 80. The peak nodal strain value is below the allowable linearized averaged plastic strain of 0.04 (4%) in accordance with DNVGL-RP-C208 [63], therefore the strain results are considered acceptable. Note, the maximum plastic strain is of a similar magnitude as determined in the previous rectangular HSS load case.

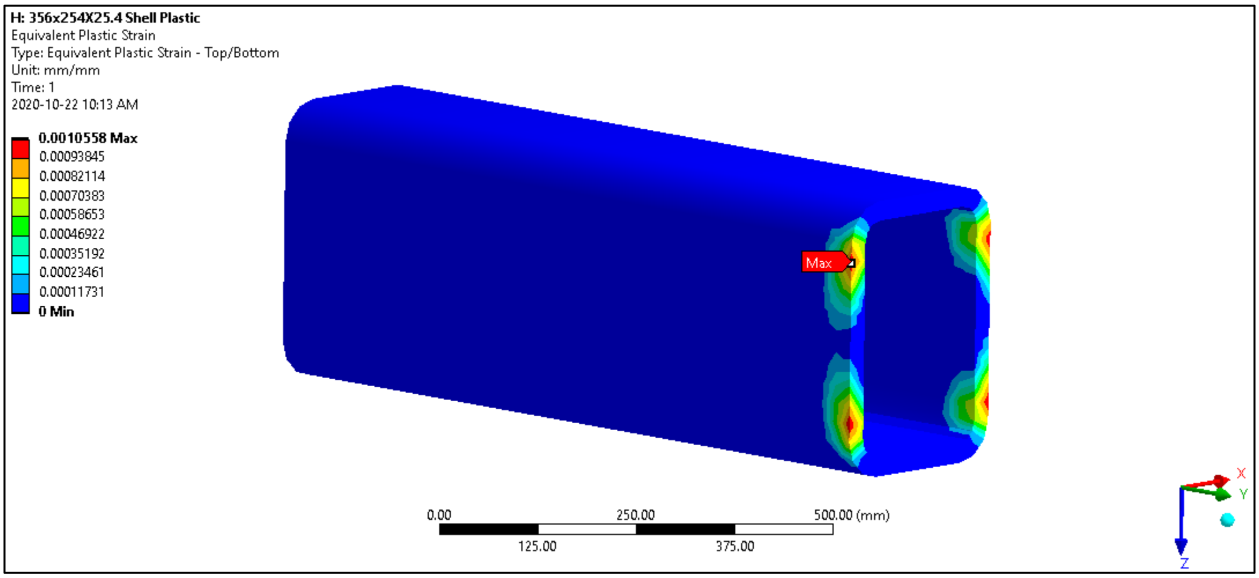


Figure 79: Load Case 6 - Rectangular HSS 356x254x25 Torsion Loading Plastic Strain

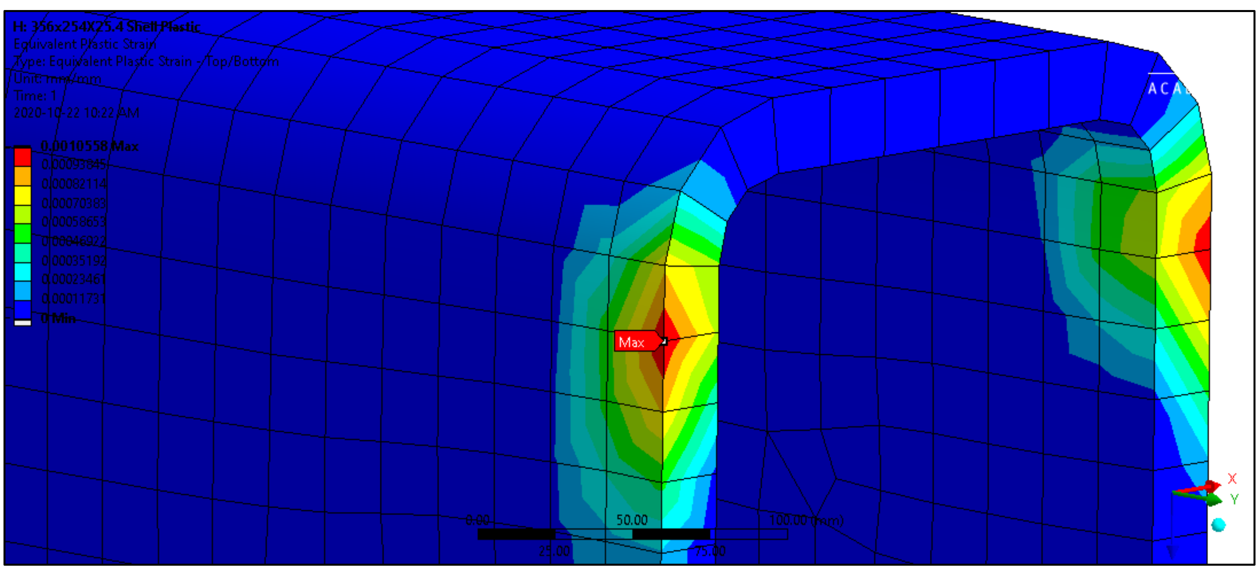


Figure 80: Load Case 6 - Rectangular HSS 356x254x25 Torsion Loading Plastic Strain

The total deflection under load case 6 is shown in Figure 81. The maximum deflection value of 2.09 mm is acceptable for a defection at failure magnitude.

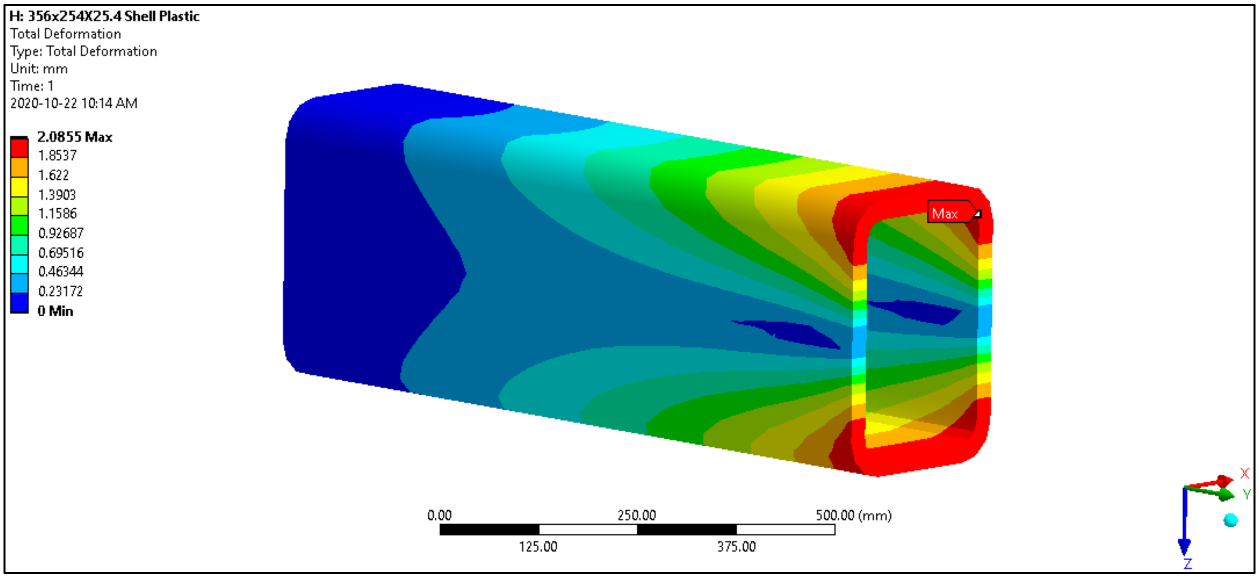


Figure 81: Load Case 6 - Rectangular HSS 356x254x25 Torsion Loading Deflection

## 5.9 Load Case 7 – Round HSS 168x13 Combined Loading

Equivalent stresses for load case 7 – round HSS 168x13 combined loading, are shown in Figure 82 with a maximum stress of 289.2 MPa. The max stress occurs at the outer diameter edge of the tubular at the fixed support as shown in Figure 83. The maximum stress is lower than allowable stress in accordance with CAN/CSA S16-19 [1].

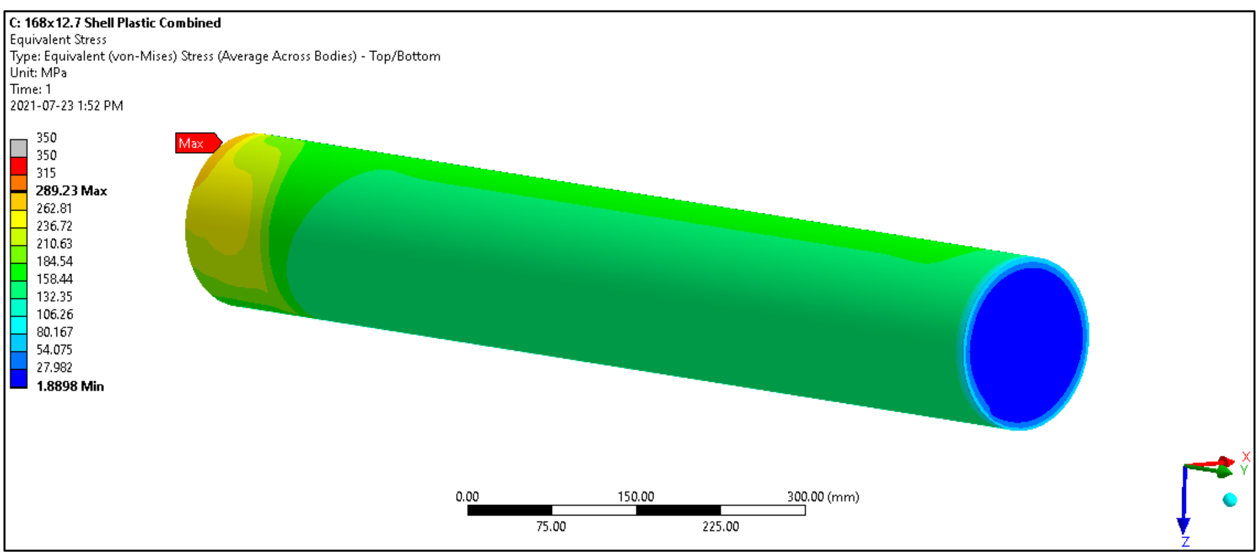


Figure 82: Load Case 7 - Round HSS 168x13 Combined Loading Stress

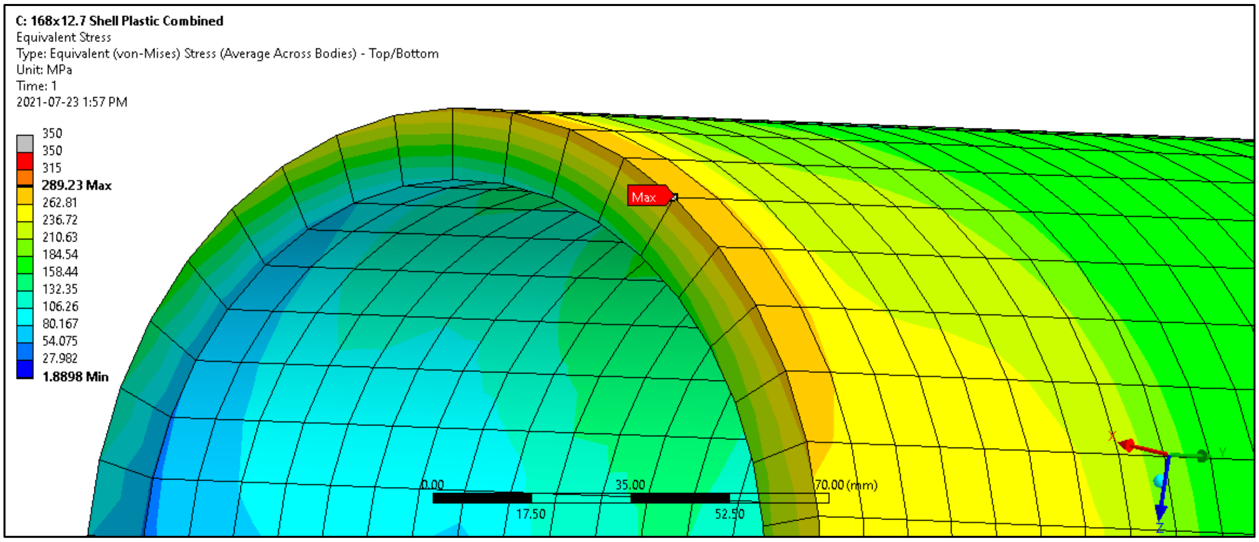

Figure 83: Load Case 7 - Round HSS 168x13 Combined Loading Stress

Equivalent plastic strains for load case 7 – round HSS 168x13 combined loading, are presented in Figure 84 with a maximum plastic strain of 0.0 (0%). Although the applied combined loading magnitudes were the calculated section capacities, they were not large enough to cause the round HSS to plastically strain to produce a strain value. The peak nodal strain value is sufficiently below the allowable linearized averaged plastic strain of 0.04 (4%) in accordance with DNVGL-RP-C208 [63], therefore the strain results are considered acceptable.

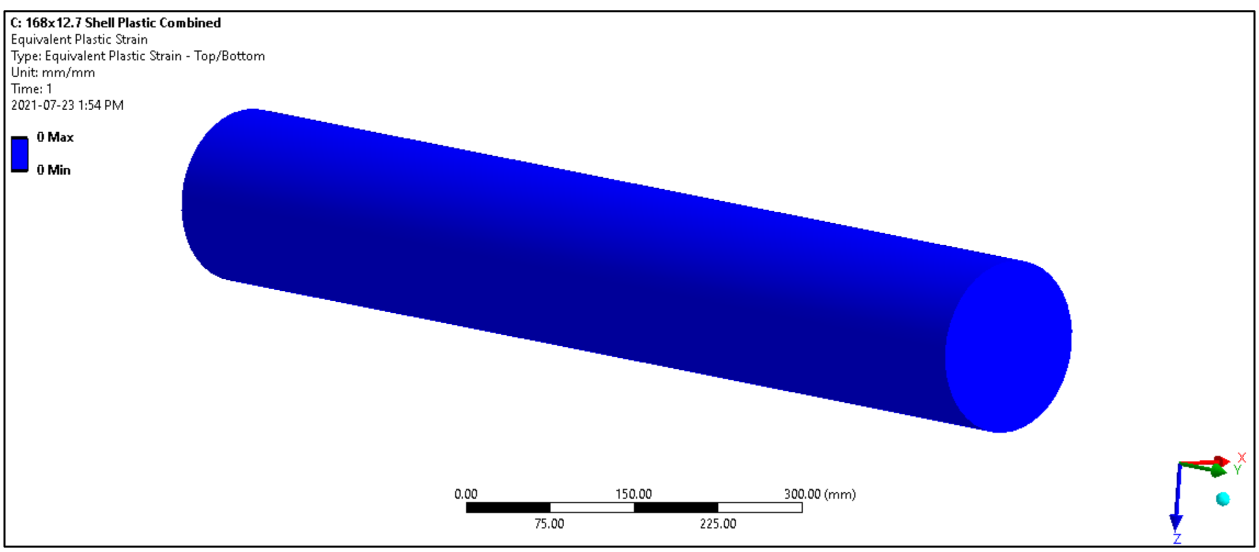

Figure 84: Load Case 7 - Round HSS 168x13 Combined Loading Plastic Strain

The total deflection under load case 7 is shown in Figure 85. The maximum deflection value of 1.76 mm is acceptable for a defection at failure magnitude.

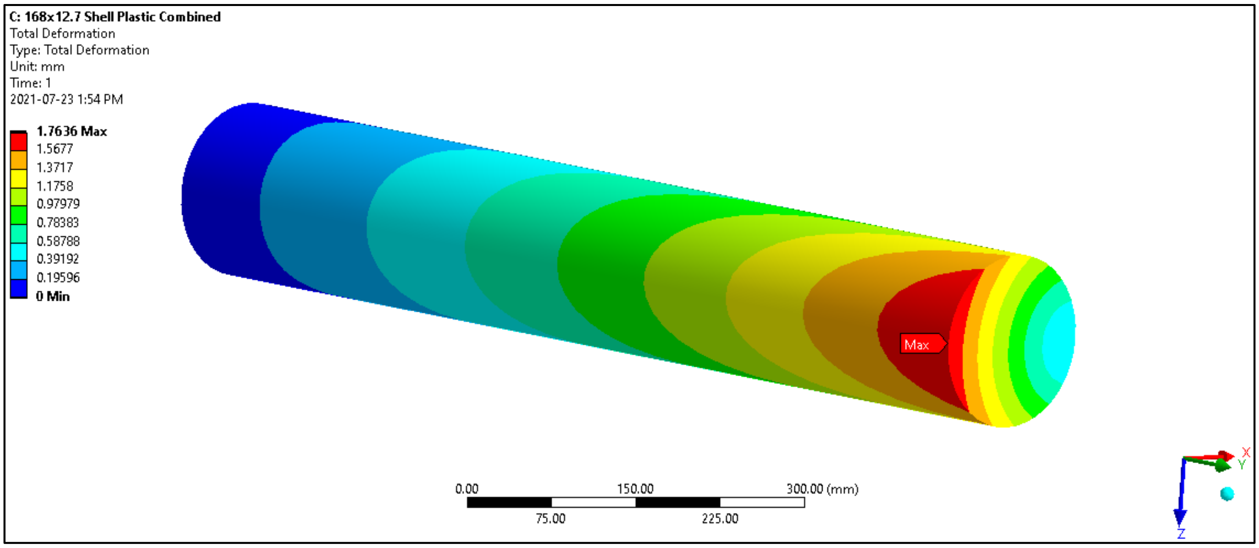


Figure 85: Load Case 7 - Round HSS 168x13 Combined Loading Deflection

## 5.10 Load Case 8 – Square HSS 168x13 Combined Loading

Equivalent stresses for load case 8 – square HSS 152x152x13 combined loading, are shown in Figure 86 with a maximum stress of 290.1 MPa. The max stress occurs at the outer edge of the tubular at the fixed support as shown in Figure 87. The maximum stress is lower than allowable stress in accordance with CAN/CSA S16-19 [1]. Note, the maximum stress is of a similar magnitude as determined in the previous combined HSS load case.

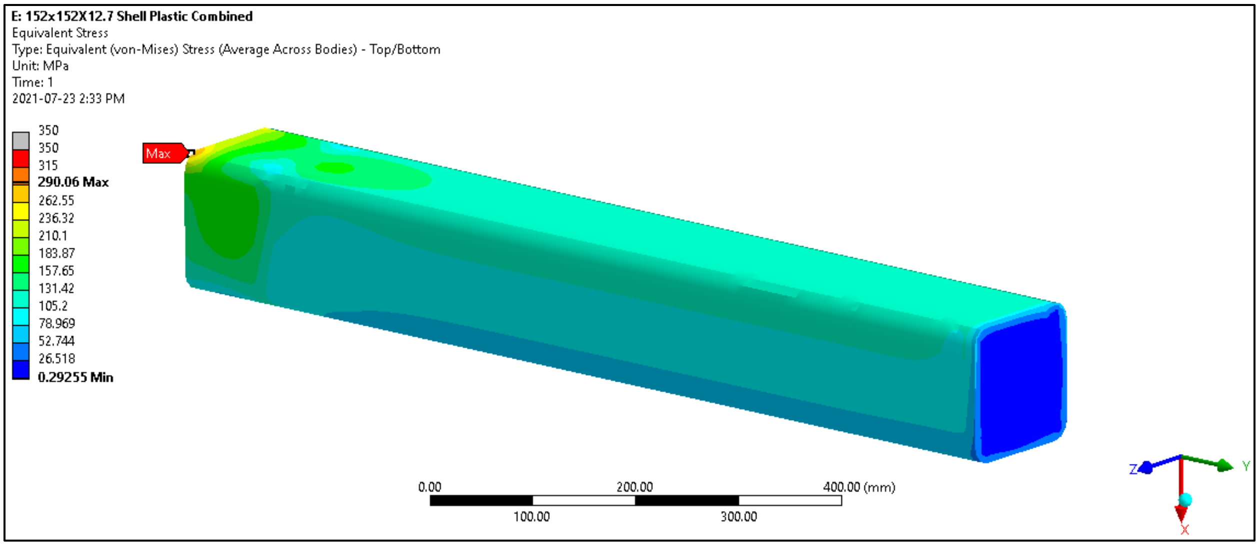


Figure 86: Load Case 8 - Square HSS 152x152x13 Combined Loading Stress

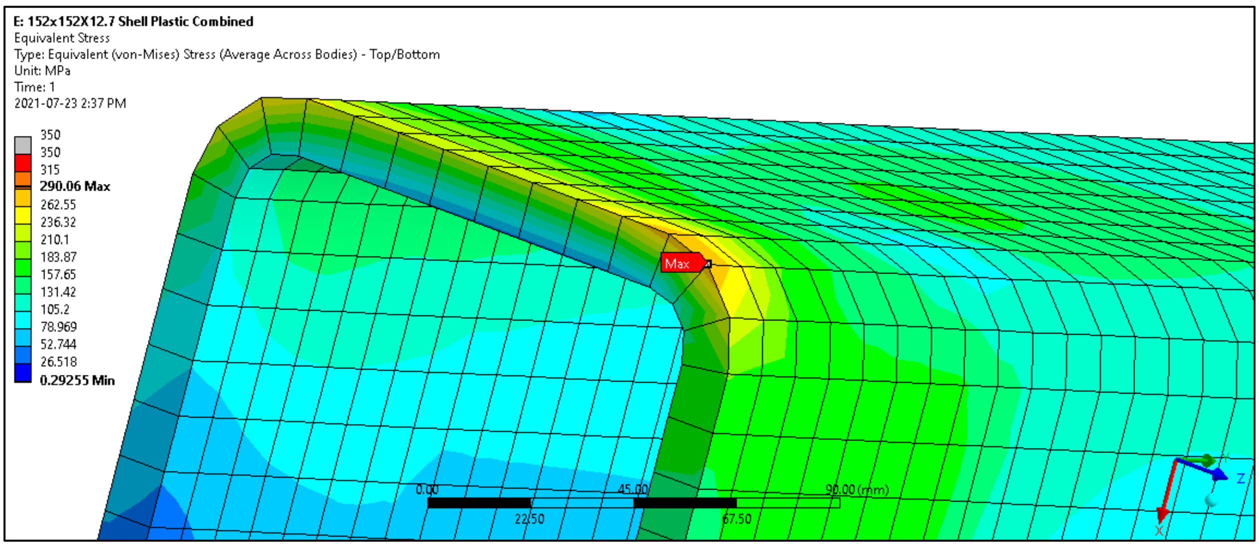


Figure 87: Load Case 8 - Square HSS 152x152x13 Combined Loading Stress

Equivalent plastic strains for load case 8 – square HSS 152x152x13 combined loading, are presented in Figure 88 with a maximum plastic strain of 0.0 (0%). Although the applied combined loading magnitudes were the calculated section capacities, they were not large enough to cause the square HSS to plastically strain producing a strain value. The peak nodal strain value is sufficiently below the allowable linearized averaged plastic strain of 0.04 (4%) in accordance with DNVGL-RP-C208 [63], therefore the strain results are considered acceptable. Note, the maximum plastic strain is the same value as determined in the previous combined HSS load case.

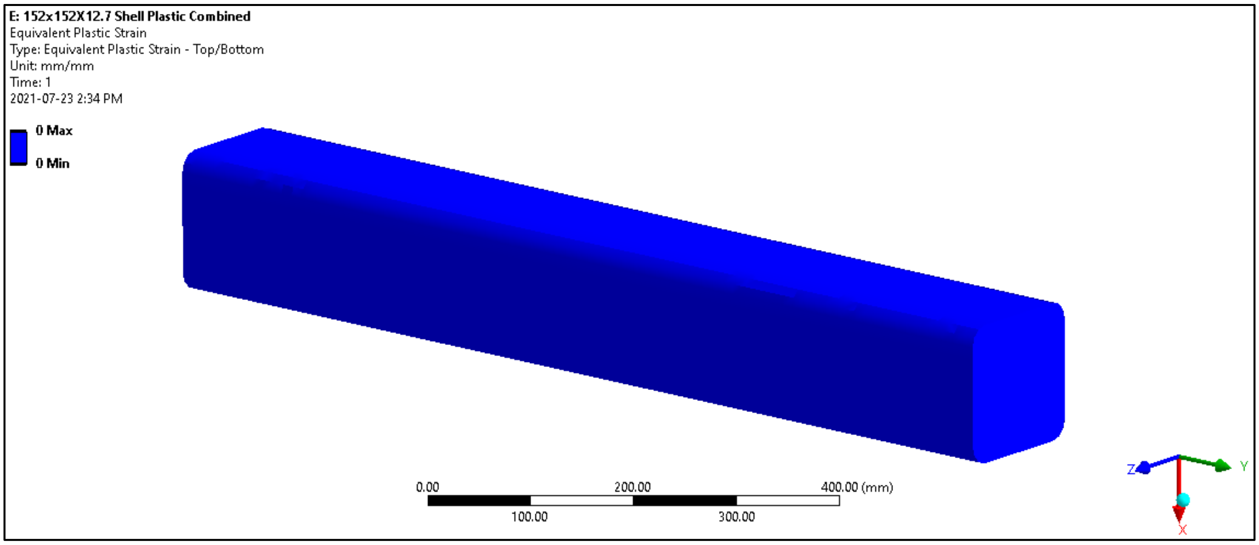

Figure 88: Load Case 8 - Square HSS 152x152x13 Combined Loading Plastic Strain

The total deflection under load case 8 is shown in Figure 89. The maximum deflection value of 1.88 mm is acceptable for a defection at failure magnitude.

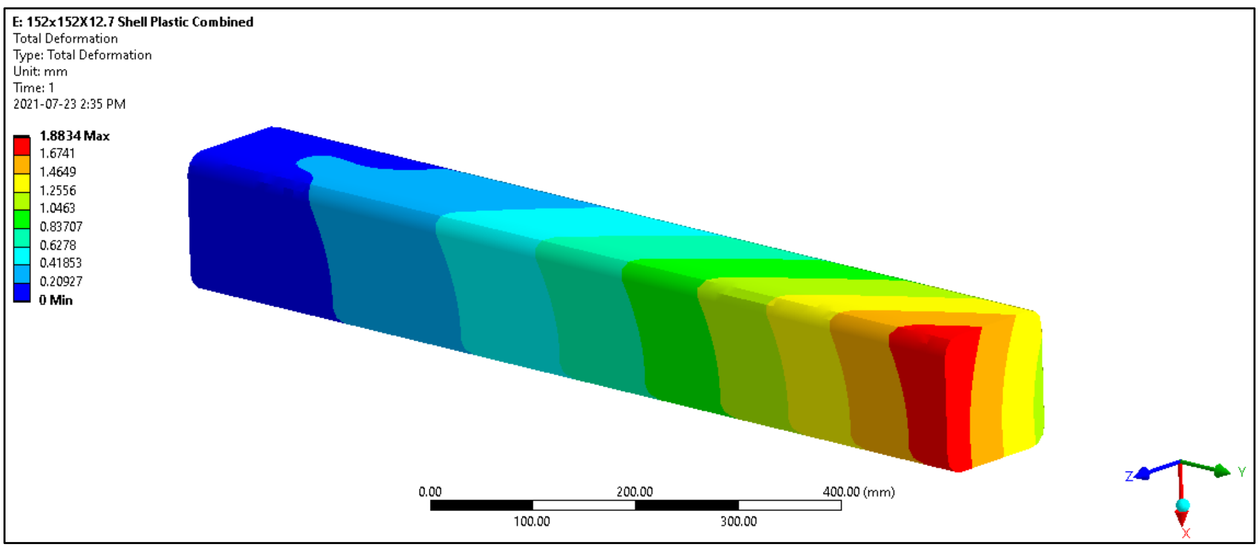

Figure 89: Load Case 8 - Square HSS 152x152x13 Combined Loading Deflection

## 5.11 Load Case 9 – Rectangular HSS 203x152x13 Combined Loading

Equivalent stresses for load case 9 – rectangular HSS 203x152x13 combined loading, are shown in Figure 90 with a maximum stress of 311.9 MPa. The max stress occurs at the outer edge of the tubular at the fixed support as shown in Figure 91. The maximum stress is lower than allowable stress in accordance with CAN/CSA S16-19 [1]. Note, the maximum stress is of a similar magnitude as determined in the previous 2 combined HSS load cases.

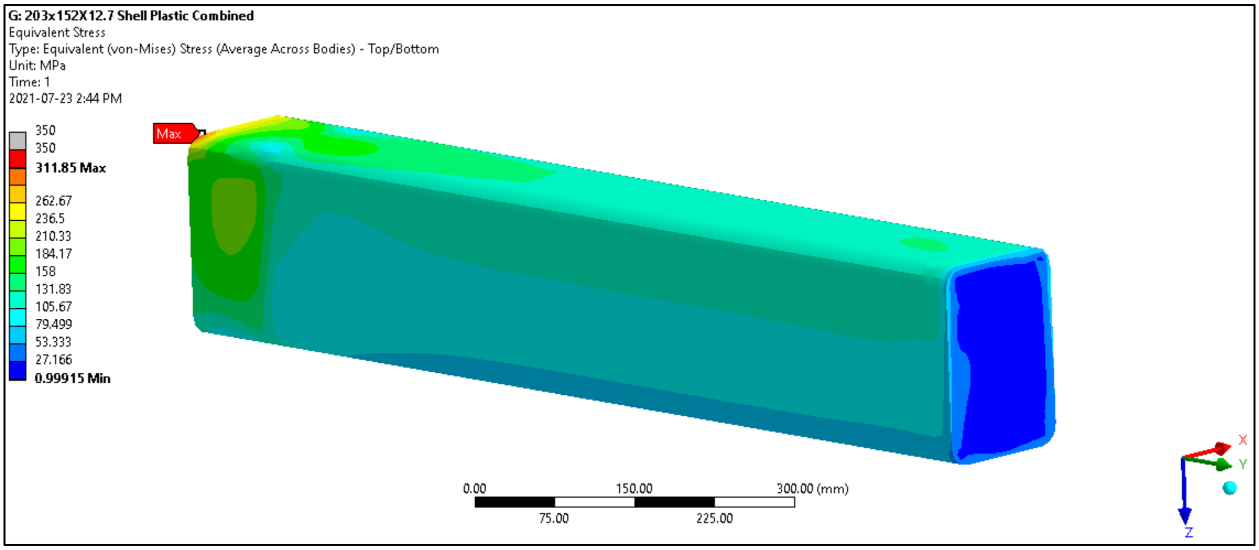


Figure 90: Load Case 9 - Rectangular HSS 203x152x13 Combined Loading Stress

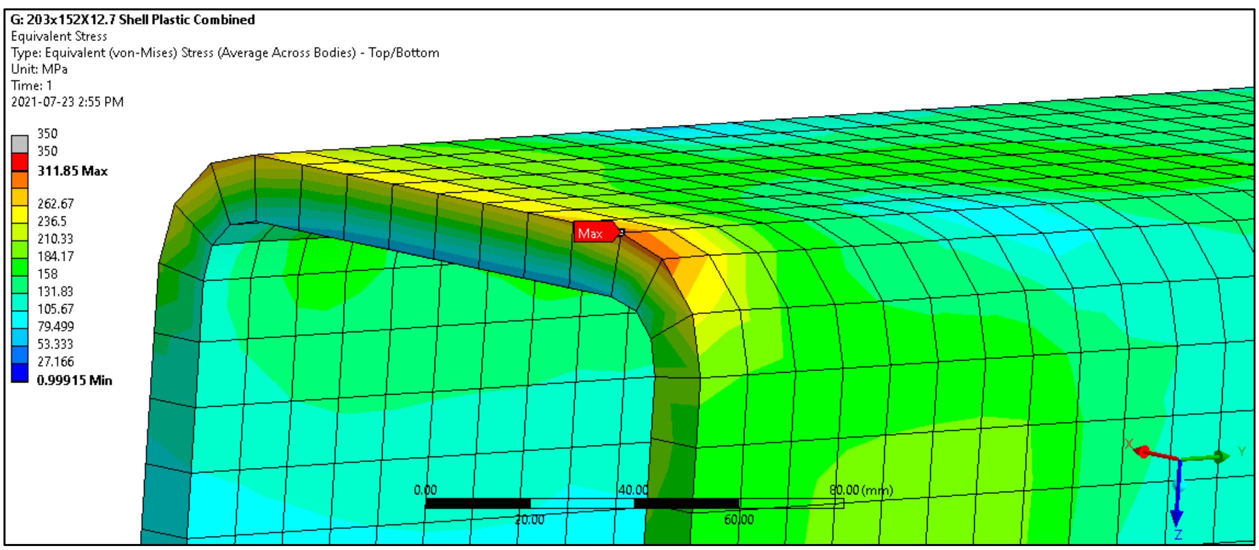


Figure 91: Load Case 9 - Rectangular HSS 203x152x13 Combined Loading Stress

Equivalent plastic strains for load case 9 – square HSS 152x152x13 combined loading, are presented in Figure 92 with a maximum plastic strain of 0.0 (0%). Although the applied combined loading magnitudes were the calculated section capacities, they were not large enough to cause the rectangular HSS to plastically strain to produce a strain value. The peak nodal strain value is sufficiently below the allowable linearized averaged plastic strain of 0.04 (4%) in accordance with

DNVGL-RP-C208 [63], therefore the strain results are considered acceptable. Note, the maximum plastic strain is the same value as determined in the previous 2 combined HSS load cases.

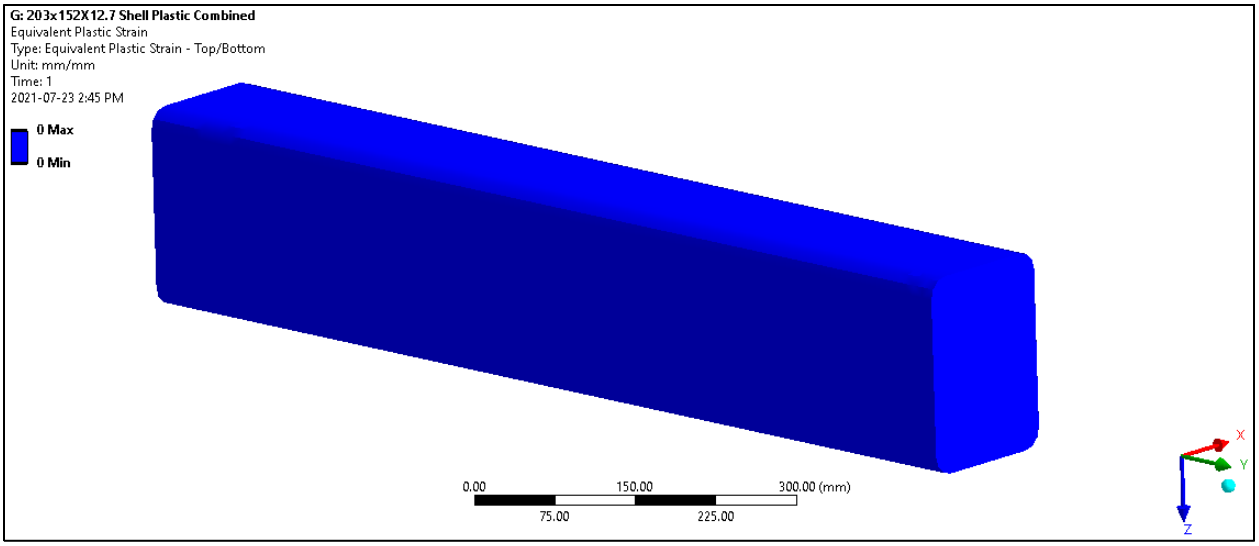


Figure 92: Load Case 9 - Rectangular HSS 203x152x13 Combined Loading Plastic Strain

The total deflection under load case 9 is shown in Figure 93. The maximum deflection value of 1.63 mm is acceptable for a defection at failure magnitude.

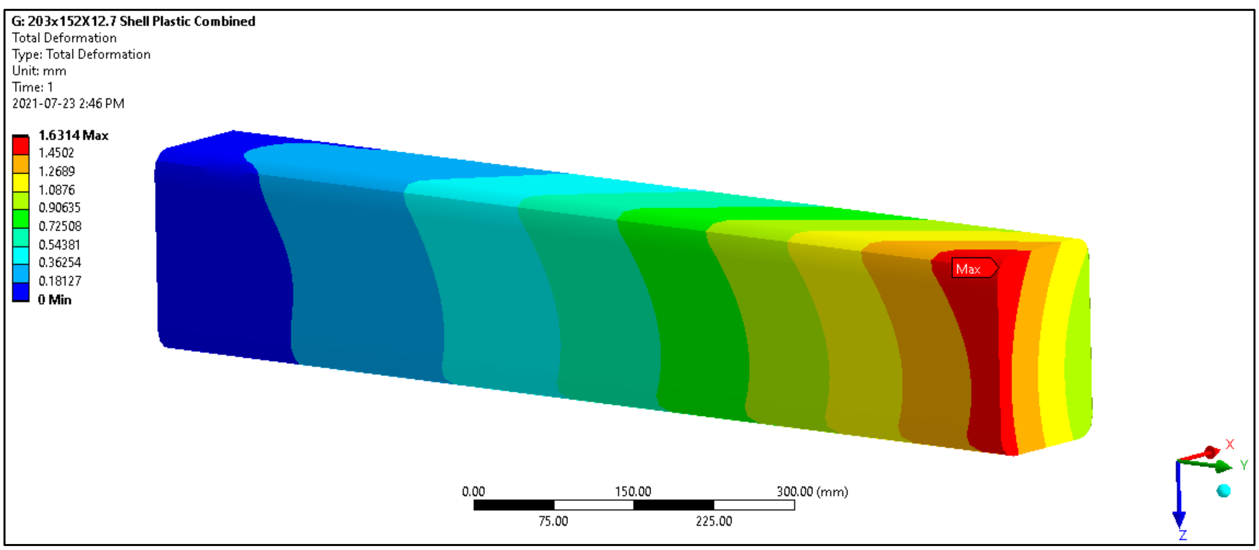


Figure 93: Load Case 9 - Rectangular HSS 203x152x13 Combined Loading Deflection

## 5.12 Analysis of Round HSS 168x13 Combined Loading with CSA Shear Capacity

It was determined the CSA shear capacity of the round HSS 168x13 section was greater than the AISC value when a comparison was completed of the capacities for the combined load cases.

The calculated section capacities are shown in Appendix A. A separate analysis was completed utilizing the load case 7 - round HSS 168x13 combined loading model except for the CSA shear capacity of 228229 N was applied to the section as shown in Figure 94.

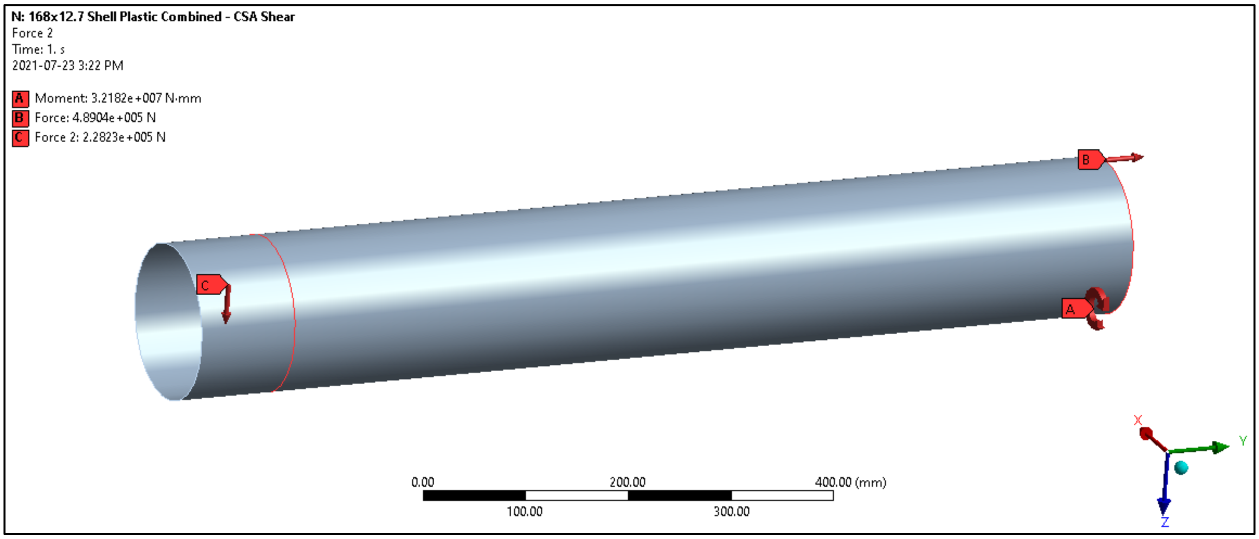


Figure 94: CSA Shear Analysis - Round HSS 168x13 (Combined Loading)

The CSA shear capacity value was determined to have a magnitude of 20748 N greater than the AISC value. In CAN/CSA S16-19 – Design of Steel Structures [1] shear capacity of a tubular member is simply determined by,

$$V_r = 0.66 \cdot \phi \cdot A/2) \cdot F_y \tag{5-1}$$

Where:

$\phi$ = Resistance Factor

A = Area

$F_y$ = Yield Strength

The CAN/CSA S16-19 [1] tubular shear capacity clause is shown in Appendix A. While using ANSI/AISC 360-16 – Specification for Structural Steel Buildings [2] to calculate round HSS shear capacity, the user needs to calculate the larger value of $F_{cr}$ but shall not exceed $0.6 \cdot F_y$. The appropriate value of $F_{cr}$ is then applied in the shear formula,

$$V_r = F_{cr} \cdot Ag/2 \tag{5-2}$$

Where:

$F_{cr}$ = Critical Stress

$A_g$ = Gross Area of Member

The ANSI/AISC 360-16 [2] round HSS shear capacity clause is shown in Appendix A. As stated in AISC "For standard sections shear yielding will usually control and $F_{cr} = 0.6 \cdot F_y$" [2] therefore providing a lower shear capacity in comparison to the CSA value.

The Equivalent stresses for the CSA shear analysis – round HSS 168x13 combined loading, are shown in Figure 95 with a maximum stress of 295.2 MPa. The max stress occurs at the outer diameter edge of the tubular at the fixed support as shown in Figure 96. The maximum stress is lower than allowable stress in accordance with CAN/CSA S16-19 [1]. Note, the maximum stress is of a similar magnitude as determined in the previous 3 combined HSS load cases.

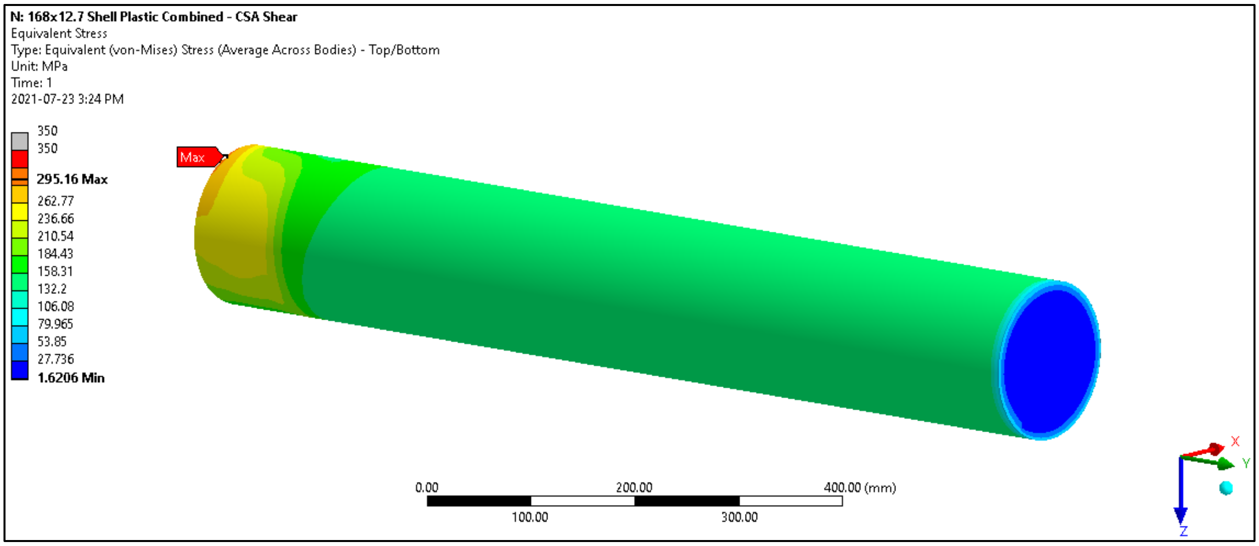


Figure 95: CSA Shear Analysis - Round HSS 168x13 Combined Loading Stress

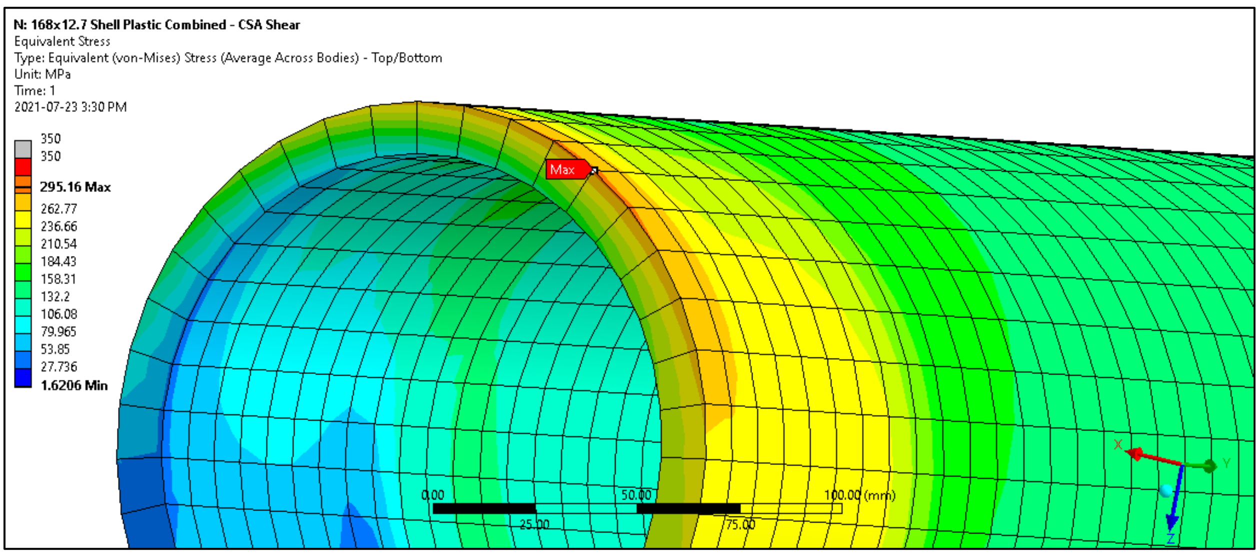


Figure 96: CSA Shear Analysis - Round HSS 168x13 Combined Loading Stress

Equivalent plastic strains for the CSA shear analysis – round HSS 168x13 combined loading, are presented in Figure 97 with a maximum plastic strain of 0.0 (0%). Although the applied combined loading magnitudes were the calculated section capacities, they were not large enough to cause the round HSS to plastically strain to produce a strain value. The peak nodal strain value is sufficiently below the allowable linearized averaged plastic strain of 0.04 (4%) in accordance with DNVGL-RP-C208 [63], therefore the strain results are considered acceptable. Note, the maximum plastic strain is the same value as determined in the previous 3 combined HSS load cases.

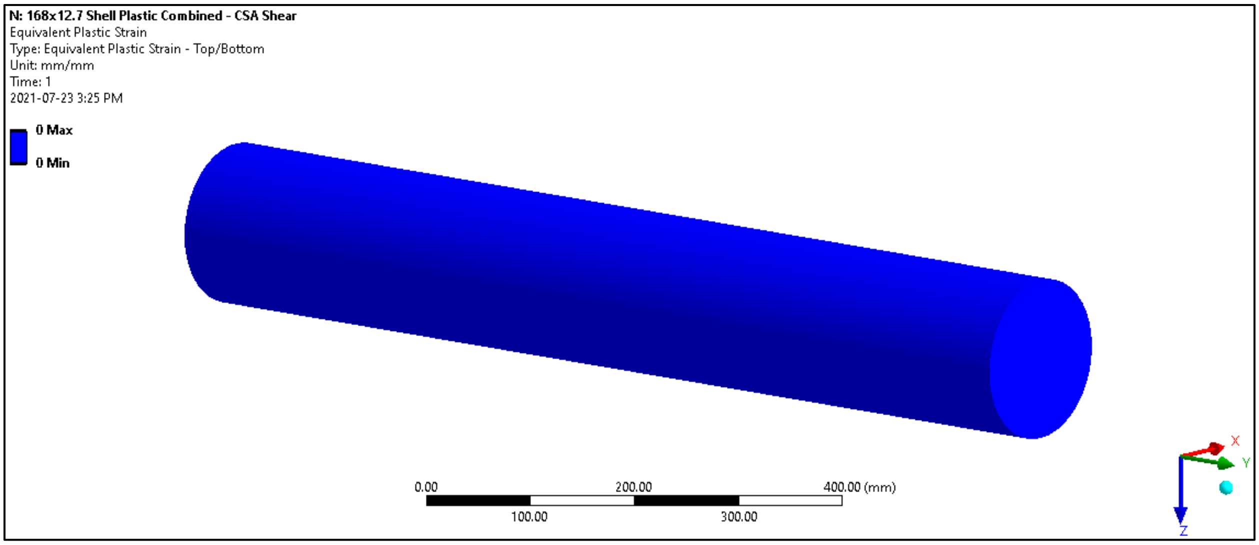


Figure 97: CSA Shear Analysis - Round HSS 168x13 Combined Loading Plastic Strain

The total deflection under CSA shear analysis combined loading is shown in Figure 98. The maximum deflection value of 1.53 mm is acceptable for a defection at failure magnitude.

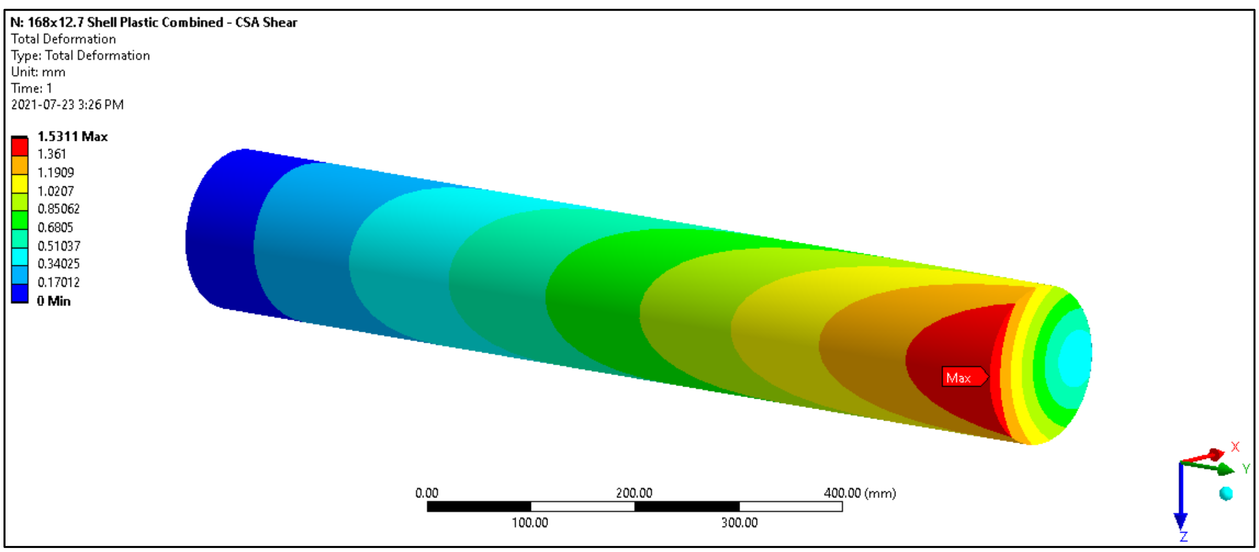


Figure 98: CSA Shear Analysis - Round HSS 168x13 Combined Loading Deflection

The results from the analysis using the larger CSA shear load combined with the AISC capacities are very similar to the load case 7 results where the AISC shear is applied. Both load cases are considered acceptable.

# Chapter 6 Conclusion and Recommendations

The overall research objective of this thesis was to determine a concise design approach through the application of theoretical equations to assess hollow structural sections (HSS) subject to torsion and combined loading for designs in Canada. The principal motivation for this work was to deliver additional literature to the field of HSS under torsion and combined loading, while potentially providing an efficient mathematical approach to assess the behavior of HSS subject to these unique loadings in Canada.

The steel design codes are based on probabilistic and reliability techniques which are used to determine appropriate factors of safety. It was determined in the thesis "Reliability-Based Development of Torsional Strength Equations for the CSA S16 Standard" [8] that both codes have a similar reliability index under various loading combinations but the American code is slightly lower. This indicates from a calibration perspective the factor of safety from the American code is marginally lower than the Canadian. Greene concluded through his reliability modeling looking specifically at the AISC torsion clause if different constants are applied for round and rectangular HSS in the AISC torsion formula the applicable level of safety can be achieved for limit states design in Canada. Greene also notes the reliability indexes need to be examined further with additional section sizes and experimental testing verification completed before it is determined if the reliabilities are completely corresponding.

From the literature review completed in this study, specifically comparing the Canadian and American steel design code clauses in detail it was determined the ANSI/AISC 360-16 – Specification for Structural Steel Buildings [2] provides equations to assess HSS in torsion and combined loading while CAN/CSA S16-19 – Design of Steel Structures [1] recommends an elastic analysis for verification. Even though both options are effective design approaches if theoretical equations were available in Canada to check HSS in torsion and combined loading it would be a practical and valuable option for design engineers. The AISC clause that was studied in this paper was Members Subject to Torsion and Combined Torsion, Shear, Flexure, and/or Axial Force which is found in Chapter H, Section H3 [2]. Through the research completed the torsion and combined loading clause was verified for the included HSS sizes using the calculated section capacities and FE techniques. The analysis results meet the DNVGL-RP-C208 [63] strain assessment criteria for the beams that were investigated. All beam equivalent plastic strains were less than 0.04 (4%) with the overall maximum plastic strain value of 0.0032 (0.32%) occurring in the load case 5 rectangular HSS 203x152x13 torsion loading. It was also determined from the calculated section capacity between the Canadian and American steel codes on the round HSS section that the Canadian shear capacity was higher than the American. From the results of the separate analysis using the CSA capacity, it was concluded using the slightly larger CSA shear load the section is still acceptable under the combined load case. Based on the analysis performed on the specific sections in this study, the results indicate the AISC torsion and combined loading clause could potentially be applied for verification in Canada. Before the AISC clauses can be recommended as an approved design approach further analysis is required on additional HSS sizes, loading conditions and all analysis results need to be verified by experimental tests. Eventually, if the AISC 360-16 [2] torsion and combined loading clauses can be confidently applied in Canada it would provide a convenient method of verification and possibly increase the quality of the designs produced resulting in safer structures for the general public. The AISC clauses could also be treated as an initial design check which would provide the engineer with a simple method of determining the beam utilization, from there a separate detailed elastic analysis could be completed based on engineering judgment if deemed required.

Some recommendations for future work could be to study the behavior of other HSS of various sizes and wall thicknesses. In this paper, the HSS sections were classed as compact in AISC or class 1 and 2 in CSA. Due to this, when the section bending capacities were calculated for the combined loading models failure mechanisms such as local buckling and lateral-torsional buckling did not apply. There is a potential that some section sizes may not be adequate under the torsion or combined loads such as larger thin wall HSS. It is noted even though the models used were laterally unsupported cantilevers for bending, due to the HSS section geometries there is no reduction in moment capacity. During this study, a sensitivity analysis was completed for a combined loading case with an additional displacement support included in the lateral direction at the end of the cantilever. It was concluded adding in the lateral support did not have any effect on the results and the model stresses/ strains were comparable to the model with no lateral support.

Different loading scenarios could be examined for the combined load case such as applying compression in the beam instead of tension from the axial load. Round and rectangular HSS torsional capacities could be calculated in accordance with the AISC torsion formula using the constants determined in Greene's study [8] then applied in FEA for verification and further alignment with the Canada code. Various load percentages that yield a utilization of 1.0 for the sections could also be investigated producing a parametric study for the combined torsion, axial, flexure, and shear, as an equal split of 25% capacity of each component was used in this thesis. All FEA results in this study should be verified by experimental testing and beam loading behavior compared to see if they are consistent with FE models. Non-HSS members subject to torsion and combined stresses could also be investigated further using FEA techniques in an attempt to determine capacity values for torsion and combined loading. Further research in this area could be to develop formulas for evaluating non-HSS members subject to torsion and combined loading similar to what's available for HSS in the American code. Currently in AISC in Chapter H, Section H3-3 - Non-HSS Members Subject to Torsion and Combined Stress it is stated "the available torsional strength for non-HSS members shall be the lowest value obtained according to the limit states of yielding under normal stress, shear yielding under shear stress, or buckling" [2] along with provided limit states equations for each case. Additional research could be investigating other international standards such as the Eurocode [27] in detail to evaluate torsion methodology and compare results to what was achieved in this study.

To implement the findings of this work supplementary research is needed for confirmation of the results. Once this has been achieved through experimental methods, the American code HSS torsion and combined loading clauses could possibly be used by structural engineers in Canada for a simple theoretical equation-based assessment. The application of this method would significantly increase the efficiency of evaluating HSS torsion and combined loading. An engineer could assess a HSS by manual calculations instead of having to complete a finite element model which also assumes they have capable finite element software available. The overall goal of researching technical engineering topics is to improve proficiency, safety, and advance the literature in these fields. If the American code HSS torsion and combined loading clauses are considered for use in Canada, they will progress the understanding of this unique loading scenario and provide engineers with further assessment options in addition to the currently available evaluation techniques.

# Chapter 7 References


[1] Canadian Standards Association, CAN/CSA S16-19 - Design of Steel Structures, Toronto, Ontario, Canada: CSA Group, 2019.

[2] American Institute of Steel Construction, ANSI/AISC 360-16 - Specification for Structural Steel Buildings, Chicago, Illinois, United States: American Institute of Steel Construction, 2016.

[3] S.-K. Choi, R. V. Grandhi and R. A. Canfield, Reliability-based Structural Design, Springer, 2007.

[4] R. E. Melchers and A. T. Beck, Structural Reliability Analysis and Prediction, John Wiley & Sons, 2018.

[5] G. L. Kulak and G. Grondin, Limit States Design in Structural Steel, Quadratone Graphics Ltd., 2006.

[6] Y. Miyata, "Frequency Distributions," 2011. [Online]. Available: https://www.researchgate.net/figure/Frequency-distributions-for-a-measured-load-and-resistance-values-b-load-bias-and_fig5_235955593.

[7] K. Ashkinadze, "Proposals for Limit States Torsional Strength Design of Wide-Flange Steel Members," *Canadian Journal of Civil Engineering,* 2008.

[8] A. Greene, "Reliability Based Development of Torsional Strength Equations for the CSA S16 Standard," St. John's, 2021.

[9] T. V. Galambos, "A Comparison of Canadian, Mexican and United States Steel Design Standards," *Engineering Journal,* pp. 52-66, 1999.

[10] J.-L. Liu, D. M. Lue and C. H. Lin, "Investigation on Slenderness Ratios of Built-up Compression Members," *Journal of Constructional Steel Research ,* pp. 237-248, 2009.

[11] American Institute of Steel Construction, AISC-ASD - Allowable Stress Design Specification for Structural Steel Buildings, Chicago, Illinois, United States, 1989.

[12] American Institute of Steel Construction, AISC-LRFD - Load and Resistance Factor Design Specification for Structural Steel Buildings, Chicago, Illinois, United States, 1986.

[13] Standards Australia, AS 4100 - Steel Structures;, 1998.

[14] Canadian Standards Association, CAN/CSA S16-01 - Design of Steel Structures, Toronto, Ontario, Canada, 2001.

[15] American Institute of Steel Construction, ANSI/AISC 360-05 - Specification for Structural Steel Buildings, Chicago, Illinois, 2005.

[16] S. Rhodes, B. Donoghue and T. Cakebread, "Steel Bridge Member Resistance - AASHTO Compared to Other International Codes," 2019.

[17] American Association of State Highway and Transportation Officials, AASHTO LRFD Bridge Design Specification, 8th Edition, 2017.

[18] British Standards Institution, BS EN 1993-2: 2006 Eurocode 3: Design of Steel Structures - Part 2: Steel Bridges, 2006.

[19] Canadian Standards Association, CSA S6-14 - Canadian Highway Bridge Design Code, Ontario, 2014.

[20] W. S. Easterling, D. R. Gibbings and T. M. Murray, "Strength of Shear Studs in Steel Deck on Composite Beams and Joists," 1993.

[21] American Institute of Steel Construction, Manual of Steel Construction - Load and Resistance Factor Design, Chicago, Illinois, 1986.

[22] Canadian Standards Association, CAN/CSA-S16.1-M89 - Limit States Design of Steel Structures, Ontario, 1989.

[23] Commission of the European Communities, Eurocode 4 - Common Unified Rules for Composite Steel and Concrete Structures, 1992.

[24] M. I. Kabir, "Lateral Torsional Buckling of Welded Wide Flange Beams," Montreal, Quebec, Canada, 2016.

[25] Canadian Standards Association , CAN/CSA S16-14 - Design of Steel Structures, Toronto, Ontario, 2014.

[26] American Institute of Steel Construction, ANSI/AISC 360-10 - Specification for Structural Steel Buildings, Chicago, Illinois, 2010.

[27] European Committee for Standardization, EN 1993-1-1 - Eurocode 3: Design of Steel Structures Part 1, General Rules for Buildings, Belgium, 2005.

[28] C. D. Eamon, A. W. Lamb and k. Patki, "Effect of Moment Gradient and Load Height With Respect to Centroid on the Reliability of Wide Flage Steel Beams Subject to Elastic Lateral Torsional Buckling," 2017.

[29] M. I. Kabir and A. K. Bhowmick, "Effect of Geometric Imperfection on lateral Torsional Buckling Capacity," 2016.

[30] M. Manarin, "Numerical Investigation of Lateral Torsional Buckling of T-Shaped Steel Beams," University of Alberta, 2019.

[31] E. Wong and R. G. Driver, "Critical Evaluation of Equivalent Moment Factor Procedures for Laterally Unsupported Beams," *Engineering Journal,* 2010.

[32] M. Leblouba and S. W. Tabsh, "Reliability-Based Shear Design of Corrugated Web Steel Beams for AISC 360 Specification and CSA-S16 Standard," *Engineering Structures,* 2020.

[33] G. Kiymaz and E. Seckin, "Strength and Design of Slotted and Gusset Plate Welded Tubular Member Connections in Stainless Steel".

[34] S. Willibald, J. A. Packer and G. Martinez-Saucedo, "Behavior of Gusset Plate Connections to Ends of Round and Elliptical Hollow Structural Section Members," *Canadian Journal of Civil Engineering,* pp. 373-383, 2006.

[35] S. J. Guravich and J. L. Dawe, "Simple Beam Connection in Combined Shear and Tension," *Canadian Journal of Civil Engineering,* pp. 357-372, 2006.

[36] American Institute of Steel Construction, AISC - Manual of Steel Construction: Load and Resistance Factored Design, Chicago, Illinois, 2001.

[37] J. L. Carril, R. A. LaBoube and W.-w. Yu, "Tensile and Bearing Capacities of Bolted Connections," Missouri University of Science and Technology, 1994.

[38] J. B. Shaback, "Behavior of Square HSS Braces with End Connections Under Reversed Cyclic Axial Loading," 2001.

[39] Canadian Standards Association, CAN/CSA S16.1-94 - Limit States Design of Steel Structures, Rexdale, Ontario, 1997.

[40] American Institute of Steel Construction, AISC - Manual of Steel Construction, Load and Resistance Factored Design, Chicago, Illinois, 1998.

[41] R. Driver and D. Kennedy, "Combined Flexure and Torsion of I-Shaped Steel Beams," *Canadian Journal of Civil Engineering,* pp. 124-139, 1989.

[42] Y. Pi and N. Trahair, "Inelastic Torsion of Steel I-beams," *ASCE Journal of Structural Engineering,* 1995.

[43] P. A. Seaburg and C. J. Carter, Torsional Analysis of Structural Steel Members, United States of America: American Institute of Steel Construction, 1997.

[44] R. Brockenbrough and B. Johnson, Steel Design Manual, Pittsburgh, PA: United States Steel Corp., 1974.

[45] R. Englekirk, Steel Structures Controlling Behavior Through Design, New York, NY: John Wiley & Sons, 1994.

[46] E. Mashaly, M. EI-Heweity, H. Abou-Elfath and M. Osman, "Finite Element Analysis of beam-to-column joints in steel frames under cyclic loading," *Alexandria Engineering Journal,* pp. 91-104, 2011.

[47] M. P. Laurendeau, "Live Load Testing and Finite Element Analysis of A Steel Cantilever Deck Arched Pratt Truss Bridge for the Long Term Bridge Performance Program," Logan, Utah, 2011.

[48] R. Zhao, R. Huang, H. A. Khoo and J. R. Cheng, "Parametric Finite Element Study on Slotted Rectangular and Square HSS Tension Connections," *Journal of Constructional Steel Research,* pp. 611-621, 2008.

[49] J. Cheng, G. Kulak and H. Khoo, "Strength of Slotted Tubular Tension Members," *Canadian Journal of Civil Engineering ,* pp. 982-991, 1998.

[50] G. Martinez-Saucedo, J. Packer and S. Willibald, "Parametric Finite Element Study of Slotted End Connections to Circular Hollow Sections," *Engineering Structures,* pp. 1956-1971, 2006.

[51] A. Hughes, D. C. IIes and A. Malik, Design of Steel Beams in Torsion, Berkshire, UK: The Steel Construction Institute, 2011.

[52] O. W. Blodgett, Design of Welded Structures, Cleveland, Ohio: The James F. Lincoln Arc Welding Foundation, 1966.

[53] F. De'nan, H. Hasan, D. Nassir, M. Osman and S. Saad, "Finite Element Analysis for Torsion Behavior of Flat Web Profile Beam Steel Section With Opening," *Procedia Engineering,* pp. 1129-1134, 2015.

[54] F. De'nan, N. Omar and M. Mustapha, "Finite Element Analysis of Torsion Behaviour of Triangular Web Profile Beam Section," 2015.

[55] C. Nandhakumar, R. Ramesh and V. Sreevidya, "Investigation of Cold Formed Steel Beam Subject to Torsion," *Materials Today: Proceedings ,* pp. 425-429, 2019.

[56] Y. P. Lin and N. S. Trahair, "Inelastic Bending and Torsion of Steel I-Beams," *Journal of Structural Engineering,* pp. 3397-3417, 1994.

[57] B. G. Estabrooks, "Combined Bending and Torsion of Steel I-Shaped Beams," University of Alberta, Edmonton, Alberta, 2008.

[58] Y. Pi and N. Trahair, "Inelastic Bending and Torsion of Steel I-Beams, Research Report No. R683," The University of Sidney, 1993.

[59] N. Trahair and Y. Pi, "Torsion, Bending and Buckling of Steel Beams," *Engineering Structures,* pp. 372-377, 1997.

[60] K. Kim and C. H. Yoo, "Ultimate Strenghts of Steel Rectangular Box Beams Subjected to Combined Action of Bending and Torsion," *Engineering Structures,* pp. 1667-1687, 2008.

[61] M. Konate, "Inelastic Behavior and Strength of Steel Beam-Columns with Applied Torsion," Old Dominion University, 2015.

[62] ANSYS, "ANSYS Mechanical Finite Element Analysis Software (FEA) for Structural Engineering," 2021. [Online]. Available: https://www.ansys.com/products/structures/ansys-mechanical.

[63] DNVGL, DNVGL-RP-C208: Determination of Structural Capacity by Non-Linear Finite Element Analysis Methods, 2019.

[64] Ansys Mechanical APDL 2021 R1, "Mechanical APDL 2021 R1," 29 March 2021. [Online]. Available: https://ansyshelp.ansys.com/account/secured?returnurl=/Views/Secured/corp/v211/en/ans_elem/Hlp_E_SHELL181.html.

[65] Mechanical Base, "Equivalent Plastic Strain in ANSYS Mechanical," April 2021. [Online]. Available: https://mechanicalbase.com/equivalent-plastic-strain-in-ansys-mechanical/.

[66] Bentley, "STAAD.Pro - 3D Structural Analysis and Design Software," 2021. [Online]. Available: https://www.bentley.com/en/products/product-line/structural-analysis-software/staadpro.

# Appendix A – AISC/ CSA Code Clauses & Section Capacities

Shown below are the ANSI/AISC 360-16 – Specification for Structural Steel Buildings [2] Torsion and combined loading, Axial, Flexure, and Shear clauses along with the calculated section capacities.

## H3. MEMBERS SUBJECT TO TORSION AND COMBINED TORSION, FLEXURE, SHEAR, AND/OR AXIAL FORCE

### 1. Round and Rectangular HSS Subject to Torsion

The design torsional strength, $\phi_T T_n$, and the allowable torsional strength, $T_n/\Omega_T$, for round and rectangular HSS according to the limit states of torsional yielding and torsional buckling shall be determined as follows:





$$T_n = F_{cr} C \tag{H3-1}$$

$$\phi_T = 0.90 \text{ (LRFD)} \qquad \Omega_T = 1.67 \text{ (ASD)}$$

where

$C$ = HSS torsional constant, in.$^3$ (mm$^3$)

The critical stress, $F_{cr}$, shall be determined as follows:

(a) For round HSS, $F_{cr}$ shall be the larger of

(1) $$F_{cr} = \frac{1.23E}{\sqrt{\frac{L}{D}}\left(\frac{D}{t}\right)^{\frac{5}{4}}} \tag{H3-2a}$$

and

(2) $$F_{cr} = \frac{0.60E}{\left(\frac{D}{t}\right)^{\frac{3}{2}}} \tag{H3-2b}$$

but shall not exceed $0.6F_y$,

where

$D$ = outside diameter, in. (mm)
$L$ = length of member, in. (mm)
$t$ = design wall thickness defined in Section B4.2, in. (mm)

(b) For rectangular HSS

(1) When $h/t \le 2.45\sqrt{E/F_y}$

$$F_{cr} = 0.6F_y \tag{H3-3}$$

(2) When $2.45\sqrt{E/F_y} < h/t \le 3.07\sqrt{E/F_y}$

$$F_{cr} = \frac{0.6F_y\left(2.45\sqrt{E/F_y}\right)}{\left(\frac{h}{t}\right)} \tag{H3-4}$$

(3) When $3.07\sqrt{E/F_y} < h/t \le 260$

$$F_{cr} = \frac{0.458\pi^2 E}{\left(\frac{h}{t}\right)^2} \tag{H3-5}$$

where

$h$ = flat width of longer side, as defined in Section B4.1b(d), in. (mm)





**User Note:** The torsional constant, $C$, may be conservatively taken as:

For round HSS: $C = \dfrac{\pi(D-t)^2 t}{2}$

For rectangular HSS: $C = 2(B-t)(H-t)t - 4.5(4-\pi)t^3$

## 2. HSS Subject to Combined Torsion, Shear, Flexure and Axial Force

When the required torsional strength, $T_r$, is less than or equal to 20% of the available torsional strength, $T_c$, the interaction of torsion, shear, flexure and/or axial force for HSS may be determined by Section H1 and the torsional effects may be neglected. When $T_r$ exceeds 20% of $T_c$, the interaction of torsion, shear, flexure and/or axial force shall be limited, at the point of consideration, by

$$\left(\frac{P_r}{P_c}+\frac{M_r}{M_c}\right)+\left(\frac{V_r}{V_c}+\frac{T_r}{T_c}\right)^2 \le 1.0 \qquad \text{(H3-6)}$$

where

**For design according to Section B3.1 (LRFD)**

$P_r$ = required axial strength, determined in accordance with Chapter C, using LRFD load combinations, kips (N)

$P_c$ = $\phi P_n$ = design tensile or compressive strength, determined in accordance with Chapter D or E, kips (N)

$M_r$ = required flexural strength, determined in accordance with Chapter C, using LRFD load combinations, kip-in. (N-mm)

$M_c$ = $\phi_b M_n$ = design flexural strength, determined in accordance with Chapter F, kip-in. (N-mm)

$V_r$ = required shear strength, determined in accordance with Chapter C, using LRFD load combinations, kips (N)

$V_c$ = $\phi_v V_n$ = design shear strength, determined in accordance with Chapter G, kips (N)

$T_r$ = required torsional strength, determined in accordance with Chapter C, using LRFD load combinations, kip-in. (N-mm)

$T_c$ = $\phi_T T_n$ = design torsional strength, determined in accordance with Section H3.1, kip-in. (N-mm)

## D2. TENSILE STRENGTH

The design tensile strength, $\phi_t P_n$, and the allowable tensile strength, $P_n/\Omega_t$, of tension members shall be the lower value obtained according to the limit states of tensile yielding in the gross section and tensile rupture in the net section.

(a) For tensile yielding in the gross section

$$P_n = F_y A_g \tag{D2-1}$$

$$\phi_t = 0.90 \text{ (LRFD)} \qquad \Omega_t = 1.67 \text{ (ASD)}$$

(b) For tensile rupture in the net section

$$P_n = F_u A_e \tag{D2-2}$$

$$\phi_t = 0.75 \text{ (LRFD)} \qquad \Omega_t = 2.00 \text{ (ASD)}$$

where

$A_e$ = effective net area, in.$^2$ (mm$^2$)
$A_g$ = gross area of member, in.$^2$ (mm$^2$)
$F_y$ = specified minimum yield stress, ksi (MPa)
$F_u$ = specified minimum tensile strength, ksi (MPa)

Where connections use plug, slot or fillet welds in holes or slots, the effective net area through the holes shall be used in Equation D2-2.

## F7. SQUARE AND RECTANGULAR HSS AND BOX SECTIONS

This section applies to square and rectangular HSS, and box sections bent about either axis, having compact, noncompact or slender webs or flanges, as defined in Section B4.1 for flexure.

The nominal flexural strength, $M_n$, shall be the lowest value obtained according to the limit states of yielding (plastic moment), flange local buckling, web local buckling, and lateral-torsional buckling under pure flexure.

### 1. Yielding

$$M_n = M_p = F_y Z \tag{F7-1}$$

where

$Z$ = plastic section modulus about the axis of bending, in.$^3$ (mm$^3$)

### 2. Flange Local Buckling

(a) For compact sections, the limit state of flange local buckling does not apply.

(b) For sections with noncompact flanges

$$M_n = M_p - \left(M_p - F_y S\right)\left(3.57 \frac{b}{t_f}\sqrt{\frac{F_y}{E}} - 4.0\right) \le M_p \tag{F7-2}$$

where

$S$ = elastic section modulus about the axis of bending, in.$^3$ (mm$^3$)

$b$ = width of compression flange as defined in Section B4.1b, in. (mm)

(c) For sections with slender flanges

$$M_n = F_y S_e \tag{F7-3}$$

where

$S_e$ = effective section modulus determined with the effective width, $b_e$, of the compression flange taken as:

(1) For HSS

$$b_e = 1.92 t_f \sqrt{\frac{E}{F_y}}\left(1 - \frac{0.38}{b/t_f}\sqrt{\frac{E}{F_y}}\right) \le b \tag{F7-4}$$

(2) For box sections

$$b_e = 1.92 t_f \sqrt{\frac{E}{F_y}}\left(1 - \frac{0.34}{b/t_f}\sqrt{\frac{E}{F_y}}\right) \le b \tag{F7-5}$$

### 3. Web Local Buckling

(a) For compact sections, the limit state of web local buckling does not apply.

(b) For sections with noncompact webs

$$M_n = M_p - \left(M_p - F_y S\right)\left(0.305\frac{h}{t_w}\sqrt{\frac{F_y}{E}} - 0.738\right) \le M_p \qquad \text{(F7-6)}$$

where
$h$ = depth of web, as defined in Section B4.1b, in. (mm)

(c) For sections with slender webs

(1) Compression flange yielding

$$M_n = R_{pg} F_y S \qquad \text{(F7-7)}$$

(2) Compression flange local buckling

$$M_n = R_{pg} F_{cr} S_{xc} \qquad \text{(F7-8)}$$

and

$$F_{cr} = \frac{0.9Ek_c}{\left(\dfrac{b}{t_f}\right)^2} \qquad \text{(F7-9)}$$

where
$R_{pg}$ is defined by Equation F5-6 with $a_w = 2ht_w/(bt_f)$
$k_c = 4.0$

**User Note:** When Equation F7-9 results in the stress, $F_{cr}$, being greater than $F_y$, member strength will be limited by one of the other limit states in Section F7.

**User Note:** There are no HSS with slender webs.

## 4. Lateral-Torsional Buckling

(a) When $L_b \le L_p$, the limit state of lateral-torsional buckling does not apply.

(b) When $L_p < L_b \le L_r$

$$M_n = C_b\left[M_p - \left(M_p - 0.7F_y S_x\right)\left(\frac{L_b - L_p}{L_r - L_p}\right)\right] \le M_p \qquad \text{(F7-10)}$$

(c) When $L_b > L_r$

$$M_n = 2EC_b \frac{\sqrt{JA_g}}{L_b/r_y} \le M_p \qquad \text{(F7-11)}$$

where
$A_g$ = gross cross-sectional area of member, in.$^2$ (mm$^2$)
$L_p$, the limiting laterally unbraced length for the limit state of yielding, in. (mm), is:

$$L_p = 0.13Er_y \frac{\sqrt{JA_g}}{M_p} \qquad \text{(F7-12)}$$

$L_r$, the limiting laterally unbraced length for the limit state of inelastic lateral-torsional buckling, in. (mm), is:

$$L_r = 2Er_y \frac{\sqrt{JA_g}}{0.7F_y S_x} \quad \text{(F7-13)}$$

**User Note:** Lateral-torsional buckling will not occur in square sections or sections bending about their minor axis. In HSS sizes, deflection will usually control before there is a significant reduction in flexural strength due to lateral-torsional buckling. The same is true for box sections, and lateral-torsional buckling will usually only be a consideration for sections with high depth-to-width ratios.

## F8. ROUND HSS

This section applies to round HSS having $D/t$ ratios of less than $\frac{0.45E}{F_y}$.

The nominal flexural strength, $M_n$, shall be the lower value obtained according to the limit states of yielding (plastic moment) and local buckling.

### 1. Yielding

$$M_n = M_p = F_y Z \quad \text{(F8-1)}$$

### 2. Local Buckling

(a) For compact sections, the limit state of flange local buckling does not apply.

(b) For noncompact sections

$$M_n = \left[\frac{0.021E}{\left(\frac{D}{t}\right)} + F_y\right] S \quad \text{(F8-2)}$$

(c) For sections with slender walls

$$M_n = F_{cr} S \quad \text{(F8-3)}$$

where

$D$ = outside diameter of round HSS, in. (mm)

$$F_{cr} = \frac{0.33E}{\left(\frac{D}{t}\right)} \quad \text{(F8-4)}$$

$t$ = design wall thickness of HSS member, in. (mm)

## G4. RECTANGULAR HSS, BOX SECTIONS, AND OTHER SINGLY AND DOUBLY SYMMETRIC MEMBERS

The nominal shear strength, $V_n$, is:

$$V_n = 0.6F_y A_w C_{v2} \tag{G4-1}$$

For rectangular HSS and box sections

$A_w$ = $2ht$, in.$^2$ (mm$^2$)

$C_{v2}$ = web shear buckling strength coefficient, as defined in Section G2.2, with $h/t_w = h/t$ and $k_v = 5$

$h$ = width resisting the shear force, taken as the clear distance between the flanges less the inside corner radius on each side for HSS or the clear distance between flanges for box sections, in. (mm). If the corner radius is not known, $h$ shall be taken as the corresponding outside dimension minus 3 times the thickness.

$t$ = design wall thickness, as defined in Section B4.2, in. (mm)

For other singly or doubly symmetric shapes

$A_w$ = area of web or webs, taken as the sum of the overall depth times the web thickness, $dt_w$, in.$^2$ (mm$^2$)

$C_{v2}$ = web shear buckling strength coefficient, as defined in Section G2.2, with $h/t_w = h/t$ and $k_v = 5$

$h$ = width resisting the shear force, in. (mm)
= for built-up welded sections, the clear distance between flanges, in. (mm)
= for built-up bolted sections, the distance between fastener lines, in. (mm)

$t$ = web thickness, as defined in Section B4.2, in. (mm)

## G5. ROUND HSS

The nominal shear strength, $V_n$, of round HSS, according to the limit states of shear yielding and shear buckling, shall be determined as:

$$V_n = F_{cr} A_g / 2 \tag{G5-1}$$

where

$F_{cr}$ shall be the larger of

$$F_{cr} = \frac{1.60E}{\sqrt{\frac{L_v}{D}}\left(\frac{D}{t}\right)^{\frac{5}{4}}} \tag{G5-2a}$$

and

$$F_{cr} = \frac{0.78E}{\left(\frac{D}{t}\right)^{\frac{3}{2}}} \tag{G5-2b}$$

but shall not exceed $0.6F_y$

$A_g$ = gross cross-sectional area of member, in.$^2$ (mm$^2$)

$D$ = outside diameter, in. (mm)

$L_v$ = distance from maximum to zero shear force, in. (mm)

$t$ = design wall thickness, in. (mm)

AISC Torsional Capacities

Round HSS

168OD x 12.7WT

| | | |
|---|---|---|
| Tr = | 90934423 | N*mm |
| ϕ = | 0.9 | |
| Fcr1 = | 3997 | MPa |
| Fcr2 = | 2494 | MPa |
| E = | 200000 | MPa |
| D = | 168 | mm |
| L = | 1000 | mm |
| t = | 12.7 | mm |
| Fy = | 350 | MPa |
| 0.6*Fy = | 210 | MPa |
| C = | 481135 | mm^3 |

324OD x 25.4WT

| | | |
|---|---|---|
| Tr = | 672349374 | N*mm |
| ϕ = | 0.9 | |
| Fcr1 = | 5809 | MPa |
| Fcr2 = | 2634 | MPa |
| E = | 200000 | MPa |
| D = | 324 | mm |
| L = | 1000 | mm |
| t = | 25.4 | mm |
| Fy = | 350 | MPa |
| 0.6*Fy = | 210 | MPa |
| C = | 3557404 | mm^3 |

AISC Combined Torsion, Shear, Flexure and Axial Force

168OD x 12.7WT

Torsion

| | | |
|---|---|---|
| Tr = | 90934423 | N*mm |
| ϕ = | 0.9 | |
| Fcr1 = | 3997 | MPa |
| Fcr2 = | 2494 | MPa |
| E = | 200000 | MPa |
| D = | 168 | mm |
| L = | 1000 | mm |
| t = | 12.7 | mm |
| Fy = | 350 | MPa |
| 0.6*Fy = | 210 | MPa |
| C = | 481135 | mm^3 |
| Tf = | 32150173 | |

Tension

| | | |
|---|---|---|
| Pc = | 1956150 | N |
| Pn1 = | 1956150 | N |
| Pn2 = | 2095875 | N |
| Ag = | 6210 | mm^2 |
| An = | 6210 | mm^2 |
| Ae = | 6210 | |
| Fu = | 450 | MPa |
| U = | 1 | |
| ϕt = | 0.75 | |
| Pf= | 489038 | N |

Bending

| | | | |
|---|---|---|---|
| Mc = | 97020000 | N*mm | |
| Mn = | 107800000 | N*mm | |
| D/t = | 13.2 | compact | |
| 0.45*E/Fy | 257.1 | | |
| λp = | 40 | | |
| λr = | 177.1 | | |
| Z = | 308000 | mm^3 | |
| Mf = | 24255000 | N*mm | |
| Applied Mf= | 3506896 | N*mm | Reduced moment applied in ANSYS due to shear load. |

Shear

| | | |
|---|---|---|
| Vc = | 586845 | N |
| Vn = | 652050 | N |
| Fcr = | 231 | |
| Fcr1 = | 7352.5 | |
| Lv = | 500 | mm |
| Fcr2 = | 3242.4 | |
| 0.6*Fy | 210 | |
| Vf = | 207481 | N |

UR = 1.0

AISC Torsional Capacities

Square HSS

152 x 152 x 12.7WT

| | | |
|---|---|---|
| Tr = | 36104025 | N*mm |
| ϕ = | 0.9 | |
| E = | 200000 | MPa |
| h = | 101.2 | mm |
| B = | 101.2 | mm |
| t = | 12.7 | mm |
| h/t | 8.0 | |
| 2.45√(E/Fy) | 58.6 | |
| Fy = | 350 | MPa |
| 0.6*Fy = | 210 | MPa |
| C = | 191027 | mm^3 |

305 x 305 x 25.4WT

| | | |
|---|---|---|
| Tr = | 292240628 | N*mm |
| ϕ = | 0.9 | |
| E = | 200000 | MPa |
| h = | 203.4 | mm |
| B = | 203.4 | mm |
| t = | 25.4 | mm |
| h/t | 8.0 | |
| 2.45√(E/Fy) | 58.6 | |
| Fy = | 350 | MPa |
| 0.6*Fy = | 210 | MPa |
| C = | 1546247 | mm^3 |

AISC Combined Torsion, Shear, Flexure and Axial Force

152 x 152 x 12.7WT

Torsion

| | | |
|---|---|---|
| Tr = | 36104025 | N*mm |
| ϕ = | 0.9 | |
| E = | 200000 | MPa |
| h = | 101.2 | mm |
| B = | 101.2 | mm |
| t = | 12.7 | mm |
| h/t | 8.0 | |
| 2.45√(E/Fy) | 58.6 | |
| Fy = | 350 | MPa |
| 0.6*Fy = | 210 | MPa |
| C = | 191027 | mm^3 |
| Tf = | 12764701 | |

| | | | |
|---|---|---|---|
| Tension | | | |
| Pc = | 2104200 | N | |
| Pn1 = | 2104200 | N | |
| Pn2 = | 2254500 | N | |
| Ag = | 6680 | mm^2 | |
| An = | 6680 | mm^2 | |
| Ae = | 6680 | | |
| Fu = | 450 | MPa | |
| U = | 1 | | |
| ϕt = | 0.75 | | |
| Pf= | 526050 | N | |
| | | | |
| Bending | | | |
| Mc = | 107730000 | N*mm | |
| Mn = | 119700000 | N*mm | |
| H/t = | 7.97 | compact | |
| λp = | 57.8 | | |
| λr = | 136.3 | | |
| Z = | 342000 | mm^3 | |
| Mf = | 26932500 | N*mm | |
| Applied Mf= | 9756144 | N*mm | Reduced moment applied in ANSYS due to shear load. |
| Lb = | 1000 | mm | ok |
| Lp = | 5942 | mm | |
| ry = | 56.1 | mm | |
| | | | |
| Shear | | | |
| Vc = | 485821 | N | |
| Vn = | 539801 | N | |
| Aw = | 2570.5 | mm^2 | |
| Cv2 | 1 | | ok |
| h/t | 8 | | |
| 1.10√(kvE/Fy) | 59 | N | |
| Kv = | 5 | | |
| Vf = | 171764 | | |
| | | | |
| UR = | 1.0 | | |

AISC Torsional Capacities

Rectangular HSS

203 x 152 x 12.7WT

| | | |
|---|---|---|
| Tr = | 57771533 | N*mm |
| ϕ = | 0.9 | |
| E = | 200000 | MPa |
| h = | 152.2 | mm |
| B = | 101.2 | mm |
| t = | 12.7 | mm |
| h/t | 12.0 | |
| 2.45√(E/Fy) | 58.6 | |
| Fy = | 350 | MPa |
| 0.6*Fy = | 210 | MPa |
| C = | 305669 | mm^3 |

356 x 254 x 25.4WT

| | | |
|---|---|---|
| Tr = | 267267907 | N*mm |
| ϕ = | 0.9 | |
| E = | 200000 | MPa |
| h = | 254.4 | mm |
| B = | 152.4 | mm |
| t = | 25.4 | mm |
| h/t | 10.0 | |
| 2.45√(E/Fy) | 58.6 | |
| Fy = | 350 | MPa |
| 0.6*Fy = | 210 | MPa |
| C = | 1414116 | mm^3 |

AISC Combined Torsion, Shear, Flexure and Axial Force

203 x 152 x 12.7WT

Torsion

| | | |
|---|---|---|
| Tr = | 57771533 | N*mm |
| ϕ = | 0.9 | |
| E = | 200000 | MPa |
| h = | 152.2 | mm |
| B = | 101.2 | mm |
| t = | 12.7 | mm |
| h/t | 12.0 | |
| 2.45√(E/Fy) | 58.6 | |
| Fy = | 350 | MPa |
| 0.6*Fy = | 210 | MPa |
| C = | 305669 | mm^3 |
| Tf = | 20425321 | |

Tension

| | | | |
|---|---|---|---|
| Pc = | 2510550 | N | |
| Pn1 = | 2510550 | N | |
| Pn2 = | 2689875 | N | |
| Ag = | 7970 | mm^2 | |
| An = | 7970 | mm^2 | |
| Ae = | 7970 | | |
| Fu = | 450 | MPa | |
| U = | 1 | | |
| ϕt = | 0.75 | | |
| Pf= | 627638 | N | |

Bending

| | | | |
|---|---|---|---|
| Mc = | 166320000 | N*mm | |
| Mn = | 184800000 | N*mm | |
| H/t = | 11.98 | compact | |
| λp = | 57.8 | | |
| λr = | 136.3 | | |
| Z = | 528000 | mm^3 | |
| Mf = | 41580000 | N*mm | |
| Applied Mf= | 15747575 | N*mm | Reduced moment applied in ANSYS due to shear load. |
| Lb = | 1000 | mm | ok |
| Lp = | 5508 | mm | |
| ry = | 58.6 | mm | |
| J = | 56000000 | mm^4 | |

Shear

| | | | |
|---|---|---|---|
| Vc = | 730651 | N | |
| Vn = | 811835 | N | |
| Aw = | 3865.9 | mm^2 | |
| Cv2 | 1 | | |
| h/t | 12 | | ok |
| 1.10√(kvE/Fy) | 59 | N | |
| Kv = | 5 | | |
| Vf = | 258324 | | |

| | |
|---|---|
| UR = | 1.0 |

Shown below are the CAN/CSA S16-19 – Design of Steel Structures [1] axial, flexure and shear clauses along with the calculated section capacities which were used for comparison to the AISC values.

### 13.2 Axial tension

The factored tensile resistance, $T_r$, developed by a member subjected to an axial tensile force shall be taken as follows:

a) the least of
   i) $T_r = \phi A_g F_y$;
   ii) $T_r$ = resistance determined using Clause 13.11; and
   iii) $T_r = \phi_u A_{ne} F_u$; and

b) for pin connections (excluding eyebars), the least of
   i) $T_r = \phi A_g F_y$;
   ii) $T_r = \phi_u A_{net} F_u$; and
   iii) $T_r = 0.6\phi_u A_{nes} F_u$,

   where $A_{net}$ and $A_{nes}$ are defined in Clause 12.4.1.

### 13.5 Bending — Laterally supported members

The factored moment resistance, $M_r$, developed by a member subjected to uniaxial bending moments about a principal axis where effectively continuous lateral support is provided to the compression flange, or where the member has no tendency to buckle laterally, shall be taken as follows:

a) for Class 1 and Class 2 sections (except that singly symmetric I-sections and T-sections shall not yield under service loads):

$$M_r = \phi Z F_y$$
$$= \phi M_p$$

### 13.4.1.3 Tubular members and concrete-filled tubular members

The shear resistance, $V_r$, of Class 1 and 2 tubular members and concrete-filled tubular members where local wall buckling is prevented shall be taken as

$$V_r = 0.66\phi\,(A/2)F_y$$

where

$A$ = cross-sectional area of the tubular member portion of the concrete-filled member

CSA Section Capacites (Shear, Flexure and Axial Force) for Comparison to AISC

Round HSS - 168OD x 12.7WT

Torsion (AISC)

| | | | |
|---|---|---|---|
| Tr = | 90934423 | N*mm | |
| ϕ = | 0.9 | | |
| Fcr1 = | 3997 | MPa | |
| Fcr2 = | 2494 | MPa | |
| E = | 200000 | MPa | |
| D = | 168 | mm | |
| L = | 1000 | mm | |
| t = | 12.7 | mm | |
| Fy = | 350 | MPa | |
| 0.6*Fy = | 210 | MPa | |
| C = | 481135 | mm^3 | |
| Tf = | 32150173 | | Can't calculate in CSA |

Tension

| | | | |
|---|---|---|---|
| Tr= | 1956150 | N | |
| ϕ = | 0.9 | | |
| Ag = | 6210 | mm^2 | |
| Fy = | 350 | MPa | |
| Pf= | 489038 | N | ok, equal to AISC value |

Bending

| | | | |
|---|---|---|---|
| Mr= | 97020000 | N*mm | |
| D/t = | 13.2 | class 1 | |
| 13000/Fy | 37.1 | | |
| Z = | 308000 | mm^3 | |
| Mf = | 24255000 | N*mm | ok, equal to AISC value |
| Applied Mf = | 1432086 | N*mm | Reduced moment applied in ANSYS due to shear load. |

Shear

| | | | |
|---|---|---|---|
| Vr= | 645530 | N | |
| ϕs = | 0.66 | | |
| Vf = | 228229 | N | Greater than AISC value of 207481 N |

CSA Section Capacites (Shear, Flexure and Axial Force) for Comparison to AISC

152 x 152 x 12.7WT

Torsion (AISC)

| | | | |
|---|---|---|---|
| Tr = | 36104025 | N*mm | |
| ϕ = | 0.9 | | |
| E = | 200000 | MPa | |
| h = | 101.2 | mm | |
| B = | 101.2 | mm | |
| t = | 12.7 | mm | |
| h/t | 8.0 | | |
| 2.45√(E/Fy) | 58.6 | | |
| Fy = | 350 | MPa | |
| 0.6*Fy = | 210 | MPa | |
| C = | 191027 | mm^3 | |
| Tf = | 12764701 | | Can't calculate in CSA |

Tension

| | | | |
|---|---|---|---|
| Tr= | 2104200 | N | |
| ϕ = | 0.9 | | |
| Ag = | 6680 | mm^2 | |
| Fy = | 350 | MPa | |
| Pf= | 526050 | N | ok, equal to AISC value |

Bending

| | | | |
|---|---|---|---|
| Mr= | 107730000 | N*mm | |
| b | 101.2 | mm | |
| b/t = | 8.0 | class 2 | |
| 170/√Fy | 9.1 | | |
| Z = | 342000 | mm^3 | |
| Mf = | 26932500 | N*mm | ok, equal to AISC value |

Shear

| | | | |
|---|---|---|---|
| Vr= | 391895 | N | |
| ϕs = | 0.66 | | |
| Aw = | 2570.5 | mm^3 | |
| h/w = | 8.0 | | |
| 1014/√Fy | 54.2 | ok | |
| Fs = | 231.0 | Mpa | |
| Vf = | 138556 | N | ok, less than AISC value of 171764 N |

CSA Section Capacites (Shear, Flexure and Axial Force) for Comparison to AISC

203 x 152 x 12.7WT

| | | | |
|---|---|---|---|
| Torsion (AISC) | | | |
| Tr = | 57771533 | N*mm | |
| ϕ = | 0.9 | | |
| E = | 200000 | MPa | |
| h = | 152.2 | mm | |
| B = | 101.2 | mm | |
| t = | 12.7 | mm | |
| h/t | 12.0 | | |
| 2.45√(E/Fy) | 58.6 | | |
| Fy = | 350 | MPa | |
| 0.6*Fy = | 210 | MPa | |
| C = | 305669 | mm^3 | |
| Tf = | 20425321 | | Can't calculate in CSA |
| | | | |
| Tension | | | |
| Tr= | 2510550 | N | |
| ϕ = | 0.9 | | |
| Ag = | 7970 | mm^2 | |
| Fy = | 350 | MPa | |
| Pf= | 627638 | N | ok, equal to AISC value |
| | | | |
| Bending | | | |
| Mr= | 166320000 | N*mm | |
| b | 101.2 | mm | |
| b/t = | 8.0 | class 2 | |
| 170/√Fy | 9.1 | | |
| Z = | 528000 | mm^3 | |
| Mf = | 41580000 | N*mm | ok, equal to AISC value |
| | | | |
| Shear | | | |
| Vr= | 589392 | N | |
| ϕs = | 0.66 | | |
| Aw = | 3865.9 | mm^3 | |
| h/w = | 12.0 | | |
| 1014/√Fy | 54.2 | ok | |
| Fs = | 231.0 | Mpa | |
| Vf = | 208382 | N | ok, less than AISC value of 258324 N |

# Appendix B – STAAD.Pro Validation for Torsion and Combined Loading Models

## Job Information

| | Engineer | Checked | Approved |
|---|---|---|---|
| Name: | | | |
| Date: | 09-Nov-20 | | |

| | |
|---|---|
| Project ID | |
| Project Name | |

| | |
|---|---|
| Structure Type | SPACE FRAME |

| | | | |
|---|---|---|---|
| Number of Nodes | 2 | Highest Node | 3 |
| Number of Elements | 1 | Highest Beam | 1 |

| | |
|---|---|
| Number of Basic Load Cases | 1 |
| Number of Combination Load Cases | 0 |

*Included in this printout are data for:*

| | |
|---|---|
| All | The Whole Structure |

*Included in this printout are results for load cases:*

| Type | L/C | Name |
|---|---|---|
| Primary | 1 | COMBINED TORSION |

## Nodes

| Node | X (m) | Y (m) | Z (m) |
|---|---|---|---|
| 1 | 0 | 0 | 0 |
| 3 | 0 | 0 | 1.000 |

## Beams

| Beam | Node A | Node B | Length (m) | Property | β (degrees) |
|---|---|---|---|---|---|
| 1 | 1 | 3 | 1.000 | 1 | 0 |

## Section Properties

| Prop | Section | Area ($in^2$) | $I_{yy}$ ($in^4$) | $I_{zz}$ ($in^4$) | J ($in^4$) | Material |
|---|---|---|---|---|---|---|
| 1 | HSSP168X13 | 9.626 | 45.407 | 45.407 | 90.881 | STEEL |

## Materials

| Mat | Name | E (kip/in$^2$) | ν | Density (kip/in$^3$) | α (/°F) |
|---|---|---|---|---|---|
| 1 | CONCRETE | 3.15E+3 | 0.170 | 8.68e-05 | 5.5E -6 |
| 2 | ALUMINUM | 10E+3 | 0.330 | 9.8e-05 | 12.8E -6 |
| 3 | STEEL_50_KSI | 29E+3 | 0.300 | 0.000283 | 6.5E -6 |
| 4 | STAINLESSSTEEL | 28E+3 | 0.300 | 0.000283 | 9.9E -6 |
| 5 | STEEL_36_KSI | 29E+3 | 0.300 | 0.000283 | 6.5E -6 |
| 6 | STEEL_275_NMM2 | 29.7E+3 | 0.300 | 0.000 | 6.67E -6 |
| 7 | STEEL | 29E+3 | 0.300 | 0.000283 | 6.5E -6 |
| 8 | STEEL_355_NMM2 | 29.7E+3 | 0.300 | 0.000 | 6.67E -6 |

## Supports

| Node | X (kN/m) | Y (kN/m) | Z (kN/m) | rX (kN·m/deg) | rY (kN·m/deg) | rZ (kN·m/deg) |
|---|---|---|---|---|---|---|
| 1 | Fixed | Fixed | Fixed | Fixed | Fixed | Fixed |

## Primary Load Cases

| Number | Name | Type |
|---|---|---|
| 1 | COMBINED TORSION | None |

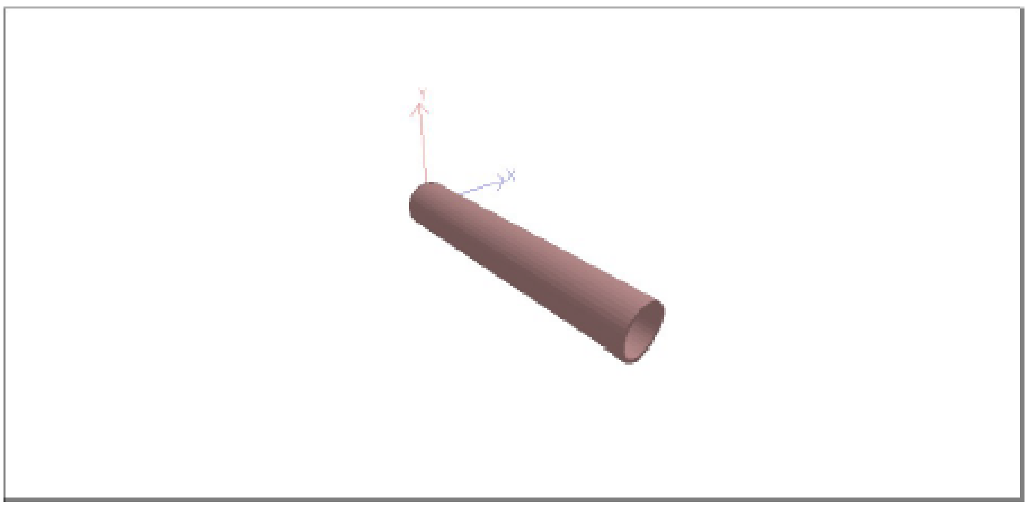


*3D Rendered View*

| | | | |
|---|---|---|---|
| Software licensed to MEMORIAL UNIVERSITY OF NEWFOUNDLAND<br>CONNECTED User: Steve Bartlett | Job No | Sheet No 3 | Rev |
| | Part | | |
| Job Title | Ref | | |
| | By | Date 09-Nov-20 | Chd |
| Client | File 168x12.7 AISC Torsion.st | Date/Time 10-Nov-2020 11:54 | |

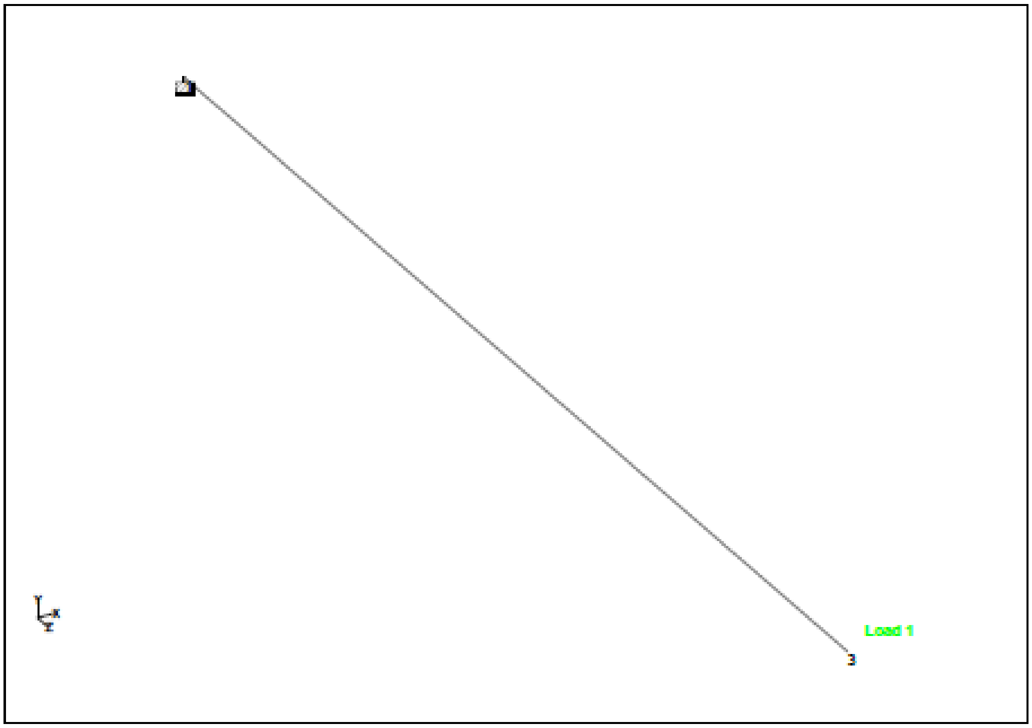


*Node Numbers*

| | | | |
|---|---|---|---|
| Software licensed to MEMORIAL UNIVERSITY OF NEWFOUNDLAND<br>CONNECTED User: Steve Bartlett | Job No | Sheet No<br>4 | Rev |
| | Part | | |
| Job Title | Ref | | |
| | By | Date 09-Nov-20 | Chd |
| Client | File 168x12.7 AISC Torsion.ST | Date/Time 10-Nov-2020 11:54 | |

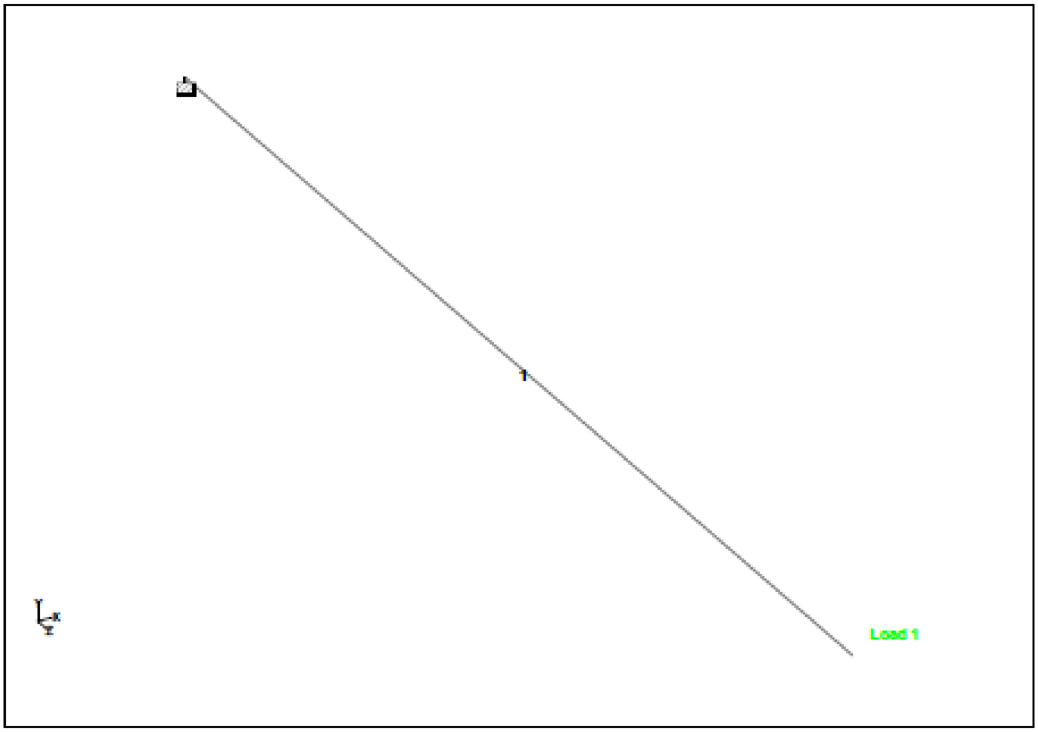


*Beam Numbers*

Print Time/Date: 10/11/2020 12:16 STAAD.Pro CONNECT Edition 22.04.00.40 Print Run 4 of 8

| Software licensed to MEMORIAL UNIVERSITY OF NEWFOUNDLAND<br>CONNECTED User: Steve Bartlett | Job No | Sheet No<br>5 | Rev |
|---|---|---|---|
| | Part | | |
| Job Title | Ref | | |
| | By | Date 09-Nov-20 | Chd |
| Client | File 168x12.7 AISC Torsion.ST | Date/Time 10-Nov-2020 11:54 | |

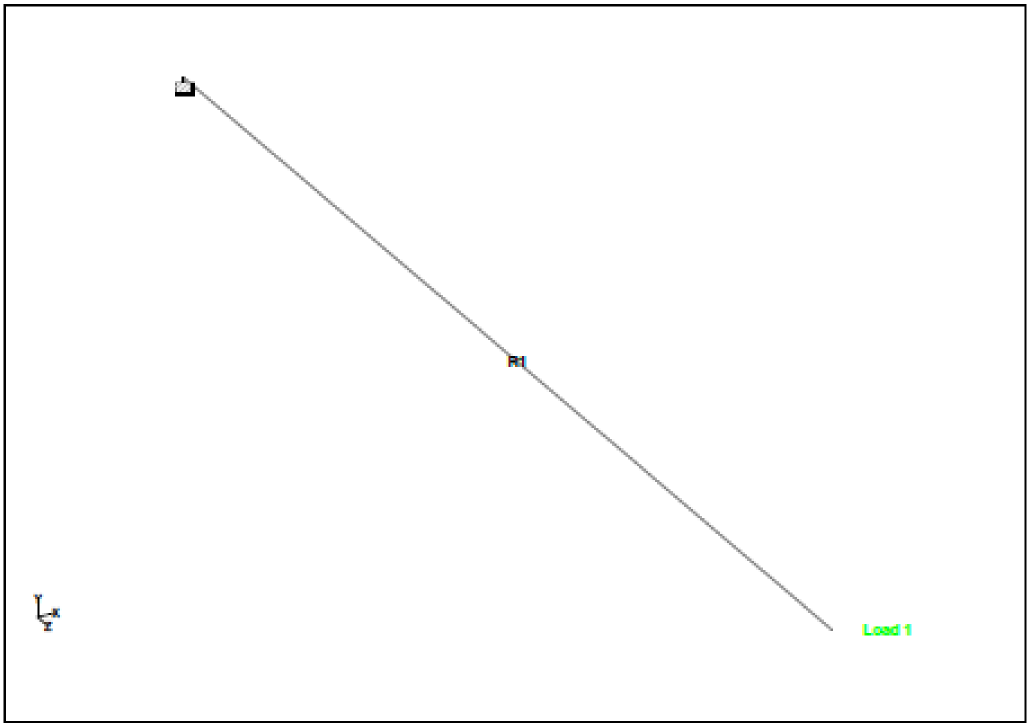


*Property Reference*

| Software licensed to MEMORIAL UNIVERSITY OF NEWFOUNDLAND<br>CONNECTED User: Steve Bartlett | Job No | Sheet No<br>6 | Rev |
|---|---|---|---|
| | Part | | |
| Job Title | Ref | | |
| | By | Date 09-Nov-20 | Chd |
| Client | File 168x12.7 AISC Torsion.st | Date/Time 10-Nov-2020 11:54 | |

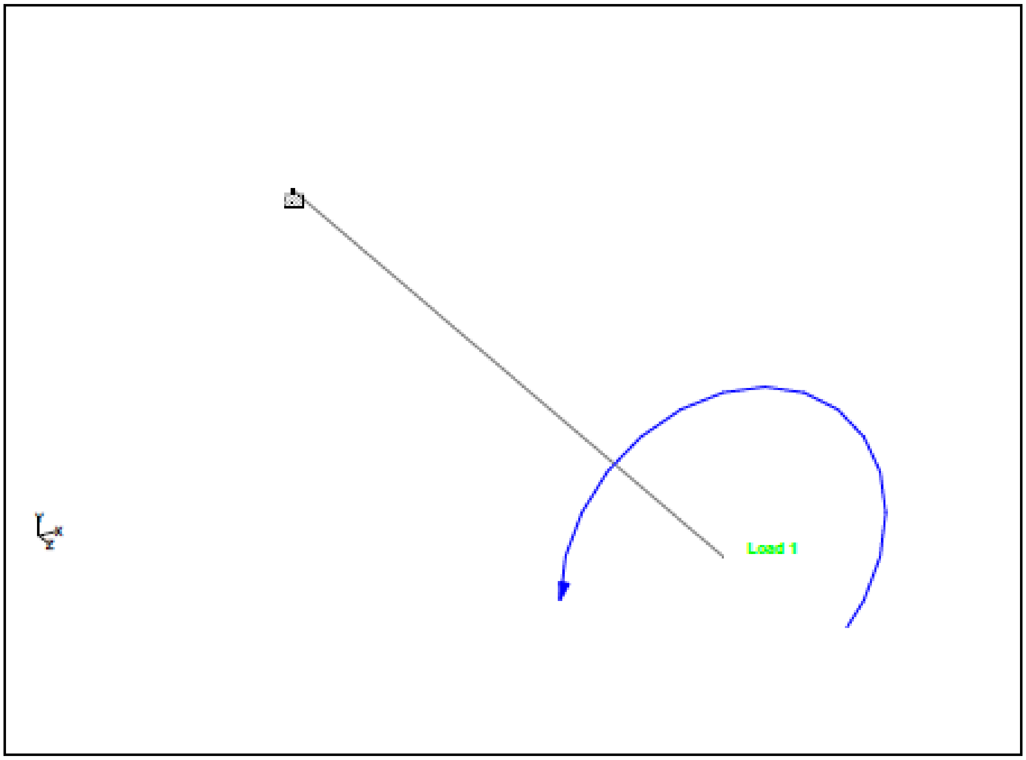


*Torsion Load*

## Node Displacement Summary

| | Node | L/C | X (m) | Y (m) | Z (m) | Resultant (m) | rX (rad) | rY (rad) | rZ (rad) |
|---|---|---|---|---|---|---|---|---|---|
| Max X | 1 | 1:COMBINED | 0 | 0 | 0 | 0 | 0 | 0 | 0 |
| Min X | 1 | 1:COMBINED | 0 | 0 | 0 | 0 | 0 | 0 | 0 |
| Max Y | 1 | 1:COMBINED | 0 | 0 | 0 | 0 | 0 | 0 | 0 |
| Min Y | 1 | 1:COMBINED | 0 | 0 | 0 | 0 | 0 | 0 | 0 |
| Max Z | 1 | 1:COMBINED | 0 | 0 | 0 | 0 | 0 | 0 | 0 |
| Min Z | 1 | 1:COMBINED | 0 | 0 | 0 | 0 | 0 | 0 | 0 |
| Max rX | 1 | 1:COMBINED | 0 | 0 | 0 | 0 | 0 | 0 | 0 |
| Min rX | 1 | 1:COMBINED | 0 | 0 | 0 | 0 | 0 | 0 | 0 |
| Max rY | 1 | 1:COMBINED | 0 | 0 | 0 | 0 | 0 | 0 | 0 |
| Min rY | 1 | 1:COMBINED | 0 | 0 | 0 | 0 | 0 | 0 | 0 |
| Max rZ | 3 | 1:COMBINED | 0 | 0 | 0 | 0 | 0 | 0 | 0.031 |
| Min rZ | 1 | 1:COMBINED | 0 | 0 | 0 | 0 | 0 | 0 | 0 |
| Max Rst | 1 | 1:COMBINED | 0 | 0 | 0 | 0 | 0 | 0 | 0 |

## Beam Displacement Detail

*Displacements shown in italic indicate the presence of an offset*

| Beam | L/C | d (m) | X (m) | Y (m) | Z (m) | Resultant (m) |
|---|---|---|---|---|---|---|
| 1 | 1:COMBINED ' | 0 | 0 | 0 | 0 | 0 |
| | | 0.100 | 0 | 0 | -0.000 | 0.000 |
| | | 0.200 | 0 | 0 | -0.000 | 0.000 |
| | | 0.300 | 0 | 0 | -0.000 | 0.000 |
| | | 0.400 | 0 | 0 | -0.000 | 0.000 |
| | | 0.500 | 0 | 0 | -0.000 | 0.000 |
| | | 0.600 | 0 | 0 | 0.000 | 0.000 |
| | | 0.700 | 0 | 0 | -0.000 | 0.000 |
| | | 0.800 | 0 | 0 | -0.000 | 0.000 |
| | | 0.900 | 0 | 0 | 0.000 | 0.000 |
| | | 1.000 | 0 | 0 | 0 | 0 |

## Reaction Envelope

| | | Horizontal | Vertical | Horizontal | Moment | | |
|---|---|---|---|---|---|---|---|
| Node | Env | FX (kN) | FY (kN) | FZ (kN) | MX (kN`m) | MY (kN`m) | MZ (kN`m) |
| 1 | +ve | 0 | 0 | 0 | 0 | 0 | 0 |
| 1 | +ve | - | - | - | - | - | - |
| 1 | -ve | 0 | 0 | 0 | 0 | 0 | -90.930 |
| 1 | -ve | - | - | - | - | - | Load: 1 |

| Software licensed to MEMORIAL UNIVERSITY OF NEWFOUNDLAND<br>CONNECTED User: Steve Bartlett | Job No | Sheet No<br>8 | Rev |
|---|---|---|---|
| | Part | | |
| Job Title | Ref | | |
| | By | Date 09-Nov-20 | Chd |
| Client | File 168x12.7 AISC Torsion.S1 | Date/Time 10-Nov-2020 11:54 | |

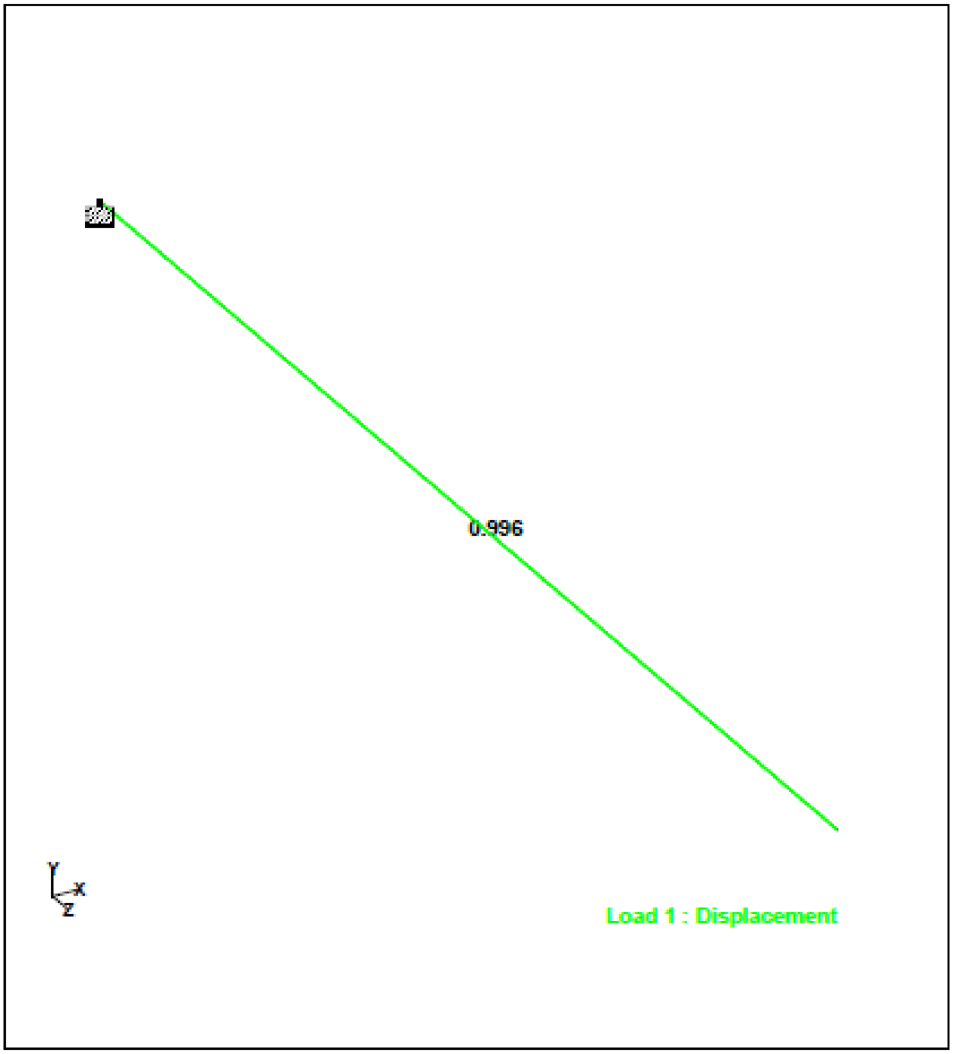


*Utilization Ratio*

## Utilization Ratio

| Beam | Analysis Property | Design Property | Actual Ratio | Allowable Ratio | Ratio (Act./Allow.) | Clause | L/C | Ax ($in^2$) | Iz ($in^4$) | Iy ($in^4$) | Ix ($in^4$) |
|---|---|---|---|---|---|---|---|---|---|---|---|
| 1 | HSSP168X1 | HSSP168X1 | 0.996 | 1.000 | 0.996 | Cl.H3.1 | 1 | 9.626 | 45.407 | 45.407 | 90.815 |

## Job Information

| | Engineer | Checked | Approved |
|---|---|---|---|
| Name: | | | |
| Date: | 09-Nov-20 | | |

| | |
|---|---|
| Project ID | |
| Project Name | |

| | |
|---|---|
| Structure Type | SPACE FRAME |

| | | | |
|---|---|---|---|
| Number of Nodes | 2 | Highest Node | 3 |
| Number of Elements | 1 | Highest Beam | 1 |

| | |
|---|---|
| Number of Basic Load Cases | 1 |
| Number of Combination Load Cases | 0 |

*Included in this printout are data for:*

| | |
|---|---|
| All | The Whole Structure |

*Included in this printout are results for load cases:*

| Type | L/C | Name |
|---|---|---|
| Primary | 1 | COMBINED TORSION |

## Nodes

| Node | X (m) | Y (m) | Z (m) |
|---|---|---|---|
| 1 | 0 | 0 | 0 |
| 3 | 0 | 0 | 1.000 |

## Beams

| Beam | Node A | Node B | Length (m) | Property | β (degrees) |
|---|---|---|---|---|---|
| 1 | 1 | 3 | 1.000 | 1 | 0 |

## Section Properties

| Prop | Section | Area ($in^2$) | $I_{yy}$ ($in^4$) | $I_{zz}$ ($in^4$) | J ($in^4$) | Material |
|---|---|---|---|---|---|---|
| 1 | HSSP168X13 | 9.626 | 45.407 | 45.407 | 90.881 | STEEL |

| Software licensed to MEMORIAL UNIVERSITY OF NEWFOUNDLAND<br>CONNECTED User: Steve Bartlett | Job No | Sheet No<br>2 | Rev |
|---|---|---|---|
| | Part | | |
| Job Title | Ref | | |
| | By | Date 09-Nov-20 | Chd |
| Client | File 168x12.7 AISC Combined | Date/Time 23-Jul-2021 16:08 | |

## Materials

| Mat | Name | E (kip/in$^2$) | ν | Density (kip/in$^3$) | α (/°F) |
|---|---|---|---|---|---|
| 1 | CONCRETE | 3.15E+3 | 0.170 | 8.68e-05 | 5.5E -6 |
| 2 | ALUMINUM | 10E+3 | 0.330 | 9.8e-05 | 12.8E -6 |
| 3 | STEEL_50_KSI | 29E+3 | 0.300 | 0.000283 | 6.5E -6 |
| 4 | STAINLESSSTEEL | 28E+3 | 0.300 | 0.000283 | 9.9E -6 |
| 5 | STEEL_36_KSI | 29E+3 | 0.300 | 0.000283 | 6.5E -6 |
| 6 | STEEL_275_NMM2 | 29.7E+3 | 0.300 | 0.000 | 6.67E -6 |
| 7 | STEEL | 29E+3 | 0.300 | 0.000283 | 6.5E -6 |
| 8 | STEEL_355_NMM2 | 29.7E+3 | 0.300 | 0.000 | 6.67E -6 |

## Supports

| Node | X (kN/m) | Y (kN/m) | Z (kN/m) | rX (kN m/deg) | rY (kN m/deg) | rZ (kN m/deg) |
|---|---|---|---|---|---|---|
| 1 | Fixed | Fixed | Fixed | Fixed | Fixed | Fixed |

## Primary Load Cases

| Number | Name | Type |
|---|---|---|
| 1 | COMBINED TORSION | None |

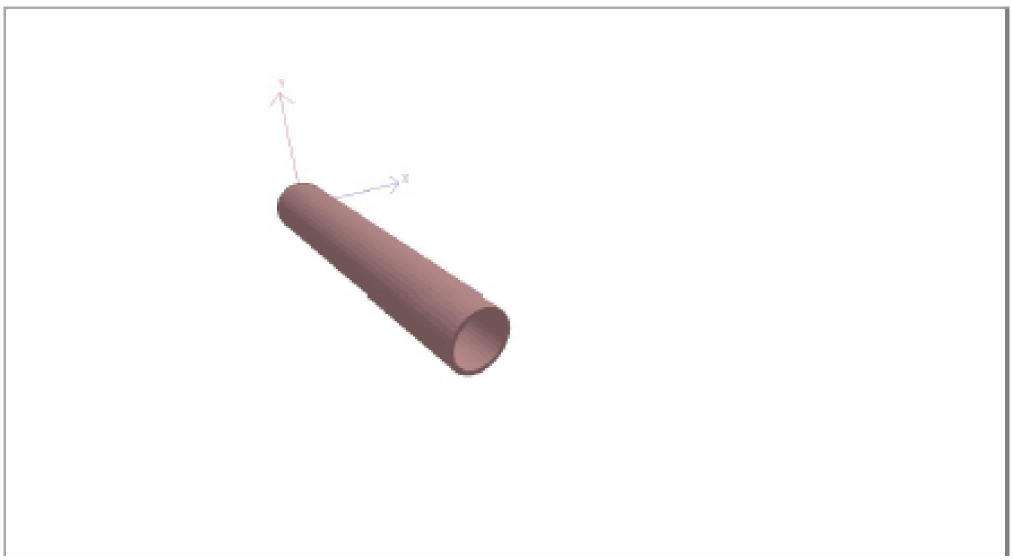


*3D Rendered View*

| Software licensed to MEMORIAL UNIVERSITY OF NEWFOUNDLAND<br>CONNECTED User: Steve Bartlett | Job No | Sheet No<br>3 | Rev |
|---|---|---|---|
| | Part | | |
| Job Title | Ref | | |
| | By | Date 09-Nov-20 | Chd |
| Client | File 168x12.7 AISC Combined | Date/Time 23-Jul-2021 16:08 | |

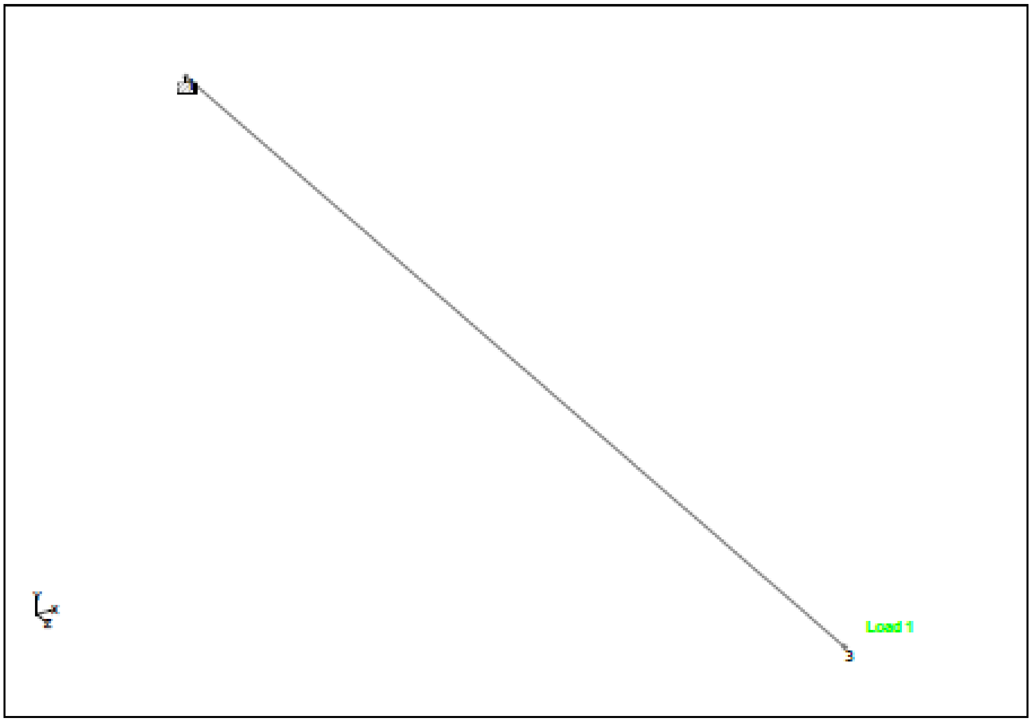


*Node Numbers*

Print Time/Date: 23/07/2021 16:17 STAAD.Pro CONNECT Edition 22.04.00.40 Print Run 3 of 8

| Software licensed to MEMORIAL UNIVERSITY OF NEWFOUNDLAND<br>CONNECTED User: Steve Bartlett | Job No | Sheet No<br>4 | Rev |
|---|---|---|---|
| | Part | | |
| Job Title | Ref | | |
| | By | Date 09-Nov-20 | Chd |
| Client | File 168x12.7 AISC Combined | Date/Time 23-Jul-2021 16:08 | |

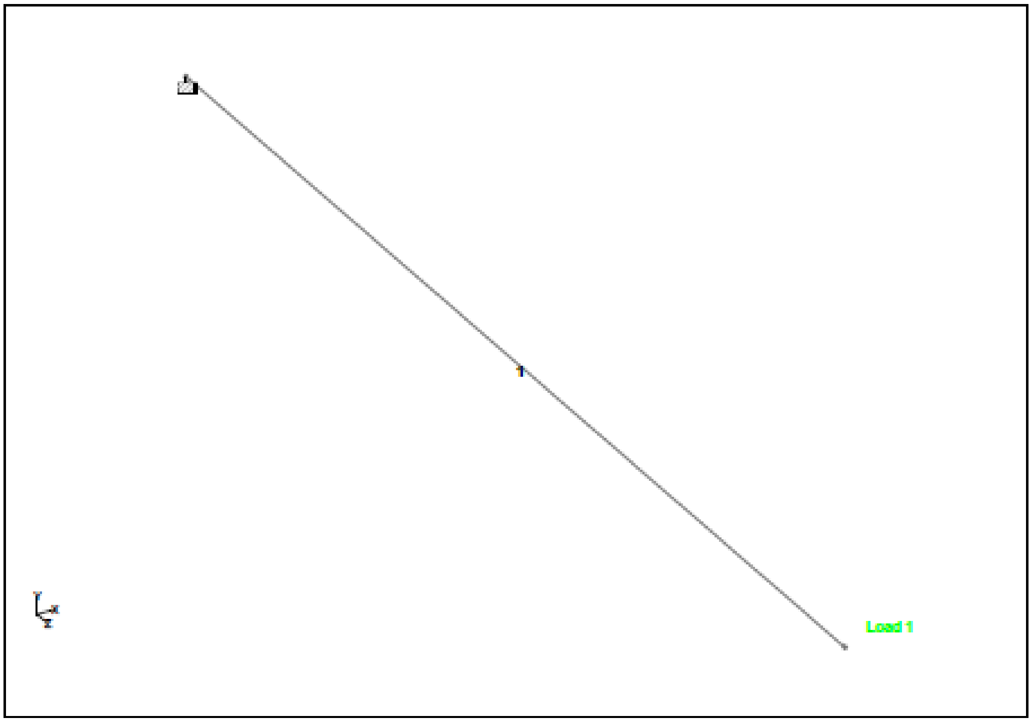


*Beam Numbers*

Print Time/Date: 23/07/2021 16:17 STAAD.Pro CONNECT Edition 22.04.00.40 Print Run 4 of 8

| Software licensed to MEMORIAL UNIVERSITY OF NEWFOUNDLAND<br>CONNECTED User: Steve Bartlett | Job No | Sheet No<br>5 | Rev |
|---|---|---|---|
| | Part | | |
| Job Title | Ref | | |
| | By | Date 09-Nov-20 | Chd |
| Client | File 168x12.7 AISC Combined | Date/Time 23-Jul-2021 16:08 | |

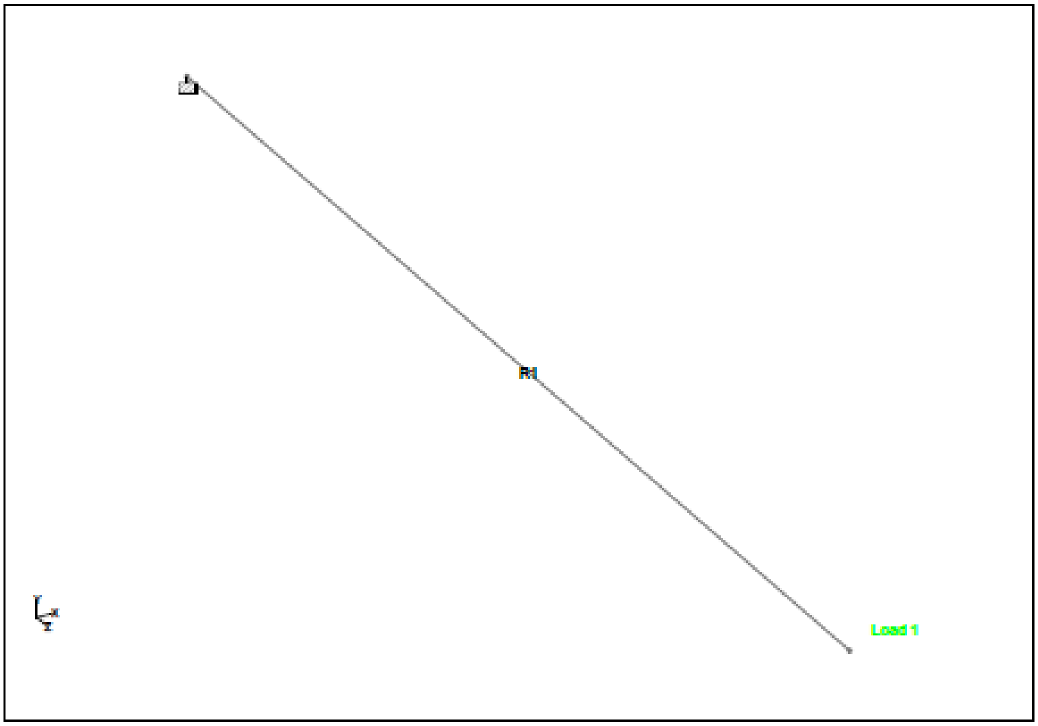


*Property Reference*

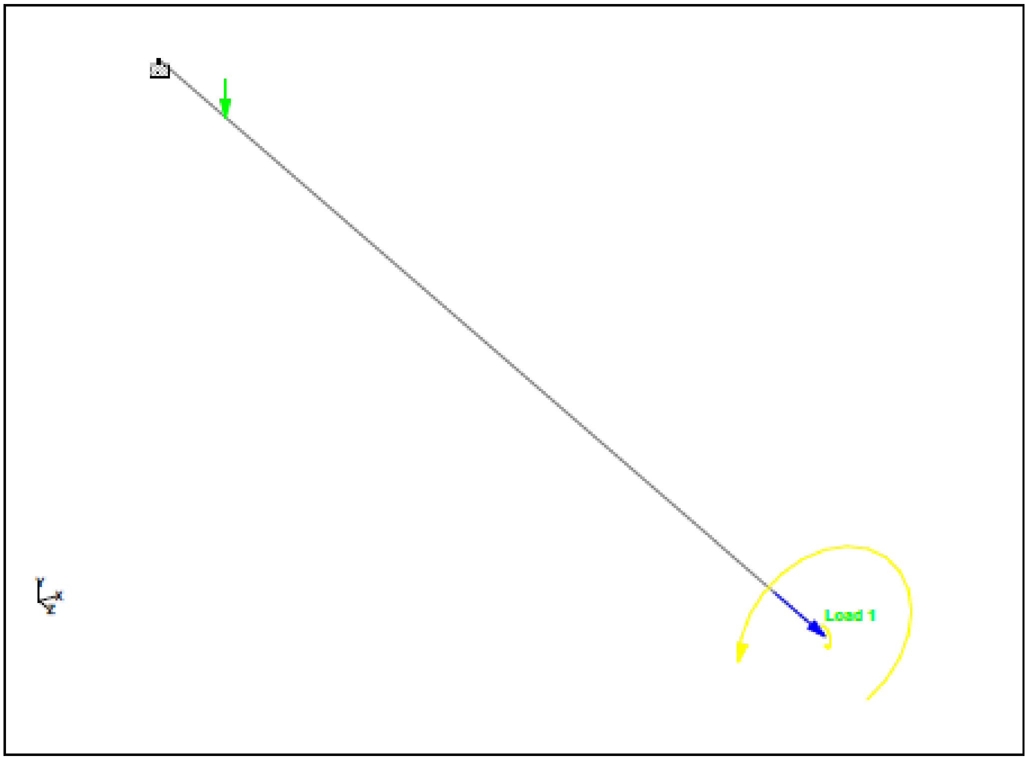


*Combined Loads*

## Node Displacement Summary

| | Node | L/C | X (m) | Y (m) | Z (m) | Resultant (m) | rX (rad) | rY (rad) | rZ (rad) |
|---|---|---|---|---|---|---|---|---|---|
| Max X | 1 | 1:COMBINED | 0 | 0 | 0 | 0 | 0 | 0 | 0 |
| Min X | 1 | 1:COMBINED | 0 | 0 | 0 | 0 | 0 | 0 | 0 |
| Max Y | 1 | 1:COMBINED | 0 | 0 | 0 | 0 | 0 | 0 | 0 |
| Min Y | 3 | 1:COMBINED | 0 | -0.001 | 0.000 | 0.001 | 0.001 | 0 | 0.011 |
| Max Z | 3 | 1:COMBINED | 0 | -0.001 | 0.000 | 0.001 | 0.001 | 0 | 0.011 |
| Min Z | 1 | 1:COMBINED | 0 | 0 | 0 | 0 | 0 | 0 | 0 |
| Max rX | 3 | 1:COMBINED | 0 | -0.001 | 0.000 | 0.001 | 0.001 | 0 | 0.011 |
| Min rX | 1 | 1:COMBINED | 0 | 0 | 0 | 0 | 0 | 0 | 0 |
| Max rY | 1 | 1:COMBINED | 0 | 0 | 0 | 0 | 0 | 0 | 0 |
| Min rY | 1 | 1:COMBINED | 0 | 0 | 0 | 0 | 0 | 0 | 0 |
| Max rZ | 3 | 1:COMBINED | 0 | -0.001 | 0.000 | 0.001 | 0.001 | 0 | 0.011 |
| Min rZ | 1 | 1:COMBINED | 0 | 0 | 0 | 0 | 0 | 0 | 0 |
| Max Rst | 3 | 1:COMBINED | 0 | -0.001 | 0.000 | 0.001 | 0.001 | 0 | 0.011 |

## Beam Displacement Detail

*Displacements shown in italic indicate the presence of an offset*

| Beam | L/C | d (m) | X (m) | Y (m) | Z (m) | Resultant (m) |
| --- | --- | --- | --- | --- | --- | --- |
| 1 | 1:COMBINED * | 0 | 0 | 0 | 0 | 0 |
| | | 0.100 | 0 | -0.000 | 0.000 | 0.000 |
| | | 0.200 | 0 | -0.000 | 0.000 | 0.000 |
| | | 0.300 | 0 | -0.000 | 0.000 | 0.000 |
| | | 0.400 | 0 | -0.000 | 0.000 | 0.000 |
| | | 0.500 | 0 | -0.000 | 0.000 | 0.000 |
| | | 0.600 | 0 | -0.000 | 0.000 | 0.000 |
| | | 0.700 | 0 | -0.000 | 0.000 | 0.001 |
| | | 0.800 | 0 | -0.001 | 0.000 | 0.001 |
| | | 0.900 | 0 | -0.001 | 0.000 | 0.001 |
| | | 1.000 | 0 | -0.001 | 0.000 | 0.001 |

## Reaction Envelope

| | | Horizontal | Vertical | Horizontal | Moment | | |
| --- | --- | --- | --- | --- | --- | --- | --- |
| Node | Env | FX (kN) | FY (kN) | FZ (kN) | MX (kN`m) | MY (kN`m) | MZ (kN`m) |
| 1 | +ve | 0 | 207.480 | 0 | 0 | 0 | 0 |
| 1 | +ve | - | Load: 1 | - | - | - | - |
| 1 | -ve | 0 | 0 | -489.038 | -24.258 | 0 | -32.150 |
| 1 | -ve | - | - | Load: 1 | Load: 1 | - | Load: 1 |

| Job Title | Job No | Sheet No 8 | Rev |
|---|---|---|---|
| | Part | | |
| | Ref | | |
| | By | Date 09-Nov-20 | Chd |
| Client | File 168x12.7 AISC Combined | Date/Time 23-Jul-2021 16:08 | |

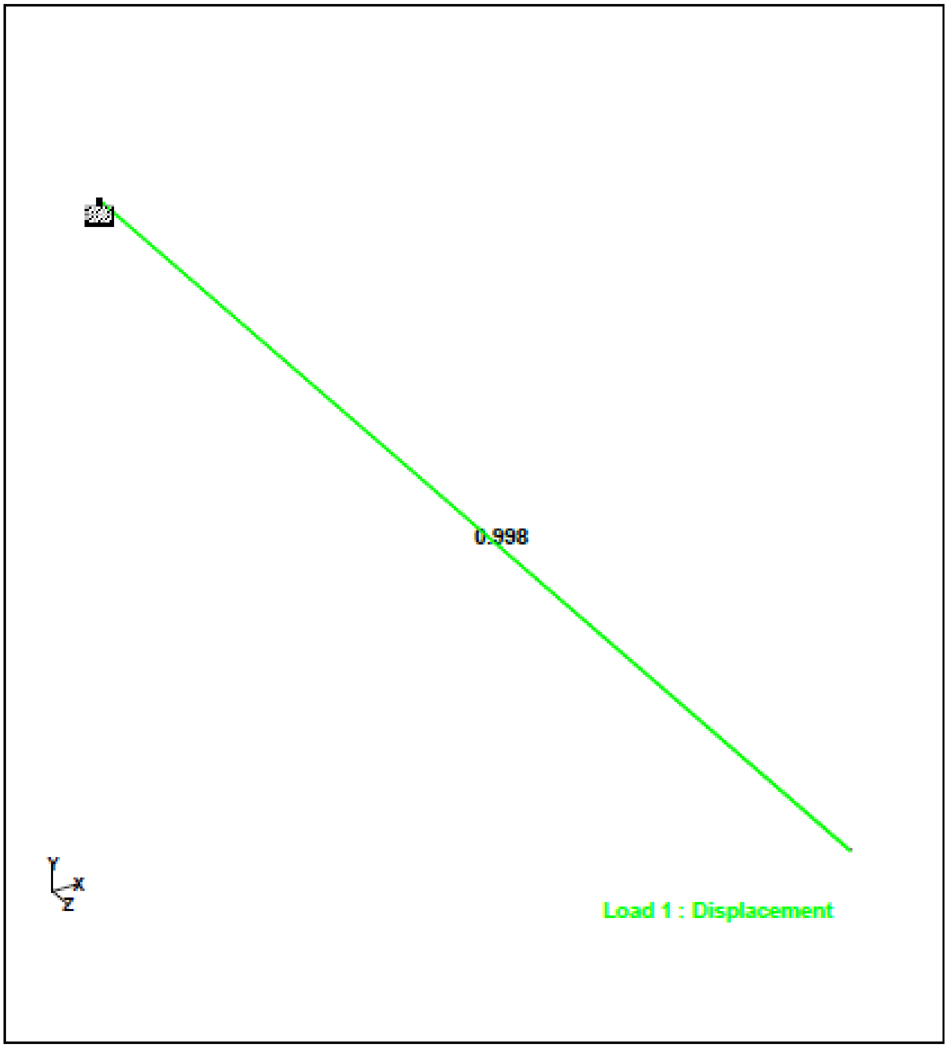


*Utilization Ratio*

## Utilization Ratio

| Beam | Analysis Property | Design Property | Actual Ratio | Allowable Ratio | Ratio (Act./Allow.) | Clause | L/C | Ax ($in^2$) | Iz ($in^4$) | Iy ($in^4$) | Ix ($in^4$) |
|---|---|---|---|---|---|---|---|---|---|---|---|
| 1 | HSSP168X1 | HSSP168X1 | 0.998 | 1.000 | 0.998 | Eq.H3-6 | 1 | 9.626 | 45.407 | 45.407 | 90.815 |